A NOVEL TRANSFORMATION MODEL FOR DEPLOYABLE SCISSOR-HINGE STRUCTURES

**A Thesis Submitted to
The Graduate School of Engineering and Sciences of
İzmir Institute of Technology
In Partial Fulfillment of the Requirements for the Degree of**

DOCTOR OF PHILOSOPHY

in Architecture

**by
Yenal AKGÜN**

**December 2010
İZMİR**

We approve the thesis of **Yenal AKGÜN**

_____
Assist. Prof. Dr. Koray KORKMAZ
Supervisor

_____
Prof. Dr. Tech. Sc. Rasim ALIZADE
Co-Supervisor

_____
Prof. Dr. Murat GÜNAYDIN
Committee Member

_____
Assist. Prof. Dr. M. Emre ERGÜL
Committee Member

_____
Assist. Prof. Dr. Abdullah SÖNMEZ
Committee Member

_____
Assist. Prof. Dr. Engin AKTAŞ
Committee Member

03 December 2010

_____   _____
Prof. Dr. H. Murat GÜNAYDIN   **Prof. Dr. Sedat AKKURT**
Head of the Department of Architecture   Dean of the Graduate School of
                                                                          Engineering and Sciences

ACKNOWLEDGEMENTS

ABSTRACT

A NOVEL TRANSFORMATION MODEL FOR DEPLOYABLE SCISSOR-HINGE STRUCTURES

Primary objective of this dissertation is to propose a novel analytical design and implementation framework for deployable scissor-hinge structures which can offer a wide range of form flexibility. When the current research on this subject is investigated, it can be observed that most of the deployable and transformable structures in the literature have predefined open and closed body forms; and transformations occur between these two forms by using one of the various transformation types such as sliding, deploying, and folding. During these transformation processes, although some parts of these structures do move, rotate or slide, the general shape of the structure remains stable. Thus, these examples are insufficient to constitute real form flexibility. To alleviate this deficiency found in the literature, this dissertation proposes a novel transformable scissor-hinge structure which can transform between rectilinear geometries and double curved forms. The key point of this novel structure is the modified scissor-like element (M-SLE). With the development of this element, it becomes possible to transform the geometry of the whole system without changing the span length. In the dissertation, dimensional properties, transformation capabilities, geometric, kinematic and static analysis of this novel element and the whole proposed scissor-hinge structure are thoroughly examined and discussed. During the research, simulation and modeling have been used as the main research methods. The proposed scissor-hinge structure has been developed by preparing computer simulations, producing prototypes and investigating the behavior of the structures in these media by several kinematic and structural analyses.

ÖZET

YAYILABİLİR MAKAS STRÜKTÜRLER İÇİN YENİ BİR ŞEKİL DEĞİŞTİREBİLME MODELİ

Bu tezin temel amacı; yayılabilir makas strüktürlere şekil değiştirebilme esnekliği sağlayabilecek bir analitik tasarım ve uygulama çerçevesi önermektir. Bugün dünyadaki mevcut şekil değiştirebilen ve yayılabilen strüktürler incelendiğinde görülecektir ki, bütün bu strüktürler sadece tanımlanmış iki form arasında, yine sadece tanımlanmış kayma, dönme veya katlanma gibi hareketler yardımıyla şekil değiştirmektedir. Ayrıca; bu sistemlerde her ne kadar dönme, kayma gibi hareketler söz konusu olsa da, aslında strüktürün temel formunda bir değişiklik olmamaktadır. Yani, bu strüktürler gerçekte şekil değiştirmemektir. Literatürdeki bu eksiği kapatmak için bu tez, çeşitli tek ve çift eğrilikli formları oluşturabilecek esneklikte, yeni bir makas sistemi önermektedir. Bu yeni sistemin kilit noktasını ise değiştirilmiş makas-benzeri eleman oluşturmaktadır. Bu eleman sayesinde önerilen makas strüktürü, geçtiği açıklığın uzunluğunu değiştirmeden, çok farklı şekillere dönüşebilme kabiliyeti kazanmaktadır. Tezde, hem bu yeni geliştirilmiş elemanın, hem de onun oluşturduğu makas strüktürün şekil değiştirebilme kapasitesi, geometrisi, kinematik ve statik analizleri kapsamlı bir şekilde anlatılmıştır. Çalışmada, araştırma yöntemi olarak simulasyon ve modelleme kullanılmıştır. Önerilen makas strüktür; bilgisayar simulasyonları, animasyonlar ve çeşitli prototip çalışmaları ile geliştirilmiş, sistemin kinematik ve strüktürel davranışları yine bilgisayar ortamında ve prototipler yardımıyla yapılan analizlerce değerlendirilmiştir.

TABLE OF CONTENTS

LIST OF FIGURES

LIST OF TABLES

CHAPTER 1

INTRODUCTION

In all periods of history, humans have tried to construct flexible buildings which are capable of adapting to ever-changing requirements and conditions. Kinetic architecture's primary objective is the design of adaptable building envelopes and spaces as the major components of the building using mechanical structures (Zuk and Clark 1970). Recent developments in construction technology, robotics, architectural computing and material science have increased the interest for deployable and transformable structures. The reasons behind this interest relate to the growing need for functional flexibility, adaptability, sustainability and extended capabilities of structural performance. The complexity of design, construction and engineering processes for this type of structures necessitates an interdisciplinary research with novel design approaches, theoretical principles and analytical methodologies that are grounded on sound research findings.

This research study posits an alternative structural design approach using above mentioned interdisciplinary principles with extensive simulation and computer modeling approach. The findings of this research study address the upstream design and implementation issues of deployable and transformable structures by incorporating theoretical models and empirical studies through simulations.

In this study, first, common examples of deployable and transformable structures are reviewed with respect to their transformation capabilities. Then, an alternative structural design approach which can meet the deficiencies of the common deployable structures is proposed. Different variations of this approach are applied to different cases; and the validity of these cases is interrogated by mathematical models and computer simulations.

The results of this study show the effectiveness and the feasibility of the proposed design approaches, structural principles and implementation strategies for deployable and transformable structures.

1.1. Problem Statement

Most of the deployable and transformable structures in the literature have predefined open and closed body forms, and transformations within the structures occur between these two forms by using one of the various transformation types such as sliding, deploying, and folding (Zuk and Clark 1970) (Figure 1). During these transformation processes, although some parts of these structures do move, rotate or slide, the general shape of the structure never changes. Thus, these examples are insufficient to offer a full formal flexibility. This deficiency constitutes the first problem area of this study.
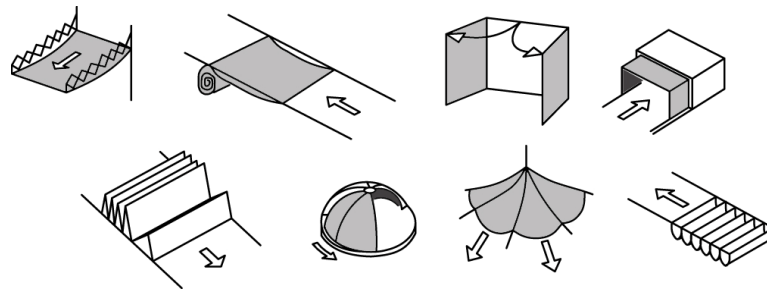
Figure 1. Examples of transformable structures

Until today, most of the research on the topic has ignored this deficiency and vast majority of the previous research on deployable and transformable structures have only focused on the following topics:

- Obtainment of defined forms by using common structural elements via different folding types: Pinero's foldable theater (Pinero 1961), novel spatial grids and patterns of Escrig and Valcarcel (Escrig 1984, 1985; Escrig and Valcarcel 1986, 1987) and structures of Calatrava in his dissertation (Calatrava 1981) are well-known examples for these studies.

- Obtainment of the defined forms by using structural elements with different geometry or material: Hoberman and Pellegrino's research on angulated elements (Hoberman 1993; You and Pellegrino 1997) and studies of Pellegrino

on scissor-hinge plates (Jensen and Pellegrino 2002) are well-known examples of these studies.

- Incorporation of additional elements to move or fix the structure: Rolling Bridge of Heatherwick (Heatherwick-Studio 2009) and Variable Geometry Truss of Inoue (Inoue, et al. 2006; Inoue 2008) have additional hydraulic arms to increase the flexibility. Moreover, Kokawa's scissor arch (Kokawa and Hokkaido 1997) has a zigzag cable system to move and fix the structure.

Except Kokawa's and Inoue's structures, all of the aforementioned examples transform via deployment and contraction. Although these structures can cover a building or a space when they are at deployed shape, they lose this property when they are at contracted position. Thus, these structures are not adequate to be used as permanent coverings. This deficiency of deployable structures constitutes the second problem area of this study.

In the case of the innovative approaches, such as in the works of Kokawa and Inoue, structures can transform without changing the size of the covered area. However, they have other deficiencies. For instance, Kokawa's structure cannot transform into asymmetrical shapes; and Inoue's Variable Geometry Truss is not feasible as a building component because of the huge number of actuators on the system.

Consequently, it can be claimed that the common deployable and transformable structures transform only between predefined body forms and during the transformation process, size of the area they cover always changes.

1.2. Objectives of the Research

Primary objective of this dissertation is to propose a novel analytical design and implementation framework for deployable structures which can offer a wide range of form flexibility without changing the size of the covered area. To arrive at this objective, a novel transformable scissor-hinge structure which can transform between rectilinear geometries and double curved forms has been proposed in this dissertation (Figure 2).

Another objective of this research study is the critical examination of common deployable and transformable structures with respect to their transformation

capabilities. During this examination, problems and shortcomings of common scissor-hinge structures are focused and identified.
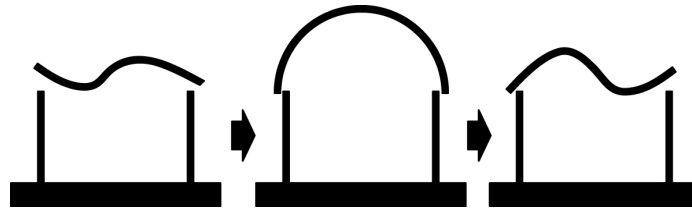
Figure 2. Schematic transformation of the proposed scissor-hinge structure

1.3. Significance of the Research and Contributions

This study analyzes the transformation capabilities of current deployable structures and proposes a flexible and transformable scissor-hinge structure, designed by novel planar and spatial scissor units. This proposed structure expands the transformation capability, adaptability and form flexibility of deployable structures. Until now, deployable structures have been only used as portative building components. However, after the model proposed in this study, deployable structures will also be used as permanent transformable building coverings.

As a hypothetical example, such a transformable structure can be used as roof of an exhibition hall. According to the activity and the necessities for the activities in that hall, the shape of the roof can be transformed by the users. This kind of a transformation offers great flexibility for spaces. As an example of functional need, the proposed scissor-hinge model can be used as a solar roof. It can be rotated according to the location of the sun and benefit from the sun more than the conventional solar panels. Scissor-hinge structures are conveniently used with control systems, so by using a few motors, these transformations can be performed easily.

This study reviews and classifies the common scissor-hinge structures and exposes the specific mathematical analysis methods for each typology. This review will also serve as a future reference for researchers to see all different typologies and their analysis methods at the same time.

1.4. Scope of the Research

This study utilizes the scissor-hinge structures combined with actuators as the main structural element. Investigation of typologies, geometric, kinematic and the structural analysis of the common scissor-hinge structures and various implementations of the proposed structural design framework form the scope of this study.

Covering materials of such kind of flexible structures is an additional research problem that is not within the scope of this study. However, in some case studies, a flexible membrane which is formed by an origami tessellation is assumed as the cover material.

Moreover, technical details, mechanical and electronic control principles of the actuators are not within the scope of this study. These could be investigated as a research topic within the fields of robotics and electronic engineering.

1.5. Methodology of the Research

The study employs "Simulation and Modeling" as the primary research methodology. Simulation and modeling includes all prototyping works, mathematical models and computer simulations. Steps of the research and the contributions of the methodological framework to the study are shown in Figure 3.

In the first phase of the study, a thorough and critical literature survey was conducted and the study exposed the general geometric principles of the common deployable structures. Simple physical models were constructed to evaluate the transformation capabilities of common scissor systems and combinations of different scissor systems in a single mechanism. This phase finished with the development of the Modified Scissor-like Element (M-SLE) and explanation of the main principles of the proposed scissor-hinge structure.

In the second phase, the study focused on the improvements of the proposed unit and the proposed structure. Several mathematical algorithms were developed by using Mathematica and Microsoft Excel (with Visual Basic extensions) in order to assess the improvements over the previous design schemes. In addition to these mathematical models, computer simulations were used to test the validity and applicability of the mathematical models. MSC Visual Nastran 4D software was used to check the

transformation capacity of the proposed structures. By Finite Element Analysis (FEA) tools of this software, strength of the elements during transformations and behavior of the struts under simple loads were simulated. Comprehensive investigations on strength of the structure are made using ADINA FEA Software. This software allows the analyses of the locations of additional actuators and the sections of the struts. Finally, prototypes in different scales were constructed according to the derived data from the computer models and the simulations.
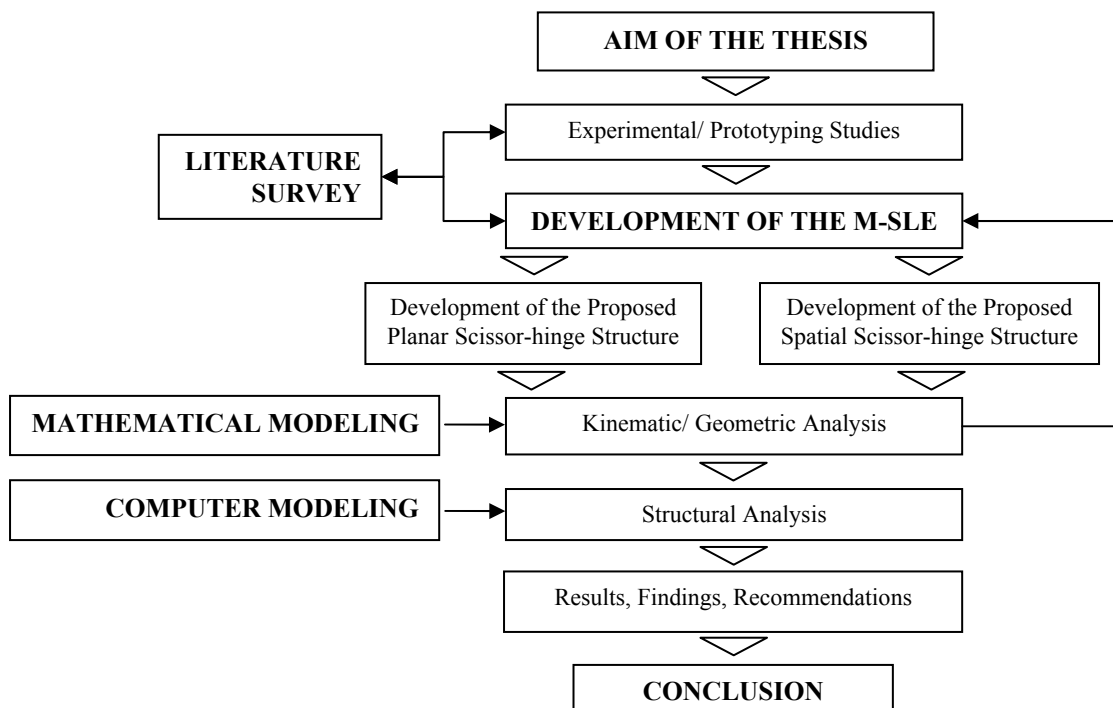
Figure 3. Process of the dissertation

1.6. Organization of the Dissertation

The dissertation is organized into following chapters:

Chapter 1 introduces the motivation, objectives, basic concepts, methodology, and significance of the study.

Chapter 2 presents a critical literature review that summarizes the previous research and practical applications on deployable and transformable structures. The

extensive literature review establishes the anchors for references and identifies the knowledge gap that justifies the current research.

Chapter 3 provides the terminology and theoretical framework of the transformable structures and mechanisms. This framework contains the main elements of a mechanism, such as typologies of the necessary actuators, and geometrical analysis methods.

Chapter 4 deals with the classification of the common scissor-hinge structures and their geometric analyses.

Chapter 5 and Chapter 6 are devoted to the presentation of the proposed scissor-hinge structural model. This model is applied to both planar and spatial scissor-hinge structures. In Chapter 5, planar version of this application is presented. Key elements of this model, mathematical and kinematic principles, static analysis, potential applications and superiority of the proposed model are presented by the help of prototypes and computer models. In Chapter 6, all these analyses and evaluations are repeated for the application of the proposed model to the common spatial scissor-hinge structures.

The main achievements of the research are summarized in Chapter 7, together with recommendations for future work, which conclude this dissertation.

CHAPTER 2

REVIEW OF PREVIOUS WORK

This chapter highlights the originality of the proposed transformable scissor-hinge structure, in comparison to common transformable examples. In this chapter, convertible works of some well-known designers are reviewed. The review includes the summary of the main characteristics of the previous examples and a discussion on their transformation capabilities, advantages, and shortcomings.

The previous works are investigated in two main groups: first, typical deployable structures which can only transform between two predefined geometries; second, structures which can transform between more than two predefined geometries. First group contains the most common examples of the transformable structures; however, they are relatively weak in meeting the requirements of wide range of flexibility. In the second group, some improved deployable structures and some mechanisms adapted for the field of structural design are listed. Although some of them are designed only for experimental purposes, this second group of structures has brought innovative issues to the concept of flexibility in transformable structures research.

2.1. Deployable Rigid Bar Structures

Deployable structures are structures capable of large configuration changes in an autonomous way. Most common configuration changes are those that change from a packaged, compact state to a deployed, large state. Usually, these structures are used for easy storage and transportation. When required, they are deployed into their service configuration (Tibert 2002). Simple examples include umbrellas or tents; or solar arrays and antennas on spacecraft, which have to be compactly stowed for launch, but then must unfold autonomously to their final state.

Today, most of the research on this topic only deal with "obtaining different forms by using common structural units via different folding types," or "obtaining the defined forms by using structural elements with different geometry or material," or

"additional elements to move or fix the structure". Thus, it can be claimed that most of the studies on this topic do not offer any significant formal flexibility. These structures change their geometries only between predefined "open-closed" or "extended-contracted" positions.

Scissor-hinge structures are typical examples of deployable structures and many key researchers such as Pinero, Hoberman, Escrig, Valcarcel, Gantes and Pellegrino have proposed different systems using scissor-hinge structures. Some important works of these key-researchers are reviewed in this chapter with respect to their flexibility and transformation capabilities.

The first example is from Pinero. In the early 1960s, the Spanish architect Emilio Perez Pinero invented a scissor mechanism, in which each rod has three pivot joints, one on each end and one toward the middle. As two ends of a scissor mechanism are brought together, the centre pivots are spread apart, lengthening the mechanism as a whole to a planar pattern (Pinero 1961). Furthermore, Pinero realized that if the interior pivot point on a rod was not at the midpoint, then it is possible to create a shell-shaped surface. He developed a full-size foldable theatre, which arrived at the site on a single wheelbarrow and was then unfolded with a scissor-hinge mechanism (Figure 4).
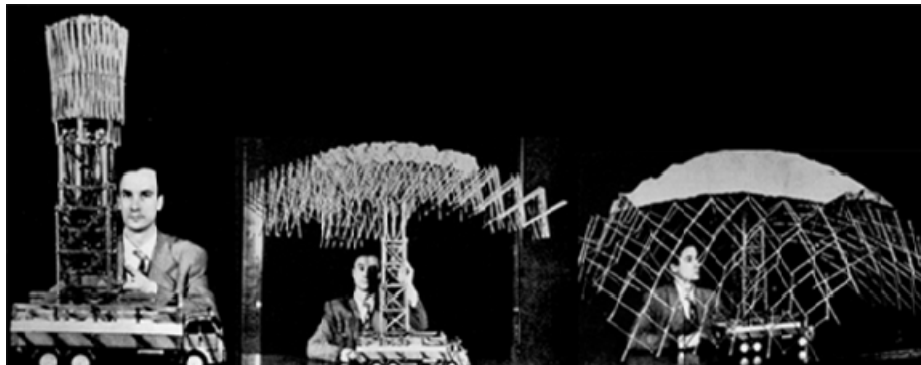
Figure 4. Pinero's transformable shell
(Source: Pinero 1962)

Felix Escrig and Juan Valcarcel improved upon Pinero's work. They developed novel planar and spatial units to obtain different geometries. They focused especially on obtaining different geometries by using the same struts and different connection

elements. Some simple examples from these studies can be seen in Figure 5. In all these three structures, simple struts are used but the connection details are different and this situation creates different grids and geometries.
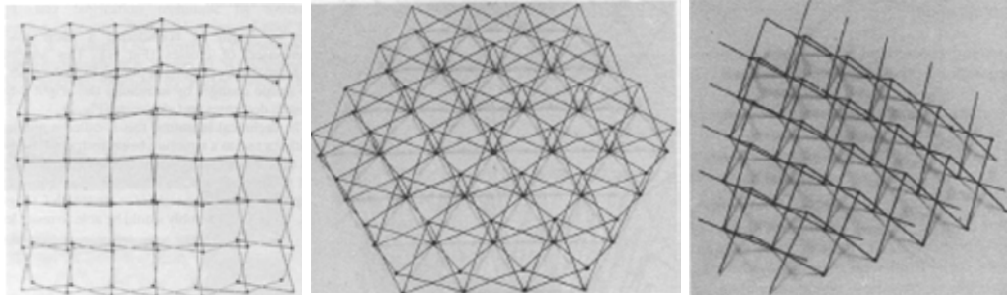
Figure 5. Deployable structures of Escrig and Valcarcel
(Source: Escrig 1985)

Besides studies on the design of new geometries, some researchers have analyzed the geometry of the scissor-hinge structures (Escrig 1985) (Escrig and Valcarcel 1986, 1987). Simple deployability conditions and the relation between span and the dimension of the elements were first explained by Escrig and Valcarcel. However, their most important work is the rigid plate roofing element. Generally, fully folded deployable structures have been covered with a thin fabric roof. However flexible materials used in deployable structures do not contribute to structural strength. Escrig determined that they are useful only in reduced spans. He has developed deployable structures with rigid plates as part of the mechanism (Figure 6). The plates overlap one another like the scales of a fish and are fixed in place once the mechanism is opened (Robbin 1996).
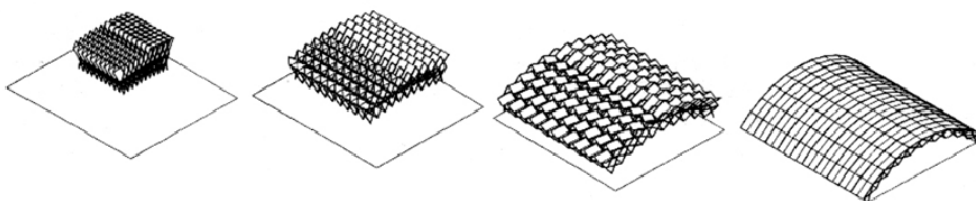
Figure 6. Escrig's deployable vault incorporating rigid panels
(Source: Robbin 1996)

Chuck Hoberman is another important designer who has focused on scissor-hinge mechanisms. Especially, he has tried to develop some primary geometric shapes by using scissor-hinge mechanisms. Expanding helicoid, Expanding Hypar (hyperbolic paraboloid), Expanding Icosahedron, Expanding Sphere, Expanding Geodesic Dome and Expanding Video Screen are examples of his designs with scissor-hinge mechanisms. These designs have been generally designed as an exhibition object (Hoberman 2009); and the latest two examples are shown in Figure 7 and Figure 8.

Figure 7. Expanding geodesic dome
(Source: Hoberman 2009)

Figure 8. Expanding video screen
(Source: Barco 2009)

Although he has many other important designs, the most important achievement of Hoberman in the design of transformable scissor-hinge mechanisms is the simple angulated element. This element consists of two identical angulated bars connected together by revolute joint and forms the basis of a new generation of transformable

structures (Figure 9). By using these angulated bars, Hoberman has created the transformable Iris Dome (Figure 10) and the Hoberman Arch. A prototype for the Iris Dome was built for an exhibition at the Museum of Modern Art in New York in 1994 and another for EXPO 2000 in Hannover (Hoberman 1993). The Hoberman Arch was constructed for the Winter Olympics in Salt Lake City in 2002. Both of these mechanisms are constructed from a number of angulated elements arranged on concentric circles. Angulated elements form a circular shape in plan and the joints connecting the end nodes of the angulated elements connect the circles to each other. This allows the structure to transform toward its perimeter, thus creating a central opening at the centre when transformed (Korkmaz 2004).
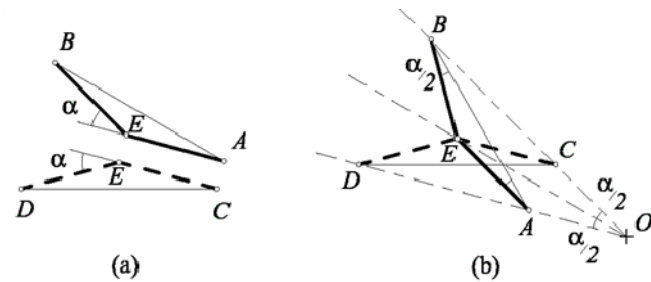
Figure 9. Angulated element
(Source: Korkmaz 2004)
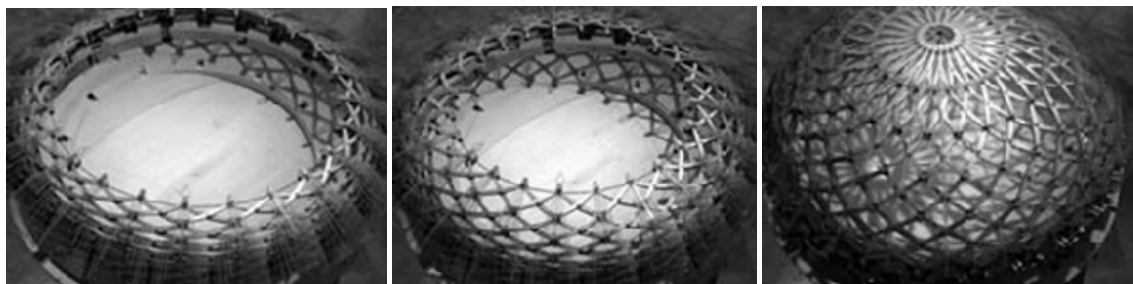
Figure 10. Iris Dome
(Source: Hoberman 1993)

Figure 11. Hoberman Arch
(Source: Hoberman 2009)

Sergio Pellegrino and Zhong You from Deployable Structures Laboratory (DSL) at Cambridge University noted that consecutive angulated bars in Figure 12 maintain a constant angle (β) when the structure is expanded, and thus can be replaced with a single multi-angulated bar. Thus, the structure shown in Figure 12 can also be made from a total of 24 bars, each having four segments with equal link angles: 12 bars are arranged in a clockwise direction and 12 anti-clockwise. At each crossover point, there is a revolute joint. An entire family of these structures has the ability to retract radially towards the perimeter and can be generated for any plan shape. This makes them particularly interesting for sporting venues where retractable roofs must be able to retract towards the perimeter of the structure (You and Pellegrino 1997).
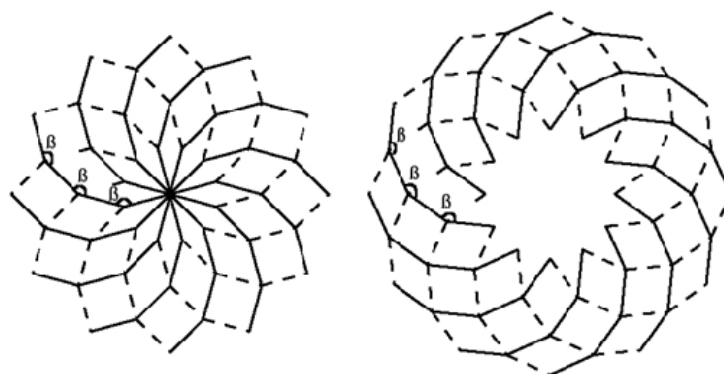
Figure 12. Multi-angulated bar and its application
(Source: Korkmaz 2004)

All of the examples summarized above can basically convert their shapes; but this shape changes occur only between limited contracted and deployed forms. These deployable examples, therefore, do not offer a complete formal flexibility. There are some studies, however, which try to bring more flexibility for deployable structures. Rippmann and Sobek's work is a good example for these studies.

Matthias Rippmann and Werner Sobek's research is one of the studies of Institute for Lightweight Structures and Conceptual Design (ILEK) at University of Stuttgart. This study is based on the development of a new Scissor-like Element (SLE). This element has various hinge points, and allows bar connections at different points. By switching the locations of hinge points, different shapes can be constituted. A Visual Basic script was also prepared to define the requested shape and the location of hinge points for every individual SLE. This structure was designed as a deployable exhibition wall, and it can adapt itself to ever changing spatial and functional needs. The disadvantage of this structure, however, is that when a change in the shape of the structure is required, all SLEs should be unplugged and the system must be connected from the beginning (Rippmann 2007).
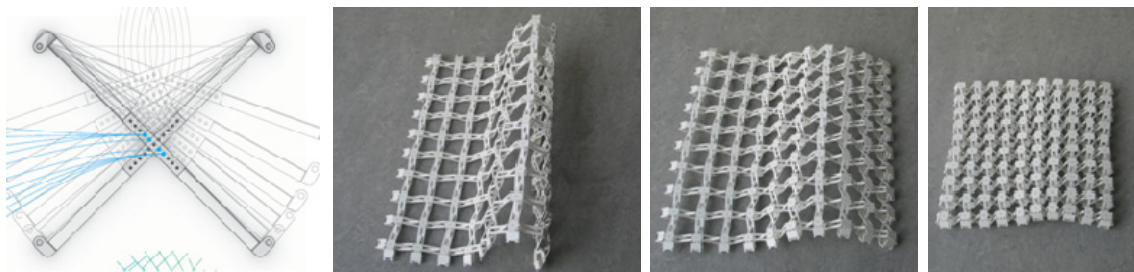
Figure 13. Rippmann's scissor structure
(Source: Rippmann 2007)

2.2. Transformable Rigid Bar Structures

Transformable structures include those which change their shapes via rotating, sliding or folding. Modified deployable structures which can transform their shapes without a change in area of the covered space can be listed in this group as well. Some of the examples investigated below have not been designed as a structural member of a

building; but they still provide clues for the probable use of a transformable structure as an adaptive building member.

First example is the transformable street lamps of Schouwburgplein in Rotterdam by Adriaan Geuze. Although this structure is just a street lamp, its flexibility gives new ideas for the novel transformable structures. The public square is designed as an interactive public space, flexible in use, and changing during day and seasons. Flexible street lamps complete the concept of the design; and with these extraordinary transformable lamps, various illumination patterns of the square are possible (Korkmaz 2004). The lamps have two transformable hydraulic arms; and by actuating these arms, various geometries can be achieved. The light source is connected to the output link and this gives the ability to illuminate the square in various positions.

Figure 14. Transformable street lamps at Schouwburgplein
(Source: West-8 2009)

Shadow Machine of Santiago Calatrava is the second example. This project was designed as an exhibition object for Museum of Modern Art in New York and Venice, Italy in 1992-1993. The idea of a concrete machine was originally developed in 1988 for the Swissbau Concrete Pavilion (Figure 15); and the Shadow Machine is the improved version of this pavilion. In this case, a socket cast into each finger engages to fully articulate upon a ball that is set into the end of the protruding supports. As with the

Swissbau Pavilion, a progressive change in the angle of engagement with an endless chain produces a staggered, synchronized motion (Tzonis 1999). Shadows of each individual element moving on the wall give the sense of continuity and change.

Figure 15. Shadow Machine and Swissbau Pavilion
(Source: Tischhauser and von Moos 1998)

Above mentioned mechanisms are not designed as a building component; but they have potentials to be used as member of a transformable roof structure. Calatrava has used this potential in several of his projects. For example, mechanisms and members of the Kuwait Pavilion and the wing-shaped louvers of the Milwaukee Art Museum are similar to the Shadow Machine. Kuwait Pavilion was designed for EXPO 92 in Seville (Figure 16). In this building, movement permits the structure of the roof to open and close. The 25-meter long cantilevered members of the pavilion come down to protect the visitors from the sun, rising up at night to accommodate the different uses of the terrace (Tischhauser and von Moos 1998). In addition, each beam can rotate individually and one can obtain infinite number of geometries as a whole roof structure by different configurations of these individual beams.
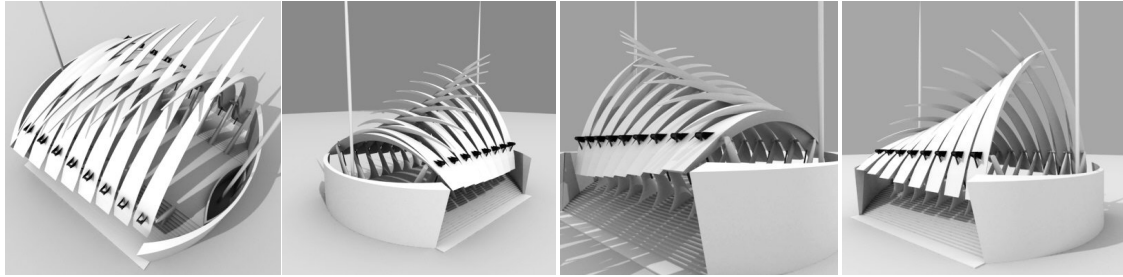
Figure 16. Model views of Kuwait Pavilion
(Source: Turbo Squid 3D Marketplace 2009)

Milwaukee Art Museum has a system of louvers that can open and close like the spreading wings of a big bird to provide shade, protection and special atmosphere (Figure 17). When open, the shape also becomes a signal against the backdrop of the lake to herald the inauguration of temporary exhibitions (Tischhauser and von Moos 1998). These louvers can also constitute infinite number of geometries as a whole.
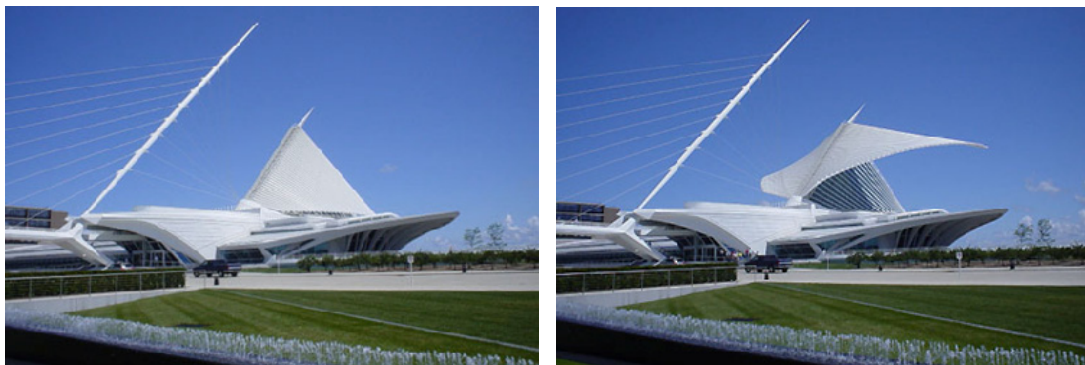
Figure 17. Louvers of Milwaukee Art Museum
(Source: Galinsky 2009)

Another example from Calatrava is the Emergency Call Center in St. Gallen-Switzerland. Mechanism of the roof of this building is more complex than the previous two examples. The symmetrically constructed, lens-shaped skylight of the Center, surrounded by a spectacular folding shade, gives the impression of a fresh, half-open flower in the green of the garden. Folding shade consists of two foldable coverings constructed with aluminum slats. Each of the coverings folds through the displacement

of a series of aligned aluminum slats, articulated in the center like a knee. When a motor hidden in the building opens the folding shade over the skylight, the slats protrude upwards to let the day light inside. The folding shade's configuration is due to the gradual and uniform change of the length of the aluminum slats and the position of articulation along series of slats (Korkmaz 2004).
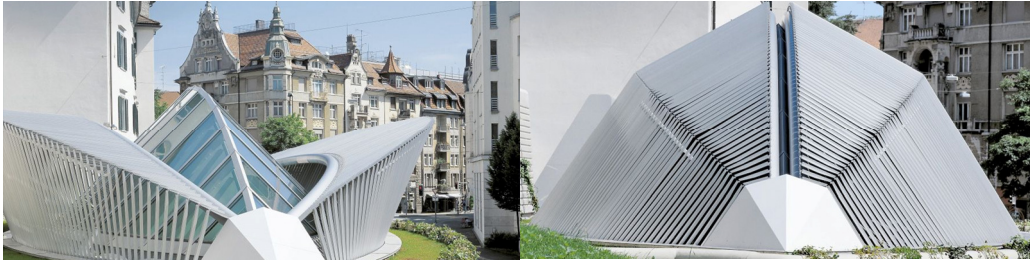
Figure 18. Transformable roof of Emergency Call Center by Santiago Calatrava
(Source: Calatrava 2009)

Rolling Bridge from Grand Union Canal in London is another example. This bridge was conceived by British designer Thomas Heatherwick, and designed by Anthony Hunt with Packman Lucas. Rather than a conventional opening bridge mechanism, consisting of a single rigid element that lifts to let boats pass, the Rolling Bridge clears the way by curling up until its two ends touch. The bridge consists of eight triangular sections hinged at the walkway level and connected above by two part links that can be collapsed towards the deck by hydraulic pistons, which are concealed in vertical posts in the bridge parapets. When extended, it resembles a conventional steel and timber footbridge, and is 12 meters long. To allow the passage of boats, the bridge curls up until its two ends join, to form an octagonal shape measuring one half of the waterway's width at that point (Heatherwick-Studio 2009). The Rolling Bridge can constitute different shapes; and by the application of the main idea of this bridge to a roof structure, a flexible roof which can offer many different shapes can be obtained.
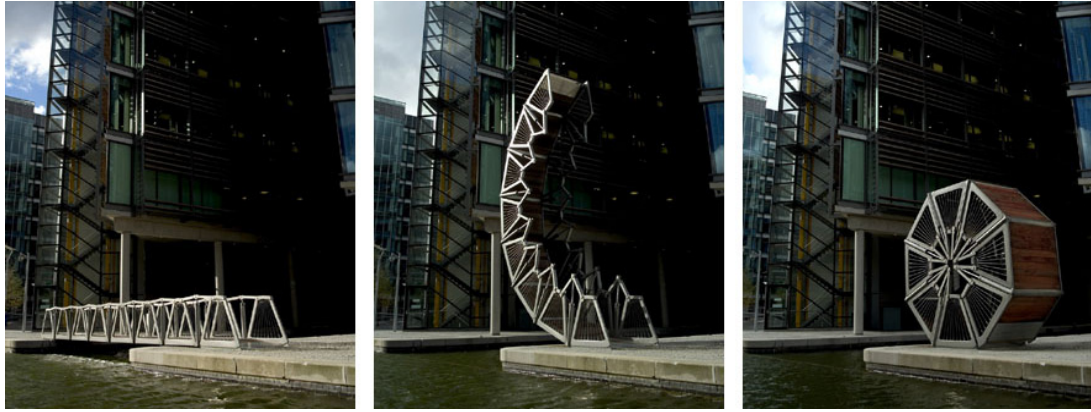
Figure 19. Opening steps of Rolling Bridge
(Source: Heatherwick Studio 2009)

Tsutomu Kokawa's research is called Cable Scissors Arch (CSA). This research is an example for transformable deployable structures. Different from and more innovative than the typical scissor-hinge structures, this structure can change its geometry without changing the span length. CSA consists of three-hinged arch scissors and zigzag flexible cables with pulleys installed at the connection points between the scissors units. During winding up of the cable by a winch, CSA expands and it is forced to lift up. It will shorten and go down by its self-weight during the winding back. The weight of the structure is in equilibrium with compression in the strut and tension in the cable, through the whole operation. CSA is a stable and statically determinate structure all the time as tension force always works in the cable under gravity load. In Figure 20, some transformations of the structure can be seen. The span in this prototype is 11m, minimum height is 175cm and maximum height is 500cm (Kokawa and Hokkaido 1997). Kokawa's structure is relatively more flexible than the other such structures. However, this structure can only provide symmetrical arc-like shapes. There should be studies which can achieve more flexible alternatives.

Figure 20. Transformations of CSA
(Source: Kokawa and Hokkaido 1997)

Fumihiro Inoue and his colleagues from Technical Research Institute of Obayashi Corporation in Japan have also claimed that the common transformable structures have no flexibility in shape; and they have proposed a flexible truss called Variable Geometry Truss (VGT). The VGT is a very simple truss structure composed of extendable members, fixed members and hinges, as shown in Figure 21. By controlling the lengths of the extendable members, it is possible to create various truss shapes (Inoue 2008). For example, when extendable members are extended at the same time, the truss extends linear. Moreover, when actuators are extended optionally and their lengths are controlled, the truss beam can be changed into any intended shape.
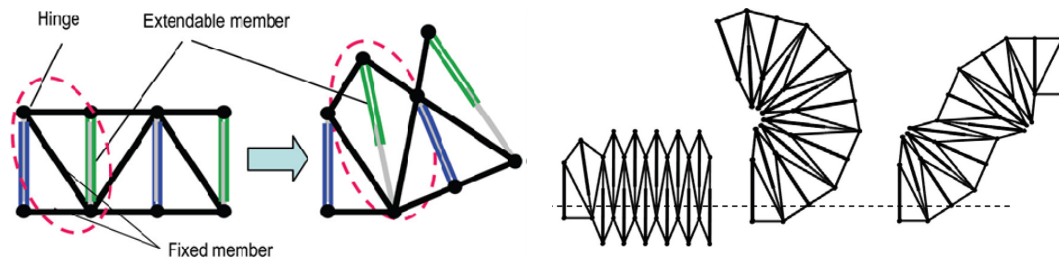
Figure 21. Basic mechanism of VGT and its transformations
(Source: Inoue 2008)

Inoue and his colleagues have applied VGT to a spatial truss structure and designed a movable monument for EXPO 2005 in Japan. The monument was composed of three movable iron towers which were spaced at 120-degree intervals around the circumference. Each tower comprised four truss members combined by VGT at joints.

Each frame comprised a solid truss structure. Transformation of the structure can be seen in Figure 22 and Figure 23 (Inoue et al. 2006).
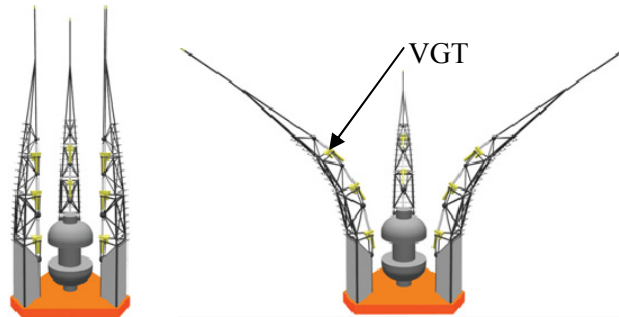
Figure 22. Schemes of the movable monument
(Source: Inoue et al. 2006)

Figure 23. Movable monument at EXPO 2005
(Source: Inoue 2008)

Another proposal of Inoue by using VGT is the Transformable Arch Structure. In this structure, all nodes are designed as hinges; and some of the members are linear actuators. Figure 24a shows the shape variations of the arch structure when the actuators are situated on the lower frame of the structure. Similarly Figure 24b shows volume changes with the extensible members sat on both lower and upper sides. In this case, a flexible member is needed for external finishing (Inoue 2008).
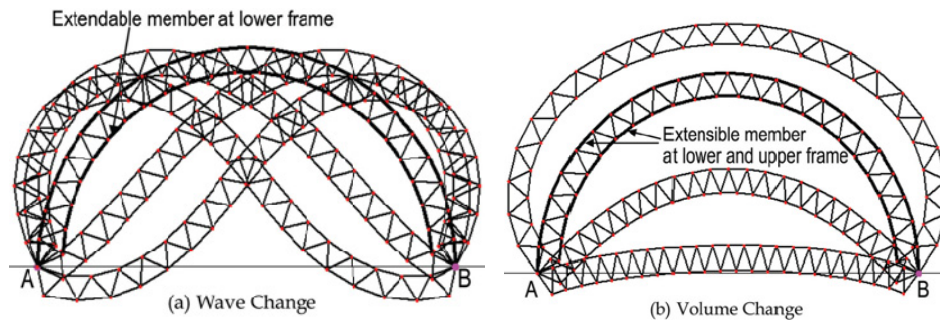
Figure 24. Arch structure with VGT mechanism
(Source: Inoue 2008)

Inoue's proposals are innovative flexible structures; but, because of the huge number of the actuators on each beam, and the necessary complicated electronic control systems, these structures are not feasible in today's technology. Achieving shape transformations with less number of actuators is a more difficult but more feasible solution.

Despite their flexibility or feasibility problems, the main ideas of the above mentioned examples about transformations in rigid bar systems are important for further studies. These studies show that it can be possible to change the shape only by changing small things such as the location of a joint or shape of the struts, and it can be easy to obtain different form alternatives by using these small modifications.

CHAPTER 3

KINEMATIC ANALYSIS OF BAR MECHANISMS

This chapter mainly introduces the basic concepts and terms of mechanisms and methods of kinematic analysis. For this introduction, first, some important terms such as kinematics, mechanism and kinematic joints are defined. Then, concept of mobility is explained by using the examples in Chapter 2. Finally, basic methods of the kinematic analysis are explained. Aforementioned concepts and kinematic analysis methods are necessary for finding the number of actuators to control a mechanism, or determining the shape limitations of any kind of mechanism or a structure.

3.1. Definition of the Terms

Kinematics is a branch of physics and a subdivision of classical mechanics concerned with the geometrically possible motion of a body or system of bodies without consideration of the forces involved. Kinematics aims to provide a description of the spatial position of bodies or systems of material particles, the rate at which the particles are moving (velocity), and the rate at which their velocity is changing (acceleration) (Kinematics - Britannica Online Encyclopedia 2009).

A *Mechanism* can be defined as a group of rigid bodies connected to each other by rigid kinematic pairs (joints) to transmit force and motion (Söylemez 1999). Thus, a mechanism transfers the input motion or work at the input point or point of actuation to one or more output points. A mechanism consists of group of rigid bodies (links) connected to each other by rigid kinematic pairs (joints) to transmit force and motion. To understand this definition thoroughly, following terms should be understood:

If a rigid body contains at least two kinematic elements, it is called as *link* (Söylemez 1999).

A *kinematic pair (joint)* is a connection between two or more links (by kinematic elements), which allows some motion, or potential motion, between the connected links (Norton 2004). The pairs are classified according to the type of contact
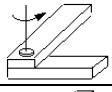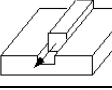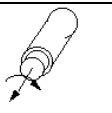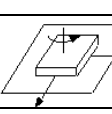
and relative motion of the members. There are two types of kinematic pairs according to the type of contact:

Lower pairs: These pairs have contact between the two mating surfaces of the members forming joint, as in the case for revolute joint ("pin", "hinge"), prismatic joint ("slider"), cylindrical joint, screw joint, planar joint, and spherical joint ("ball").

Higher pairs: These pairs have the contact between the mating surfaces as point or line contact as in the case for cams and gears (Bright-Hub 2009).

In this research, only lower pairs are used, so only this type of pairs is thoroughly explicated. In Table 1, six lower pairs can be seen.

Table 1. Lower pairs and their kinematic properties

Pair Type	Scheme	Motion Type	DoF
Revolute Joint		Rotation	1
Prismatic Joint		Translation	1
Helical Joint		Rotation and translation	1
Cylindrical Joint		Rotation and translation	2
Planar Joint		Rotation and translation	3
Spherical Joint		Rotation	3

To understand the kinematic properties of these pairs, first, concept of mobility and degree of freedom should be understood. A mechanical system's *mobility (M)* can be classified according to the number of *degrees of freedom (DoF)* that it possesses. The system's DoF is equal to the number of independent parameters (measurements) that are needed to uniquely define its position in space at any instant of time (Norton 2004). For example, an unrestrained rigid body in space has 6-DoF: three translations along the x, y

and *z* axes and three rotations around the *x*, *y* and *z* axes respectively. A system of particles could have up to 6-DoF, but would normally have less because of constraints.

3.2. Degrees of Freedom (DoF) or Mobility (M) of a System

Another definition of the mobility is "the number of inputs that need to be provided in order to create a predictable output" (Norton 2004). Thus, mobility of a mechanical system describes the number of additional actuators needed to fix or move the system safely.

The degree of freedom of an assembly of links completely predicts its character. There are only three possibilities. If the DoF is positive, it is a mechanism and the links have relative motion. For all transformable and deployable structures, mobility of the system is bigger than zero (M≥1). If mobility of the kinematic system is equal to zero (M=0), then it is a *structure* and no motion is possible (Escrig and Valcarcel 1986). If the DoF is negative, then it is a preloaded structure, which means that no motion is possible and some stresses may also be present at the time of assembly (Norton 2004).

From the aforementioned definitions, it can be said that if a mechanism is fixed by additional motors, stabilizers and actuators, it converts to a structure. All deployable and transformable structures in the field of architecture and civil engineering behave as a mechanism during their deployment and transformation process. However, they behave as a structure when they are fixed. Thus, they have the characteristics of both a mechanism and a structure. These kinds of mechanisms are called as *structural mechanism* (Chen 2003). All deployable structures including scissor-hinge structures are the typical examples of structural mechanisms.

From the beginning of the kinematics research, several formulas have been derived. All these formulas can be seen according to the chronological order in Alizade et.al. (Escrig and Valcarcel 1986). In this study, Freudenstein and Alizade formula (Freudenstein and Alizade 1975) is used; because this formula can meet both planar and spatial mechanisms. Here is the formula:

$$M = \sum_{i=1}^{j} f_i - \lambda L + q - j_p$$

<div align="right">(3.1)</div>

where;

L = Number of closed loops in the system

M = Mobility

$\sum_{i=1}^{j} f_i$ = Sum of DoF all joints

λ = DoF of space where the mechanism operates (λ=3 for planar systems and λ=6 for spatial systems)

q = Number of over-constraint links

j_p = Passive mobilities in the joints

In order to understand this formula, it is applied to the mechanisms in Chapter 2. First application is the transformable street lamp of Adriaan Geuze. In Figure 25, a schematic view of this lamp is illustrated. The mechanism has seven links, six revolute joints (five on platforms, 1 between platforms), and two prismatic joints in the kinematic diagram. Also, λ is equal to three and there are two loops. According to the Freudenstein and Alizade formula;

$$M = 8 - 3 \times 2 = 2$$

M=2 indicates that the mechanism requires two inputs to determine the position of its links relative to the ground. In reality, these inputs are supplied by two hydraulic motors which actuate the prismatic joints.
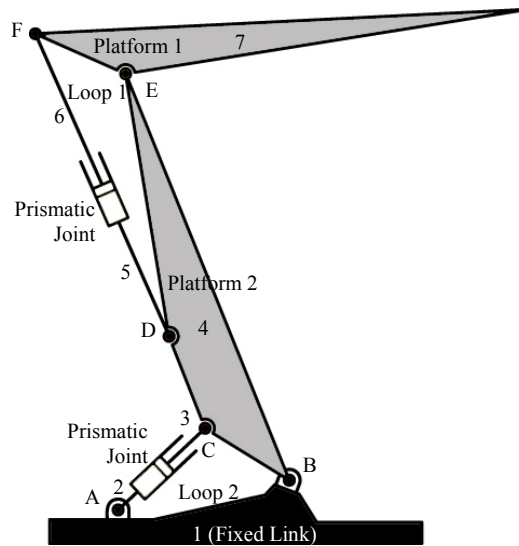
Figure 25. Kinematic diagram of the kinetic street lamp

Second example is the movable roof of Emergency Call Center in St. Gallen designed by Calatrava. This roof is the simplest closed loop linkage which is called four-bar mechanism. When Figure 26 is investigated, it can be seen that the mechanism has three moving links, one fixed link (the base) and four revolute joints. The link 2, which is connected to the power source (a revolute motor), is called as the input link: and the link 4 is called as the output link. The coupler link 3 connects the two joints, B and C, thereby coupling the input to the output link. Mobility   of   this   structural mechanism can be calculated as follows:

$$M = 4 - 3 \times 1 = 1$$
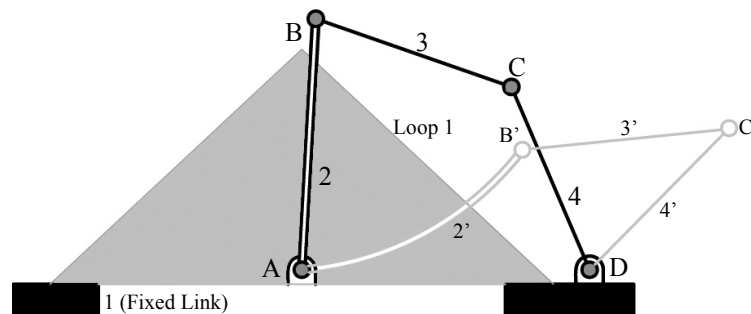
Figure 26. Kinematic diagram of the Emergency Call Center

Simple four-bar mechanisms are always M=1 systems. According to this data, Calatrava designed input link numbered 2 as an arc form to drive the various planar four-bar mechanisms with one power source which is located at Point A.

Third example is the Rolling Bridge. Figure 27 shows the kinematic diagram of the first two sections of the Rolling Bridge. This structural mechanism has 2 loops, 6 links (each trapezoid is assumed as a single link), 6 revolute joints (there are 2 joints at points D and E) and 1 prismatic joint. When the mobility formula is applied to this mechanism;

$$M = 7 - 3 \times 2 = 1$$
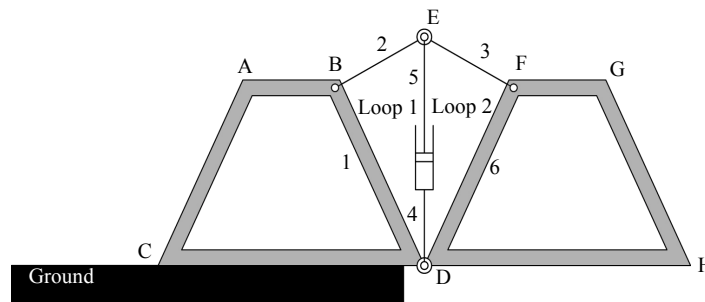
Figure 27. Kinematic diagram of two units of the Rolling Bridge

As it can be seen in Figure 28, there are 8 sections in the Rolling Bridge. This means that it has 42 revolute joints, 7 prismatic joints and 14 loops. According to the mobility formula;

$$M = 49 - 3 \times 14 = 7$$

This result means that this structural mechanism needs minimum 7 inputs (actuators) to fix or move. These inputs are supplied by seven hydraulic motors which actuate the prismatic joints.
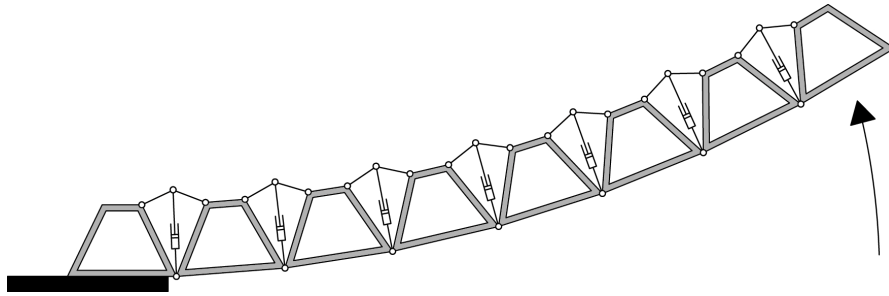
Figure 28. Kinematic diagram of the Rolling Bridge

After general examples, it can be useful to make an exercise about scissor-hinge structures. A typical planar scissor-hinge structure can be seen in Figure 29. This structure has 11 joints, 3 loops and 8 links. In addition, it is known that λ is 3 for planar systems. When this data is applied to the Freudenstein and Alizade formula;

$$M = 11 - 3 \times 3 = 2$$

This result shows that this system as a whole has two transformations. One of them is rotation around point A_0, and the other is sliding which is expressed by dashed lines; and two additional actuators are needed to control the system (one actuator is for rotation, one is for translation).
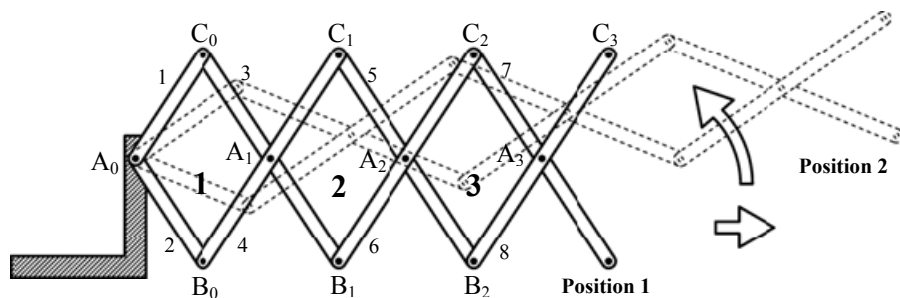
Figure 29. Mobility diagram of a common scissor-hinge structure

The system in Figure 29 has only one support at point A_0, and the other side is free. However, this study deals with the scissor-hinge structures is fixed to the both

29

edges. In Figure 30, an example curvilinear scissor-hinge structure can be seen. This structure has 21 joints, 14 links and 7 independent loops. 7th loop is the loop between two supports which closes the whole system. When the Freudenstein and Alizade formula is applied to the system;

$$M = 21 - 3 \times 7 = 0$$
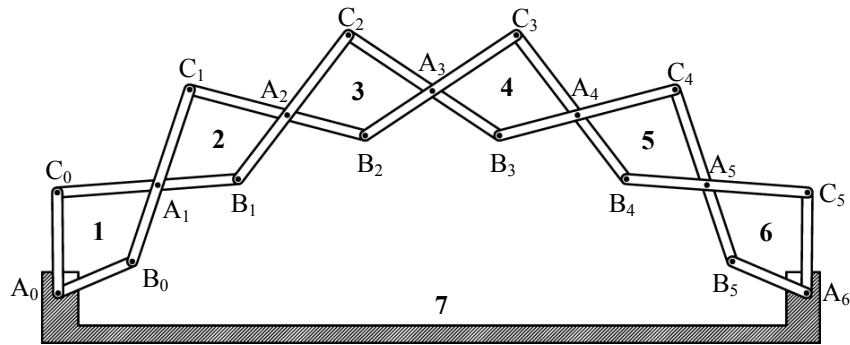
Figure 30. Mobility diagram of a scissor-hinge structure when it is fixed to the edges

M=0 means that the system is a rigid structure and do not need any additional elements to fix the system. Normally, scissor-hinge structures are all rigid bodies when they are fixed from two edges.

To show the application of the Alizade's formula to spatial structures, Felix Escrig's deployable vault is investigated. This structure is a very typical spatial scissor-hinge structure. In Figure 31, primary unit of this structure can be seen.

The unit in figure is a $\lambda=5$ mechanism. It has 12 joints, 10 elements and 3 loops (4th loop is dependent to the other 3 loops, so it is ignored). When the structure is investigated thoroughly, it can be seen that the gray branches are not necessary to constitute the same shape configuration, so these two branches are over constrained links.
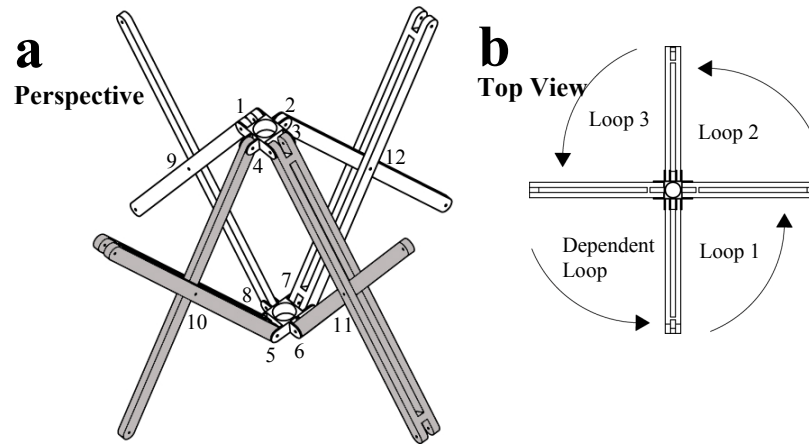
Figure 31. Basic spatial unit of Escrig's structure

According to Freudenstein and Alizade formula;

$$M = 12 - 3 \times 3 - 0 + 4 = 1$$

For all structural mechanisms derived from the multiplication of the aforementioned unit, mobility is always equal to one. In Figure 32, an example mechanism can be seen.
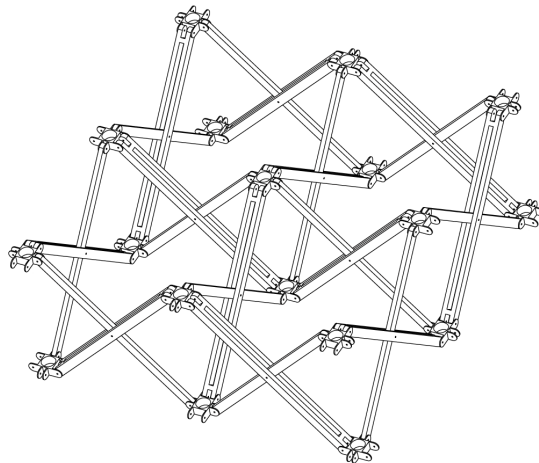
Figure 32. A 1-DoF spatial scissor-hinge structure

3.3. Position Analysis

Kinematic analysis deals with the derivation of relative motions among various links of a given manipulator (Tsai 1999). Thus, it is the study of motion characteristics in a known mechanism. One of the main principal goals of the kinematic analysis is to determine the location and rotations of the rigid bodies. Location of a rigid body (link) or a particle (point) in a rigid body with respect to a given reference frame is called as the *Position* of that point or body (Söylemez 1999).

Position of a mechanism can be analyzed by two different ways: Graphical method and algebraic method. Algebraic method includes trigonometric method, vector loop method, matrices method and etc. During this research study, graphical method is used in experimental works, and vector loop method for the programming.

3.3.1. Graphical Position Analysis

Graphical analysis method is introduced via two different examples: A typical four-bar mechanism and a scissor-hinge structure.

For a 1-DoF mechanism, such as a four-bar, only one parameter is needed to define the positions of all links graphically. This parameter can be chosen as the angle of the input link. There is an example four-bar mechanism in Figure 33. All link lengths (*a, b, c, d*) and input angle (θ_2) is known, and it is possible to define θ_3 and θ_4 according to the known parameters.

To find the unknowns, first, the ground link (1) and the input link (2) are drawn to a convenient scale such that they intersect at the origin O_2 of the global coordinate system with link 2 placed at the input angle θ_2. Link 1 is drawn along the *x* axis for convenience. The compass is set to the scaled length of link 3, and an arc of that radius swung about the end of link 2 (Point A). Then the compass is set to the scaled length of link 4, and a second arc swung about the end of link 1 (Point O_4). These two arcs have two intersections at B and B' that define the two solutions to the position problem for a four-bar mechanism which can be assembled in two configurations. Finally, θ_3 and θ_4 angles can be measured with a protractor (Norton 2004).
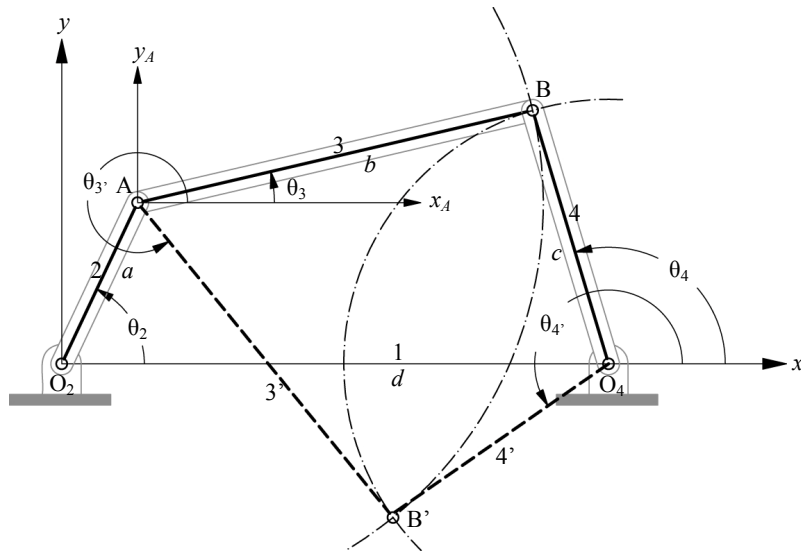
Figure 33. Graphical position analysis of the four-bar mechanism

Graphical position analysis of a scissor-hinge structural mechanism is very similar to the four-bar mechanism. There is an example in Figure 34. This mechanism is very similar to the mechanism in Figure 29, and its mobility is equal to two. This means that two parameters should be known to define the positions of all links. For this structure, these two parameters are the input angles (θ_1, θ_2). All link lengths (*a*, *b*) are known as well; so the problem is to define θ_3 and θ_4 angles, and position of A, B, C, D, E points.
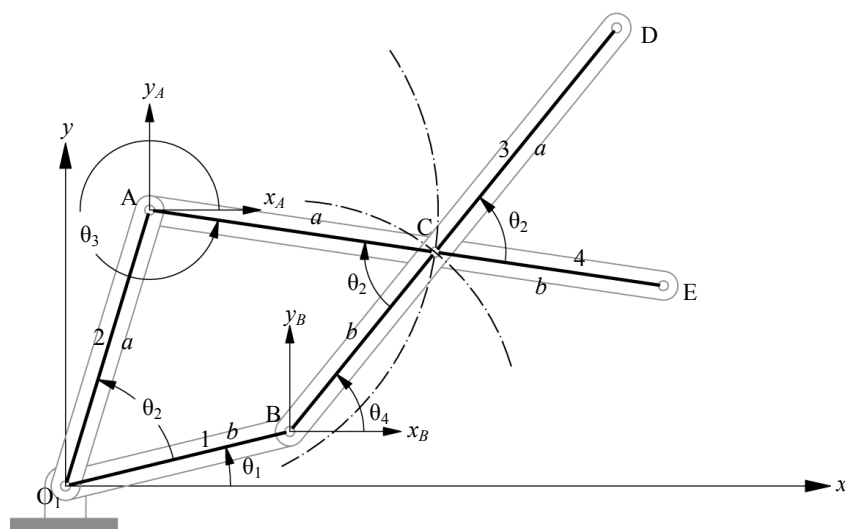
Figure 34. Graphical position analysis of the scissor-hinge structural mechanism

To find the unknowns, first, beginning point (O_1) of the mechanism is placed to the origin of the global coordinate system. Lengths of links and input angles are known, so by using a protractor, position of A and B points can be found. According to the point A, possible locations of the point C can be defined with a circle whose center is on the point A and the radius length is *a*. Similarly, this point can be defined according to the point B with a circle whose radius is *b*. Intersection point of these circles gives the exact location of Point C. Points B, C and D are collinear; and the distance between C and D is equal to *a*. Similarly, A, C and E are collinear and the distance between C and E is equal to *b*. From this information, exact locations of all points according to the defined two inputs can be found. Finally, θ_3 and θ_4 angles can be measured with a protractor.

3.3.2. Algebraic Position Analysis: Vector Loop Method

In order to understand the algebraic position analysis, first, representation of vectors should be understood. Vectors may be defined in *Polar Coordinates*, by their magnitude and angle, or in *Cartesian Coordinates* as x and y components. Examples to these representations can be seen as follows:

Polar Form	**Cartesian Form**	
$R @ \angle \theta$	$r \cos \theta\, \mathbf{i} + r \sin \theta\, \mathbf{j}$	(3.2)
$r\, e^{j\theta}$	$r \cos \theta + j\, r \sin \theta$	(3.3)

Equation 3.2 uses unit vectors to represent the x and y vector component directions in the Cartesian form (Figure 35a). Equation (3.3) uses complex number notation wherein the x direction component is called the *real portion* and the y direction is called the *imaginary portion* (Figure 35b). The term imaginary comes about because of the use of the notation j to represent the square root of minus one ($\sqrt{-1}$), which cannot be evaluated numerically. However, this imaginary number is used in a complex number as an operator, not as a value (Norton 2004).

Complex number in the equation (3.3) ($e^{j\theta}$) is known as Euler identity, and it is the exponential form of $\cos \theta + j \sin \theta$. The exponential form contains the polar parameters and the exponent $e^{j\theta}$ represents a unit vector along the direction of OA.
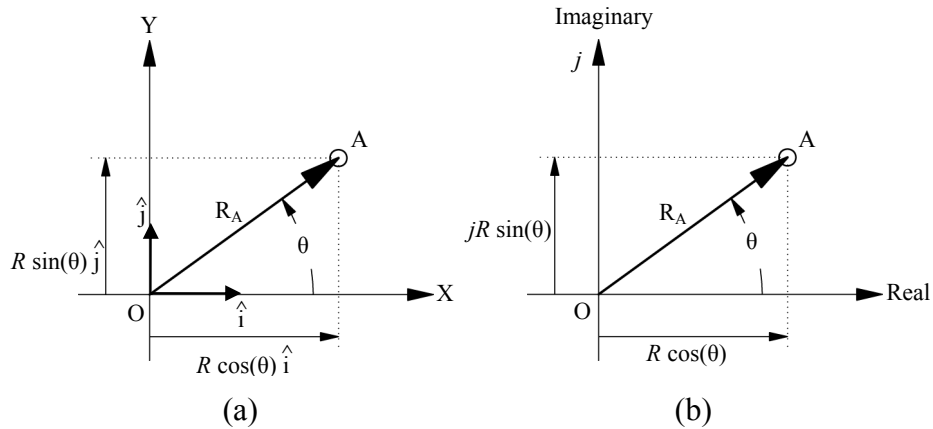
Figure 35. Unit vector representation (a) and complex number representation (b) for position vectors

Vector loop method which is first proposed by Raven (Raven 1958) is a common approach for position analysis. In this method, the links are presented as position vectors. Figure 36 shows the same fourbar mechanism as in Figure 33, but the links are now drawn as position vectors that form a vector loop. This loop closes on itself making the sum of the vectors around the loop zero (Söylemez 1999).
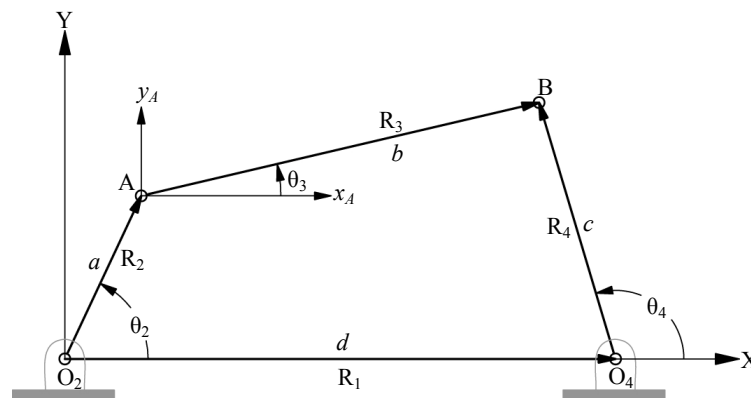
Figure 36. Position vector loop for a four-bar mechanism

According to the figure, it can be written as;

$$R_2+R_3-R_4-R_1=0 \tag{3.4}$$

Next, complex number notation should be substituted to each position vector.

$$a\, e^{j\theta_2} + be^{j\theta_3} - ce^{j\theta_4} - de^{j\theta_1} = 0 \tag{3.5}$$

When the Euler equivalents are substituted for the $e^{j\theta}$ terms, and then separate the resulting Cartesian form vector equation into two scalar equations which can be solved simultaneously for θ_3 and θ_4;

$$a\,(\cos\theta_2 + j\sin\theta_2) + b\,(\cos\theta_3 + j\sin\theta_3) - c\,(\cos\theta_4 + j\sin\theta_4) - d\,(\cos\theta_1 + j\sin\theta_1) = 0 \tag{3.6}$$

This equation can be separated into its real and imaginary parts and each set to zero. (In these e equations, it is known that $\theta_1 = 0$, so it is eliminated in both of the equations. In addition, j's can be divided out in the imaginary part);

$$a\,\cos\theta_2 + b\,\cos\theta_3 - c\,\cos\theta_4 - d = 0 \tag{3.7}$$

$$a\,\sin\theta_2 + b\,\sin\theta_3 - c\,\sin\theta_4 = 0 \tag{3.8}$$

The scalar equations can be solved simultaneously for θ_3 and θ_4. To solve this set of two trigonometric equations, first θ_3 isolated to find θ_4.

$$b\,\cos\theta_3 = -a\,\cos\theta_2 + c\,\cos\theta_4 + d \tag{3.9}$$

$$b\,\sin\theta_3 = -a\,\sin\theta_2 + c\,\sin\theta_4 \tag{3.10}$$

After square both sides and add them, θ_3 is eliminated and b can be found as;

$$b^2 = a^2 + c^2 + d^2 - 2ad\,\cos\theta_2 + 2cd\,\cos\theta_4 - 2ac\,(\sin\theta_2\,\sin\theta_4 + \cos\theta_2\,\cos\theta_4) \tag{3.11}$$

This equation can be simplified as follows;

$$K_1\,\cos\theta_4 - K_2\,\cos\theta_2 + K_3 = \cos(\theta_2 - \theta_4) \tag{3.12}$$

where;

$$K_1 = \frac{d}{a} \qquad K_2 = \frac{d}{c} \qquad K_3 = \frac{a^2 - b^2 + c^2 + d^2}{2ac}$$

Equation (3.12) is known as Freudenstein's equation. In order to reduce equation (3.12) to a more tractable form, $\sin\theta_4$ and $\cos\theta_4$ terms are converted to $\tan\theta_4$. It is known that;

$$\sin\theta_4 = \frac{2\tan\left(\frac{\theta_4}{2}\right)}{1+\tan^2\left(\frac{\theta_4}{2}\right)}; \qquad \cos\theta_4 = \frac{1-\tan^2\left(\frac{\theta_4}{2}\right)}{1+\tan^2\left(\frac{\theta_4}{2}\right)} \tag{3.13}$$

By using equation (3.12) and (3.13),

$$A\tan^2\left(\frac{\theta_4}{2}\right) + B\tan\left(\frac{\theta_4}{2}\right) + C = 0 \tag{3.14}$$

where;

$A = \cos\theta_2 - K_1 - K_2\cos\theta_2 + K_3$

$B = -2\sin\theta_2$

$C = K_1 - (K_2+1)\cos\theta_2 + K_3$

Finally, the solution for θ_4 can be found as;

$$\theta_{4_{1,2}} = 2\,\tan^{-1}\left(\frac{-B \pm \sqrt{B^2 - 4AC}}{2A}\right) \tag{3.15}$$

According to the equation (3.15), θ_4 can have two different solutions. However, one of these solutions is geometrically impossible. To test the validity of the solutions, they should be drawn and checked graphically.

The solution for θ_3 is essentially similar to that for θ_4. By returning to equation (3.7) and (3.8), θ_4 can be isolated on the left side.

$$c\cos\theta_4 = -a\cos\theta_2 + b\cos\theta_3 - d \tag{3.16}$$

$$c\sin\theta_4 = -a\sin\theta_2 + b\sin\theta_3 \tag{3.17}$$

Squaring and adding these equations eliminates θ_4. The resulting equation can be solved for θ_3 as was done above for θ_4, yielding this expression;

$$K_1 \cos\theta_3 + K_4 \cos\theta_2 + K_5 = \cos\theta_2 \cos\theta_3 + \sin\theta_2 \sin\theta_3 \qquad (3.18)$$

where;

$$K_1 = \frac{d}{a} \qquad\qquad K_4 = \frac{d}{b} \qquad\qquad K_5 = \frac{c^2 - d^2 + a^2 - b^2}{2ab}$$

This equation also reduces to a quadratic form;

$$D \tan^2\left(\frac{\theta_3}{2}\right) + E \tan\left(\frac{\theta_3}{2}\right) + F = 0 \qquad (3.19)$$

where;

$D = \cos\theta_2 - K_1 + K_4 \cos\theta_2 + K_5$

$E = -2 \sin\theta_2$

$F = K_1 + (K_4-1) \cos\theta_2 + K_5$

Finally, the solution for θ_3 can be found as;

$$\theta_{3_{1,2}} = 2\ \tan^{-1}\left(\frac{-E \pm \sqrt{E^2 - 4DF}}{2D}\right) \qquad (3.20)$$

In this dissertation, both of the graphic and algebraic position analysis methods are used. Graphical methods are used especially for experimental works and quick trials; but these trials are not represented in the dissertation. On the other hand, a computer program which is based on the vector loop method is used for the position analysis of the proposed scissor-hinge structural mechanism. This program and the analysis principles are thoroughly explained in Chapter 5.

CHAPTER 4

COMMON SCISSOR-HINGE STRUCTURES: TYPOLOGIES AND GEOMETRIC PRINCIPLES

In this chapter, typologies, main principles and geometric aspects of common deployable scissor-hinge structures are investigated. For this investigation, first, basic terms, concepts and conditions of the scissor-hinge structures are defined. Then, current scissor-hinge structures are investigated in two groups: Translational and curvilinear scissor-hinge structures. This investigation mainly encompasses the calculation methods for such kind of structures. In addition to the common methods, a new calculation method for the curvilinear scissor-hinge structures is presented in the text as well. These calculation methods are explained only for planar scissor-hinge structures, but they can be applied to the spatial modules as well.

4.1. Terms and Definitions

4.1.1. Scissor-Like Element (SLE)

To form a basic scissor-hinge unit, two bars are connected to each other at an intermediate point through a pivotal connection which allows them to rotate freely about an axis perpendicular to their common plane but restrains all other degrees of freedom (Figure 37). At the same time, end points of these bars are hinged to the next scissor units from their end points.
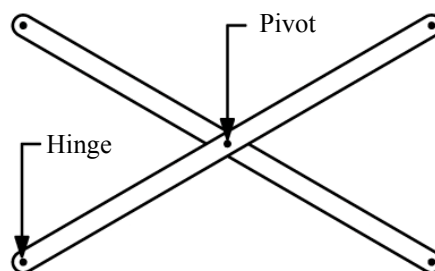
Figure 37. Scissor-like element (SLE)

Different researchers prefer to use different terms for this unit. Pinero calls it as "Pantograph" (Pinero 1961, 1962); Gantes as scissor-like element (SLE) (Gantes 1991, 2001) and some researchers as Pivot-hinge structure unit. In this dissertation, Gantes's terminology is used.

Geometry of a scissor-hinge structure is directly dependent to the geometry of SLE. According to the changes in dimensions of the lengths of bars or location of pivot point of SLE, whole systems shape is changed as well. To understand the logic of the scissor-hinge systems, first, simple shape conditions related to the lengths of bars should be understood.

4.1.2. General Deployability Condition

One of the most important requirements of the scissor-hinge structures is that the configuration is able to be stored in a compact shape. In Figure 38, there is a simple example of deployable scissor-hinge structure. At the compact configuration, all three SLEs in the figure should theoretically have one dimension and B_0, C_0, A_1, B_1, C_1, A_2, B_2, C_2, A_3, B_3, C_3 would be co-linear. When the cosine rule is applied to $A_1B_1C_1$ and $A_2B_1C_1$ triangles at contracted configuration;

$$a_2 + b_2 - 2a_2b_2 \cos 180 = a_3 + b_3 - 2a_3b_3 \cos 180$$

When this equation is generalized;

$$a_{i-1} + b_{i-1} = a_i + b_i \qquad\qquad (4.1)$$
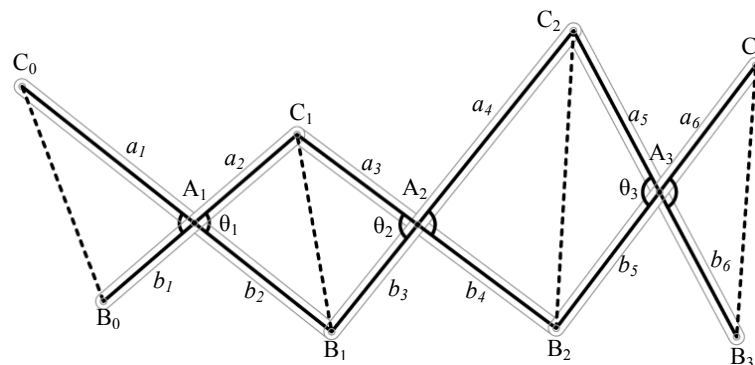
Figure 38. Deployability condition for scissor-hinge structures

Equation (4.1) is the basic deployability condition for all deployable scissor-hinge structures and derived by Felix Escrig. This equation uses purely geometric approach and ignores the effect of joint size. From a structural point of view, the equation imposes no limitations on members' sizes and materials and hence does not guarantee that stresses will be kept to an acceptable level during the deployment process (Rosenfeld, Ben-Ami and Logcher 1993). Moreover this equation cannot be applied to the angulated scissor-hinge structures such as Hoberman's structures (Hoberman 1993).

4.2. Typologies of Scissor-hinge Structures

4.2.1. Translational Scissor-hinge Structures

This type of scissor-hinge structures can only translate without any rotation. The main rule to meet this condition is that all axles which connect the hinges should be parallel to each other. According to their bar lengths and location of pivot points, there can be various types of translational scissor structures. Some of these types are investigated in this dissertation.

4.2.1.1. Translational Scissors with Constant Bar Length

When all bars have the same lengths (*2a*) and the pivots are located in the middle of the bars, system constitutes a perfect planar surface (Figure 39). This type of scissor structures is commonly used in daily life; but when it is used as an architectural structure, these are the variables to solve: Span of the whole system (*p*), span of one SLE unit (*s*), number of SLE units (N), angles between bars, depth of the whole beam (*2t*), the length of bars (*2a*) and the angle between bars (θ).
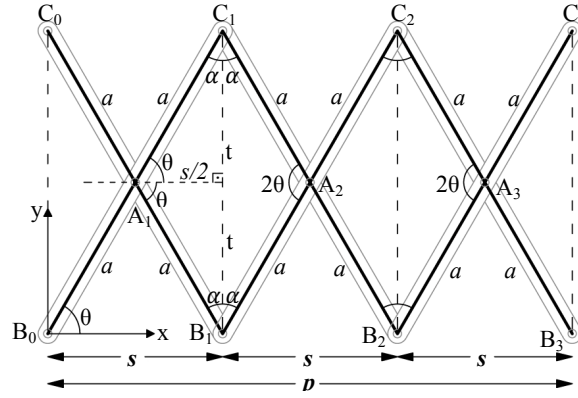
Figure 39. Geometry of translational scissor-hinge structure with constant bar lengths

System can be solved by the determination of at least three of the aforementioned variables. For these structures, the span of one SLE can be found according to the span of the whole system and the number of SLEs by the formula of:

$$s = \frac{p}{N} \qquad (4.2)$$

After finding s, it is possible to define the angles of one SLE. Basic geometry of one SLE for a linear extendable scissor-hinge system can be seen in Figure 39. A reference system is taken with its origin in point A.

According to the Figure 39, coordinates of the points can be found as follows:

$$\theta = \cos^{-1}\left(\frac{s}{2a}\right) \qquad (4.3)$$

$$x_{A_1} = \frac{s}{2} = a\cos\theta \qquad (4.4)$$

$$y_{A_1} = a\sin\theta \qquad (4.5)$$

$$x_{B_1} = x_{C_1} = 2a\cos\theta \qquad (4.6)$$

$$y_{B_1} = 0 \qquad (4.7)$$

$$y_{C_1} = 2a\sin\theta \qquad (4.8)$$

According to equations (4.3)-(4.8), span length of the whole system and the coordinates of the nth scissor unit can be found as:

$$p = \text{N } 2a \cos \theta \tag{4.9}$$

$$x_{C_n} = n \, 2a \cos \theta \tag{4.10}$$

$$y_{C_n} = y_{C_1} = 2a \sin \theta \tag{4.11}$$

4.2.1.2. Translational Scissors with Different Bar Lengths

For this type of scissor-hinge structures (Figure 40), $|C_0A_1| = |A_1B_1| = a_1$, $|C_1A_1| = |A_1B_0| = a_2$. Thus, it can be said that two bars which constitute the SLEs have different lengths, but pivots are located in the middle for both bars. System still translates and axles of the hinges are still parallel.

Variables of this condition are similar with the previous type: the span of the whole system (p), span of one SLE unit (s), number of SLE units (N), angles between bars, depth of the whole beam (h), the length of bars (a_1 and a_2) and the angle between bars (θ). Again, at least three of these variables should be known to solve the system.
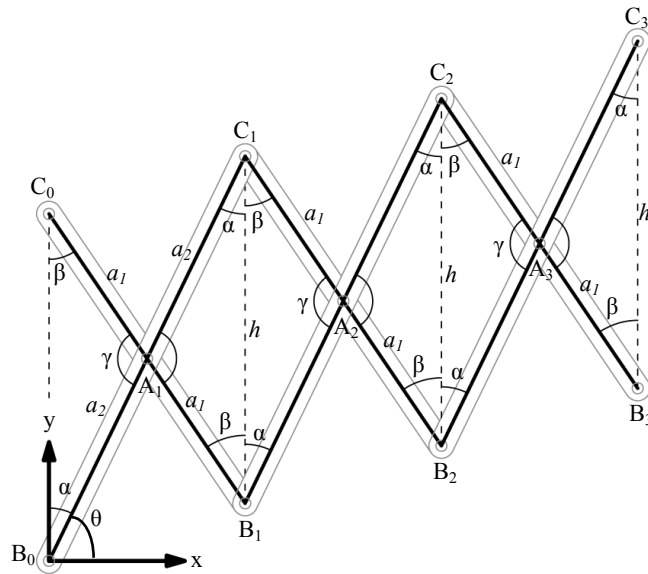
Figure 40. Geometry of translational scissor-hinge structure with different bar lengths

Coordinates of C_1 and B_1 can be found as;

$$x_{B_1} = x_{C_1} = 2a_2 \cos \theta = 2a_1 \sin \beta \qquad (4.12)$$

$$y_{C_1} = 2a_2 \sin \theta \qquad (4.13)$$

$$y_{B_1} = 2a_2 \sin \theta - h \qquad (4.14)$$

When the formulas are generalized for the nth point;

$$x_{C_n} = x_{B_n} = n(2a_2 \cos \theta) \qquad (4.15)$$

$$y_{C_n} = h + n\big((2a_2 \sin \theta) - h\big) \qquad (4.16)$$

$$y_n = n\big((2a_2 \sin \theta) - h\big) \qquad (4.17)$$

4.2.1.3. Translational Scissors with Arbitrary Geometry

Last option for translational scissor-hinge structures can be seen in Figure 41. In this example, all struts have different dimensions and pivot points are located randomly. However, as long as the system keeps its parallelism between hinge points, it can translate without rotation.
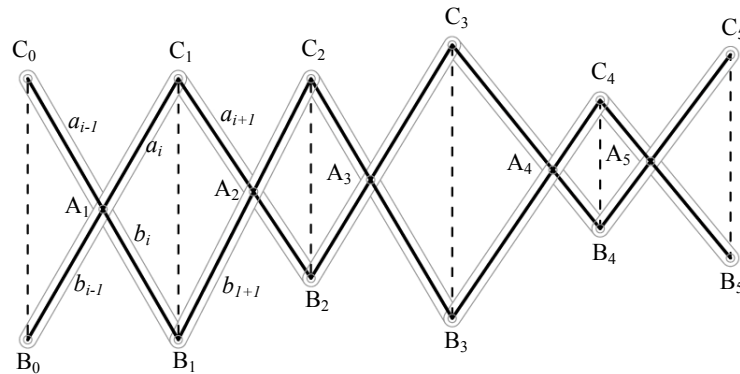
Figure 41. Translational scissor-hinge structure with arbitrary geometry

4.3. Curvilinear Scissor-hinge Structures

Curvilinear Scissor-hinge structures can have two shape alternatives. In first alternative, the structure expands as a circular system with one center point. In second alternative, the structure has an arbitrary curvilinear shape.

4.3.1. Curvilinear Scissors with one Center

As the main properties of this kind of scissor-hinge structures (Figure 42), they deploy and contract as a part of a single arc; and all axles between hinges meet in one point. These conditions can be possible when;

$$\frac{a_{i-1}}{b_{i-1}} = \frac{a_i}{b_i} = \frac{a_{i+1}}{b_{i+1}} = \text{constant} \tag{4.18}$$
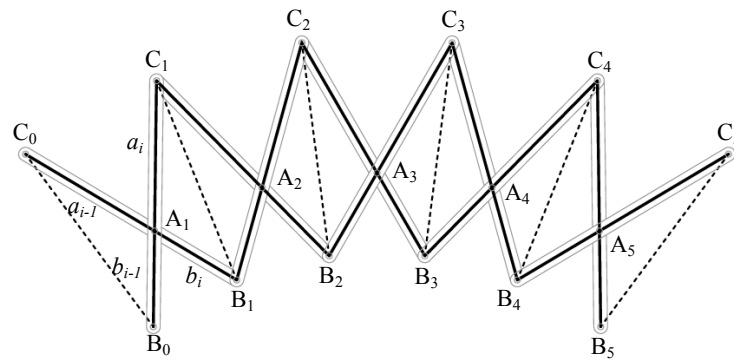
Figure 42. Curvilinear scissor-hinge structure with one center

For constituting a circular structure with constant bar lengths and constant pivot points, the equation (4.18) can be deviated as $a_{i-1} = a_i$, $b_{i-1} = b_i$

According to this data, a typical SLE for constituting a circular condition can be analyzed. Zanardo (1986) has explained the SLE for a circular shape condition as like in Figure 43. For the structure in the figure, it can be said that;

$$|C_0A_1|=|C_1A_1|= a \text{ and } |B_0A_1| = |A_1B_1|= b \qquad (4.19)$$

$$|C_0H|=|H\,C_1|= a\,\sin\theta=p\,\sin\varphi \qquad (4.20)$$

$$|B_0K|=|KB_1|=b\,\sin\vartheta \qquad (4.21)$$

$$|A_1H|=a\,\cos\vartheta \qquad (4.22)$$

$$|A_1K|=b\,\cos\vartheta \qquad (4.23)$$
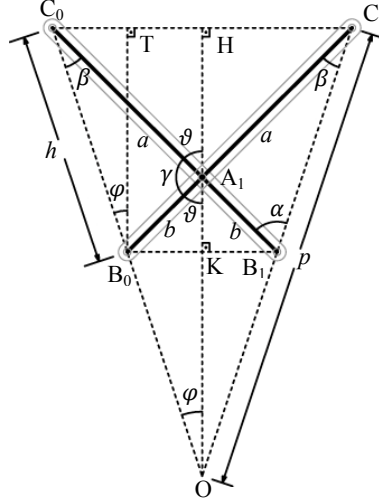
Figure 43. Geometric properties of an SLE for circular scissor-hinge structures

According to the (C_0TB_0) triangle, it is known that;

$$\tan\varphi = \frac{a\sin\vartheta - b\sin\vartheta}{a\cos\vartheta + b\cos\vartheta} \qquad (4.24)$$

When an "n" is defined as;

$$n = \frac{a}{b} \qquad (4.25)$$

Then, equation (4.24) and (4.25) can be joined as;

$$\varphi = \tan^{-1}\left(\left(\frac{n-1}{n+1}\right)\tan\vartheta\right) \qquad (4.26)$$

$$\vartheta = \tan^{-1}\left(\left(\frac{n+1}{n-1}\right)\tan\varphi\right) \qquad (4.27)$$

According to the equation (4.20) and cosines theorem onto the $(C_0A_1B_0)$ triangle;

$$p = \frac{a \sin \vartheta}{\sin \varphi} \tag{4.28}$$

$$h = \sqrt{(a^2 + b^2 - 2ab \cos \gamma)} \tag{4.29}$$

By using the main principles of the previous trigonometric methods, a new deductive calculation method has been developed for the scissor-hinge structures with fixed span. In this method, only the span length (S), the height (h) and the dimension of one bar (b or a) are enough to find the number of SLEs (N), other length of SLE (a or b), (φ) and (ϑ) angles (Figure 44).
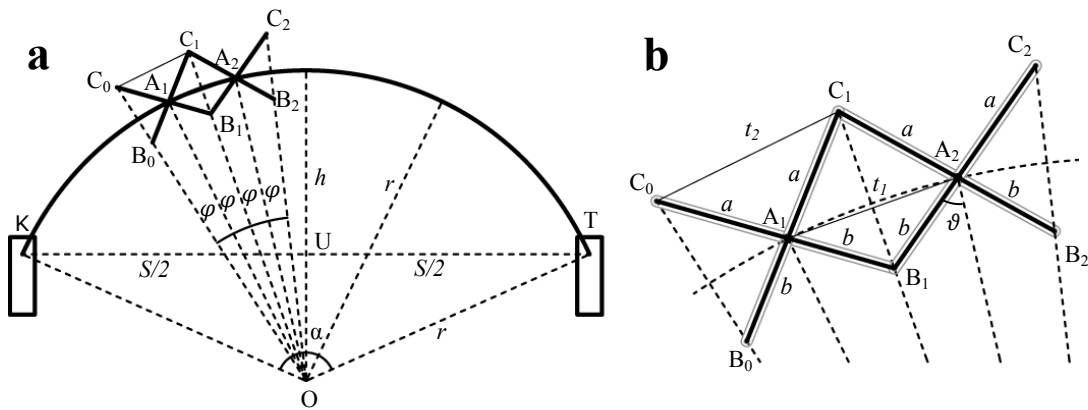
Figure 44. Placement of the variables onto a circular scissor-hinge structure

In this method, firstly, radius of the roof (r) and (α) angle should be found according to the S and h. According to the UOT triangle and chords formula for circles;

$$r = \frac{4h^2 + S^2}{8h} \tag{4.30}$$

$$\alpha = 2 \sin^{-1} \left(\frac{S}{2r}\right) \tag{4.31}$$

$$t_1 = 2r \sin \varphi \tag{4.32}$$

According to Figure 44b, $|A_1B_1|+|B_1A_2|$ should be bigger than t_1, thus;

$$2b \geq t_1 \qquad (4.33)$$

According to the α and φ angles and number of SLEs (N);

$$\varphi = \frac{\alpha}{2(N-1)} \qquad (4.34)$$

By penetrating equations (4.32), (4.33) to the (4.34);

$$b \geq \frac{S}{2 \sin\frac{\alpha}{2}} \sin\left(\frac{\alpha}{2N-2}\right) \qquad (4.35)$$

According to (4.35), it can be written as;

$$N \geq \frac{\alpha}{2 \sin^{-1}\left[\frac{(2b) \sin\left(\frac{\alpha}{2}\right)}{S}\right]} + 2 \qquad (4.36)$$

According to the equation (4.24) (ϑ) angle can be found as;

$$\vartheta = \tan^{-1}\left[\frac{\tan\varphi(a+b)}{a-b}\right] \qquad (4.37)$$

These trigonometric equations are not enough to find (a) and angle (θ), so an analytical geometry based method is needed to define these variables (Figure 45).
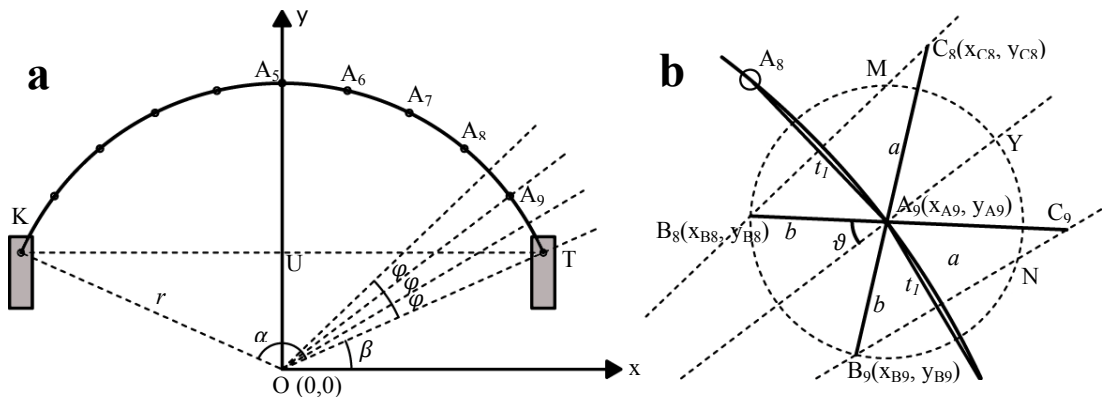
Figure 45. Second step for the calculation of a circular scissor-hinge structure

Coordinates of pivot points (A_9) and (T) are $A_9[r\cos(\beta + 2\varphi)\,;\, r\sin(\beta + 2\varphi)]$, $T[r\cos(\beta)\,;\, r\sin(\beta)]$. When the lines between pivot points (such as $|A_9T|$ and $|A_9A_8|$) are drawn, and connect the middle points of these lines to the centre point ($|MO|$ and $|NO|$), the space which one SLE covers can be defined. Functions of these lines can be written as follows;

$$\text{for } |OT|;\ y = \tan(\beta)\,x \tag{4.38}$$

$$\text{for } |OM|;\ y = \tan(\beta + 2\varphi)\,x \tag{4.39}$$

$$\text{for } |ON|;\ y = \tan(\beta + \varphi)\,x \tag{4.40}$$

It is known that (C_8) and (B_8) points are somewhere on $|MO|$ line; and (C_9) and (B_9) points on $|NO|$ line. Moreover, both of $|C_8B_9|$ and $|C_9B_8|$ lines pass through pivot point A_9. From this information, location of (B_9) and (B_8) points can be found by drawing a circle whose center point is on (A_9) and the radius is b. A circle can be defined as;

$$(x - a)^2 + (y - b)^2 = r^2 \tag{4.41}$$

When this function is applied to the circle whose center is (A_9) and radius is b;

$$\left[x_{B_9} - r\cos(\beta + 2\varphi)\right]^2 + \left[y_{B_9} - r\sin(\beta + 2\varphi)\right]^2 = b^2 \tag{4.42}$$

When this circle is intersected with the line $|ON|$ in equation (4.40);

$$\left[x_{B_9} - r\cos(\beta + 2\varphi)\right]^2 + \left[\tan(\beta + \varphi)x_{B_9} - r\sin(\beta + 2\varphi)\right]^2 = b^2 \tag{4.43}$$

When this non-linear equation is solved, two solutions can be found as:

$$x_{B_9 1,2} = \frac{r}{2}[\cos(\beta) + \cos(\beta + 2\varphi)] \pm \frac{\cos(2\beta + 2\varphi) + 1}{2}\left[\left(\frac{-r^2 + r^2\cos(2\varphi) + 2b^2}{\sqrt{\cos(2\beta + 2\varphi) + 1}}\right)\right] \tag{4.44}$$

Two solutions show that this circle has two intersections with (MO) and (NO) lines. The intersection points which are nearer to the center point must be defined as $B_8[x_{B8};\ y_{B8}]$ and $B_9[x_{B9};\ y_{B9}]$. By drawing a straight line from (B_9) to (A_9), the

intersection point of this line to the |MO| line can be defined as the point (C_8). The function of |MO| is known as in equation (4.41) and the function of $|B_9A_9|$ can be written as:

$$\left[\frac{y_{A_9}-y_{B_9}}{x_{A_9}-x_{B_9}}\right] x + \frac{x_{A_9}y_{B_9}-x_{B_9}y_{A_9}}{x_{A_9}-x_{B_9}} = y \tag{4.45}$$

where the coordinates of A_9 and B_9 are A_9 [r cos(β+2φ); r sin(β+2φ)] and $B_9[x_{B9} ; y_{B9}]$. When $|B_9A_9|$ and |MO| lines are intersected:

$$x_{B_8} = \frac{(-x_{A_9}y_{C_9}+x_{C_9}Y_{A_9})}{y_{A_9}-y_{C_9}-\tan(\beta+2\varphi)x_{A_9}+\tan(\beta+2\varphi)x_{C_9}} \tag{4.46}$$

$$y_{B_8} = \tan(\beta + 2\varphi)\, x_{B_8} \tag{4.47}$$

Similarly, when a line through $|B_8A_9|$ is drawn, the intersection point of this line with |NO| is point (C_9). Finally, when the SLE is drawn, the angle (θ) and the length (a) can be easily found from the above mentioned equations:

$$a = \sqrt{\left(x_{B_8} - x_{A_9}\right)^2 + \left(y_{B_8} - y_{A_9}\right)^2} \tag{4.48}$$

4.3.2. Curvilinear Scissors with Arbitrary Geometry

Scissor-hinge structures with this geometry are generated arbitrarily according to the dimensions of individual SLEs. There is no definite center point and relation between the SLEs. It can be said that:

$$\frac{a_{i-1}}{b_{i-1}} \neq \frac{a_i}{b_i} \neq \frac{a_{i+1}}{b_{i+1}} \neq \cdots \tag{4.49}$$

Only deployability condition (4.1) is valid for these structures. Arbitrary scissor-hinge structures (Figure 46) have different bar lengths and different angles between bars; this means lots of different unknowns to solve. Therefore, it is difficult to generalize solutions and rules for arbitrary systems.
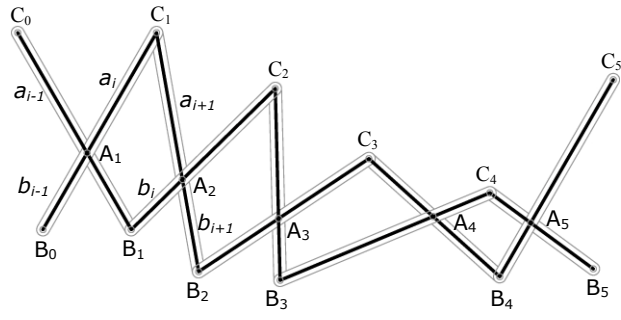
Figure 46. Curvilinear scissor-hinge structure with arbitrary geometry

CHAPTER 5

PROPOSED PLANAR SCISSOR-HINGE STRUCTURE: PRINCIPLES, ANALYSIS AND USE

Main objective of this research is to provide novel methods and techniques for the design of roof systems which are capable to transform from various curvilinear geometries to double curved shapes. In order to achieve this research objective, as a first step, the study has proposed a planar scissor-hinge structure which can achieve various curvilinear shape alternatives. This chapter presents this novel planar scissor-hinge structure: main differences from common scissor-hinge structures, primary elements (SLEs, M-SLEs and the actuators), transformation capabilities, kinematic and static analysis, and prospective uses of the proposed planar structure.

5.1. Main Properties of the Proposed Planar Scissor-hinge Structure

For comprehending the proposed scissor system framework, it is critical to examine the major differences to a common scissor structure.

As it is explained in Chapter 4, common planar scissor-hinge structures are generally fixed only from one side; and the other side is usually unfixed. In addition, both sides can be unfixed during the deployment. However the proposed planar scissor-hinge structures in this study are always fixed from the both sides either to the ground or to the appropriate surfaces of a building. This approach expects to provide increased deployability with the flexibility in form.

Second, the proposed system framework is capable to constitute various curvilinear forms without changing the span length. In order to achieve these transformations and form alternatives, Modified Scissor-like Element (M-SLE) is developed and utilized as the prototypical solution. By using this system component, various shape alternatives can be obtained without changing the span length.

Consequently, the proposed structure is based on curvilinear scissor-hinge structures and all SLEs are identical for the facilitation of the calculations and optimization of the structural lengths.

In Figure 47, schematic view of a proposed planar structure instance is given. In this figure, components of the structure, M-SLEs, SLEs and actuators can be seen.
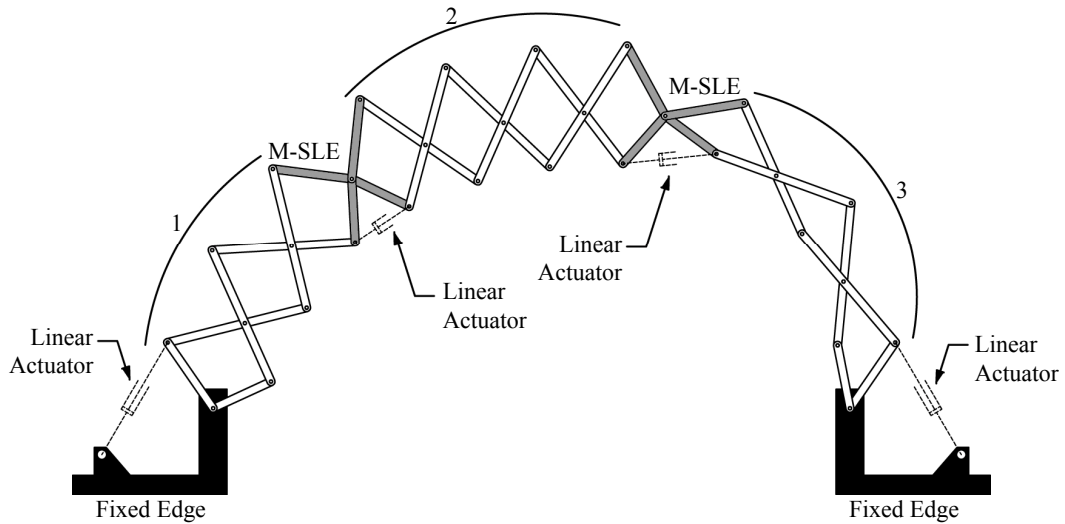
Figure 47. Proposed planar scissor-hinge and its elements

The structure in Figure 47 has nine identical SLEs, two identical M-SLEs and four actuators; but the proposed structure is flexible to incorporate different numbers of these components. Differences of the systems with various numbers of M-SLEs and SLEs are investigated in the following sections. At this step, in order to understand the structure better; first, M-SLE should be described.

5.2. Modified-SLE (M-SLE): Principles and Typologies

The core idea of the proposed scissor-hinge structure is the M-SLE. The difference of an M-SLE to a normal SLE is the additional revolute joints on various locations of the bars. These revolute joints increase not only the degree of freedom (DoF) of the unit; but also the transformation capacity of the whole system. In Figure

48, three different variations of M-SLE are illustrated. In Figure 48a, these additional revolute joints are located on the point B; in Figure 48b, on the points D' and E', and in Figure 48c, on the points D and E.

All scissor-hinge structures between two M-SLEs or between one M-SLE and a support point behave consistently. This means that, when one of these SLEs moves, all other SLEs follow this movement. However, in the proposed structure, M-SLEs divide the whole system into sub-structures, acting as "isolators" of these sub-structures, so that each sub-structure can transform without directly affecting the other sub-structures. For example, in the system of Figure 47, there are two M-SLEs, dividing the whole structure into three "isolated" parts. Thus, movement of one SLE in any group is followed only by the SLEs in this group, not by the others. This independency of the sub-groups creates the desired additional geometric mobility.
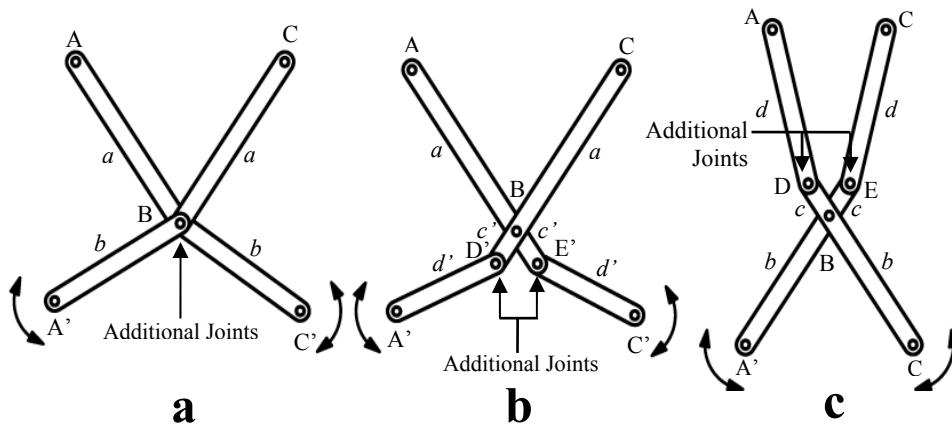
Figure 48. Variations of M-SLEs

5.3. Transformation Ability of the Proposed Planar Scissor-hinge Structure

The transformation ability of the proposed scissor-hinge structure is related to three factors: First, the number of M-SLEs in the system; second, the dimensions of the SLEs and M-SLEs; third, the support points. In this section these three factors are thoroughly elaborated.

5.3.1. Transformation Ability according to the Number of M-SLEs

For the proposed structure, the number of the M-SLEs is the most important factor that affects its transformation capacity. This factor can be explained with an example. All SLEs and M-SLEs in Figure 49a and Figure 49b have the same dimensional properties. The only difference is that the structure in Figure 49a has one M-SLE, while the structure in Figure 49b has two. Due to this difference, the number of the independent sub-structures changes from two to three; and this affects the transformation capability of the system. When the curves passing through the pivot points are investigated, the shape difference between the two examples can be observed.

The increase in the number of M-SLEs enhances the transformation capacity and flexibility, but also leads to an increase of the required number of actuators. Besides, in the experimental studies, it was seen that the use of three or more M-SLEs complicates the control and transformation of the system. For this reason, minimum number of M-SLEs must be used for achieving the desired forms; and in the examples presented hereafter, one and two M-SLEs are used.
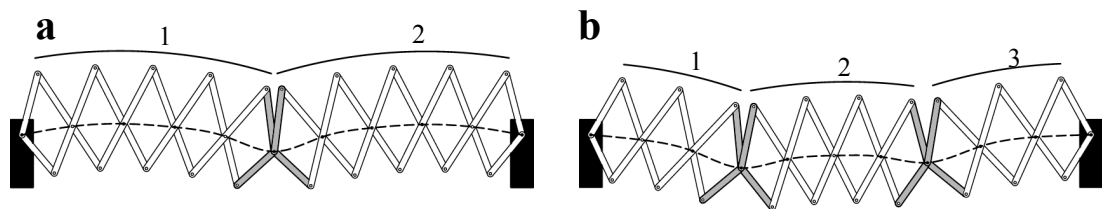
Figure 49. Proposed planar structures with one and two M-SLEs

5.3.2. Transformation Ability according to the Dimensions of M-SLEs

There are two options for the dimensions of M-SLEs. In the first one, M-SLEs have the same dimensions as the other SLEs in the system and all axes connecting hinge points intersect at one point (Figure 50a). In this situation, the structure can constitute an arc. In the second option, M-SLEs are dimensionally different from other SLEs

(*c≠b*). Then, the axes of the three independent substructures intersect at three different points, and the system can never constitute an arc or a circular arch (Figure 50b).
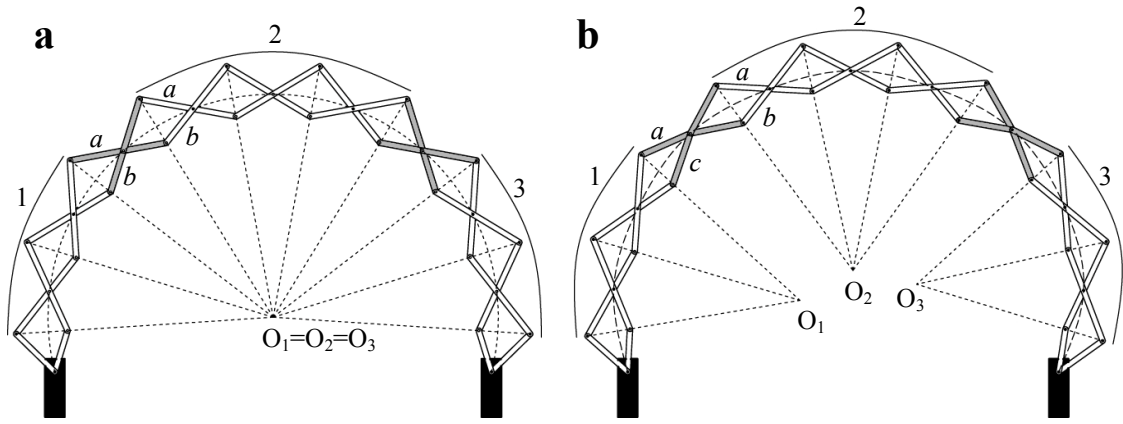
Figure 50. Situations according to the intersection of the axles

Both of the systems in Figure 50 are able to achieve similar form transformations. However, the structure in Figure 50a is more feasible than the structure in Figure 50b. This is an immediate result of the geometrical layout of the system. In a case where all the axles intersect in one point, the structure can be calculated like a typical scissor-hinge system without any M-SLEs as elaborated in Chapter 4. This provides more simplicity in the calculation of structural loads and system integrity. On top of this, standard and modular use of structural components is a major advantage for feasibility.

Because of the aforementioned advantages, the geometric layout of the M-SLEs in this study has always met the condition in Figure 50a as all axles intersecting at a common point. This condition can be met with three different kinds of M-SLEs. These conditions are illustrated in Figure 51. In these examples it is given that *d+c=a*, *d'+c'=b*.

Experimental and theoretical inquiries are conducted in order to determine the feasibility of the various layout alternatives. Preliminary results indicate that all of the given three alternatives are capable of achieving similar form transformations; but they have minor differences. For example, the condition in Figure 51a can be easily got knotted during the transformation process. In addition, the given systems in Figure 51a

and Figure 51b have more system constraints such as *c*, *c'*, *d*, *d'* compare to the system in Figure 51c. This makes the calculation harder in terms of the locations of all joint points. In addition, less number of knots decreases the number of critical points that are exposed to the shear forces.

According to these findings, it is understood that the most feasible M-SLE alternative is the unit in Figure 51c; and the geometric layout of the M-SLEs in this figure is benefited during the study.
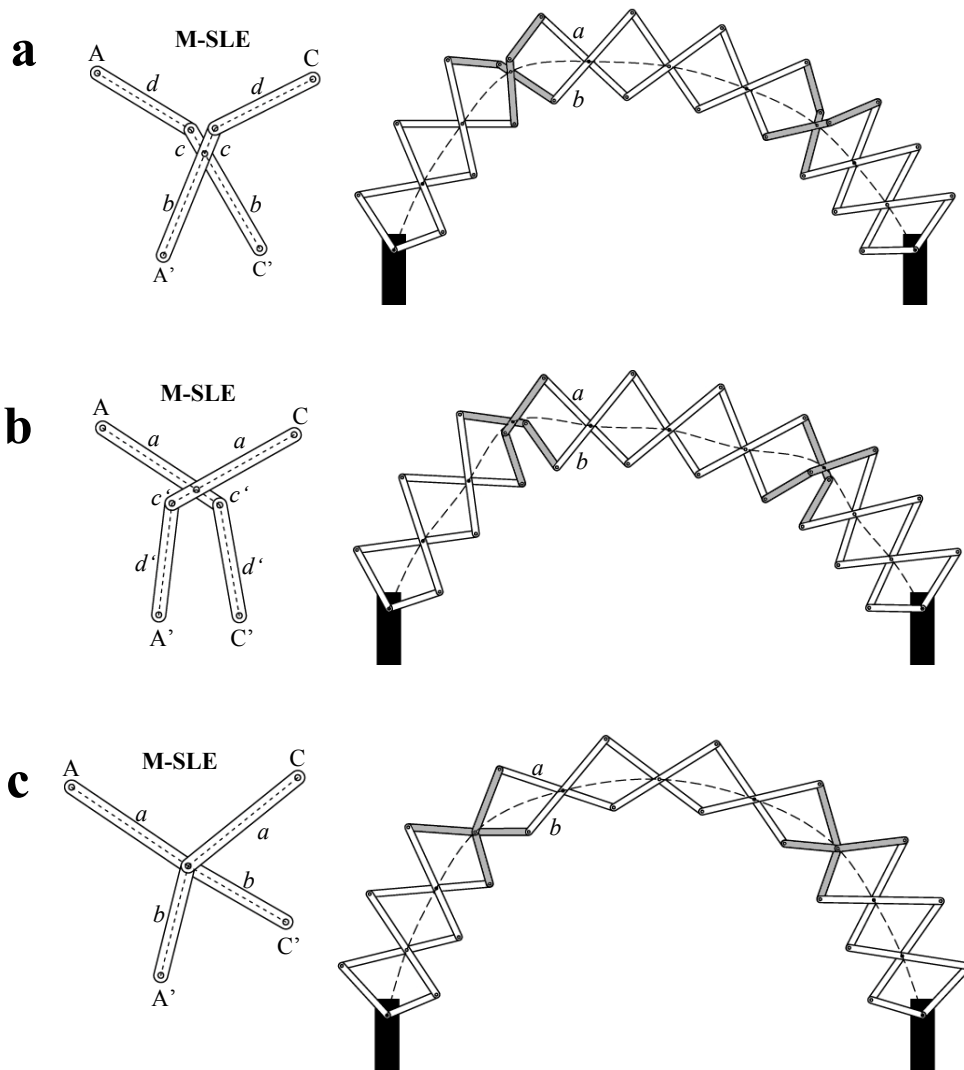
Figure 51. Situations according to the dimensions of M-SLEs

5.3.3. Transformation Ability according to the Support Points

The transformation capability of the proposed structure as well as their overall behavior can also change according to the support points. In Figure 52 two alternatives are offered. The system in Figure 52a is supported on the ground at a hinge. This causes large shear forces occur on the corresponding bottom bars on each side. The system in Figure 52b is supported on the ground at a pivot, thus avoiding the previous disadvantage. This is why structures that connect to the ground at pivot points are used in this study.
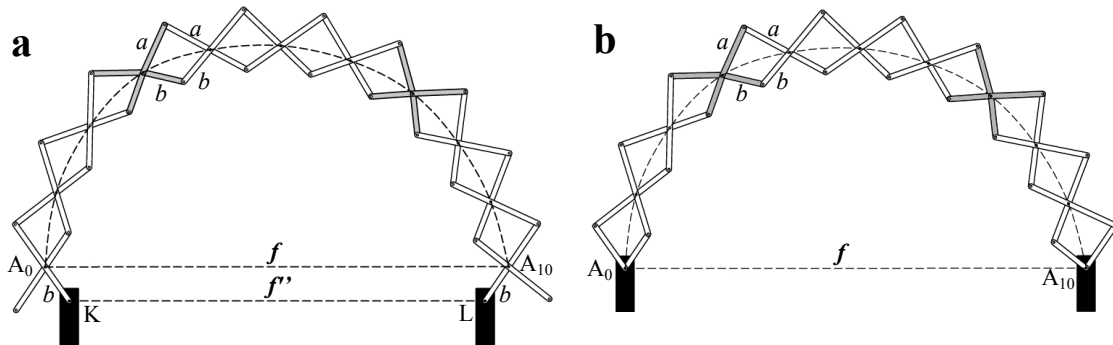
Figure 52. Situations according to fixing points

5.4. Kinematic Analysis of the Proposed Planar Scissor-hinge Structure

Transformation capability of the planar scissor-hinge structure changes according to the dimensions and the number of M-SLEs. However, the most feasible solutions are got with the M-SLE in Figure 48a; and the structures whose mobility is equal to two or four. Because of this reason, M=2 and M=4 versions of the proposed planar structure are investigated in this section. The purpose of this investigation is to establish a methodology for finding the possible shape configurations and capabilities of the proposed planar structure with M=2 and M=4 conditions.

For this analysis, first SLE, the primary unit of the mechanism, is investigated.

5.4.1. Kinematic Analysis of a Single SLE

The shape limitations of one SLE directly affect the kinematics of the whole system, so that geometric analysis of a single element should be performed first. In Figure 53, two successive identical SLEs can be seen. From experimental studies on physical models, it was observed that when θ_1' angle becomes smaller than 180°, the whole system becomes unstable. Thus, this angle must be larger than 180° for all SLE pairs. It is then possible to calculate the upper and lower bounds of (γ_1) and (α_1) angles.

$$180° > \theta_1 \geq 0 \tag{5.1}$$

$$180° \geq \alpha_1 > \cos^{-1}\left(\frac{b}{a}\right) \tag{5.2}$$

$$0° \leq \frac{\gamma_1}{2} \leq \sin^{-1}\left(\frac{b}{a}\right) \tag{5.3}$$
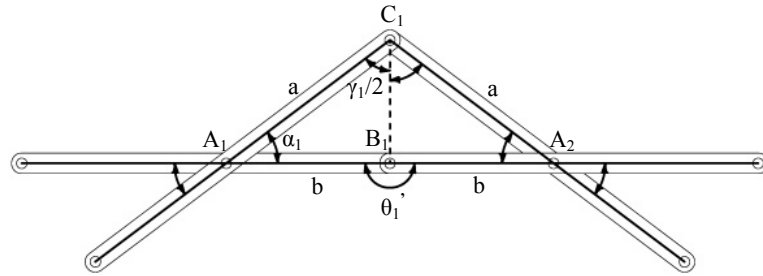
Figure 53. Definition of angles for a single SLE

5.4.2. Kinematic Analysis of M=2 Condition

In order to understand the transformation capability of a mechanism, kinematic analysis of that mechanism should be made. At kinematic analysis, the mechanism is investigated as a whole. Geometric relations of the elements and shape limitations of that mechanism are found by several methods. In this section, kinematic analysis of the proposed planar structure are made both for M=2 and M=4 conditions.

In Figure 54, a proposed planar scissor-hinge structure with M=2 condition is depicted. In this structure, all SLEs are identical, and there is only one M-SLE, which is

located in the middle of the whole structure. This means, M-SLE divides the structure into two symmetrical modules (this symmetry is not obligatory).

When every module has n number of SLEs, this means, it has also $2n$ bars and $3n-2$ revolute joints. Thus, the whole structure has $4n+1$ bars and $2(3n-2)+3=6n-1$ revolute joints. When the Figure 54 is investigated, it can be seen that $n=6$, number of bars is 25 (25th bar is the fixed ground line which connects points A_0 and A_{10}), number of revolute joints is 35 (there are two joints on points A_0 and A_{10}, three joints on A_5) and number of loops is 11 (11th loop connects points A_0 and A_{10}).

According to Alizade-Freudenstein formula which was described in (3.1);

$$M = 35 - 3 \times 11 = 2$$
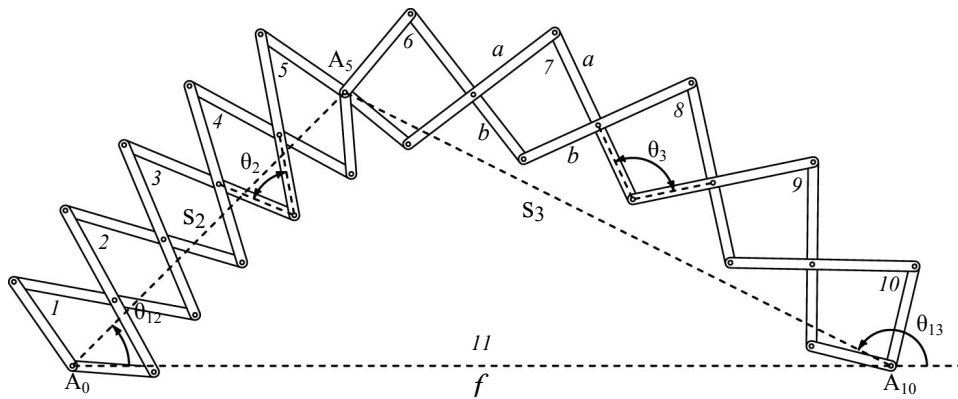
Figure 54. Proposed planar scissor structure with M=2 condition

When the structure in Figure 54 is investigated, it is seen that the structure can be abstracted as a triangle by using f as the constant element, and s_2 and s_3 as the variables. Thus, the kinematic of this structure is the same with a structure which has 5 bars, 3 revolute joints, 2 prismatic joints (f, s_2 and s_3 are connected with 3 revolute joints and each of s_2 and s_3 is divided into 2 by a prismatic joint). The kinematic analysis of this structure can be made according to this triangular mechanism.

For an M=1 module with 2n bars, determination of the position A_k and the distance s_k (k=2, 3...) is possible by using the angles between two connected bars (α_k or θ_k) as the input parameter. For the structure in Figure 54, input parameters are θ_2 and θ_3,

and α_k, β_k and r_k variables which were determined in Figure 55 should be known (All deltoids in the system are identical, so all θ_k, α_k, β_k and r_k values are equal).
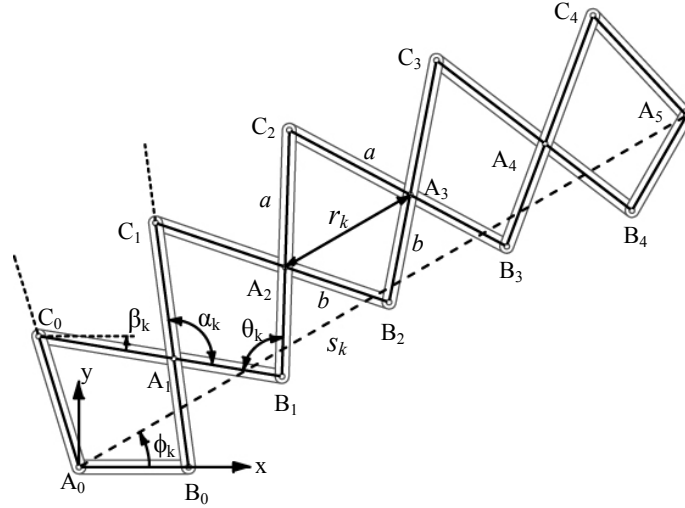
Figure 55. Variable parameters in one module of a proposed scissor-hinge structure

When the law of cosines is applied to $A_2B_2A_3$ triangle;

$$r_k = b\sqrt{2 - 2\cos\theta_k} \tag{5.4}$$

From the symmetry of the deltoid (from the $A_2B_2A_3$ and $A_2C_2A_3$ triangles);

$$\alpha_k = \cos^{-1}\left(\frac{\frac{r_k}{2}}{b}\right) + \cos^{-1}\left(\frac{\frac{r_k}{2}}{a}\right) \tag{5.5}$$

$$\beta_k = \alpha_k + \pi + (-2\alpha_k - \theta_k) = \pi - \alpha_k - \theta_k \tag{5.6}$$

When a scissor module with *n* deltoids is aligned to the *x* and *y* coordinate system as it is seen in Figure 55, A_0 locates on the center of coordinate system; and k^{th} deltoid can be defined with the vectors as follows (Euler equation is used to define vectors):

$$\overrightarrow{A_0 A_{m+1}} = \overrightarrow{A_0 A_m} + r_k e^{i\left(\pi/2 - \theta_k/2 - m\beta_k\right)} \tag{5.7}$$

$$\overrightarrow{A_0 B_m} = \overrightarrow{A_0 A_m} + b e^{-im\beta_k} \tag{5.8}$$

$$\overrightarrow{A_0 C_m} = \overrightarrow{A_0 A_m} + a e^{i(\alpha_k - m\beta_k)}, \ (m=0, \dots, n\text{-}1) \tag{5.9}$$

When the following equations are investigated, it is seen that every deltoid rotates as β_k, according to the previous deltoid. From this information;

$$s_k = \left|\overrightarrow{A_0 A_n}\right| \text{ and } \varphi_k = \angle \overrightarrow{A_0 A_n} \tag{5.10}$$

According to the application of cosines theorem on s_2 and s_3 variables;

$$\theta_{12} = \cos^{-1}\left(\frac{f^2 + s_2{}^2 - s_3{}^2}{2fs_2}\right) \tag{5.11}$$

$$\theta_{13} = \pi - \cos^{-1}\left(\frac{f^2 + s_3{}^2 - s_2{}^2}{2fs_3}\right) \tag{5.12}$$

This kinematic analysis method was tested in Microsoft Excel 2007® Medium. This method is efficient to see the final shape according to the inputs. The algorithm of this Microsoft Excel program is based on the kinematic analysis which is described above. In this program, the span of the whole structure, dimension of the elements and the angles between the elements (θ_2, θ_3) are the input variables. By a spin button, users can vary θ angles between 0 and 180; and according to the changes on these input variables, the graphic interface can update itself simultaneously Also, the system gives error for unavailable shapes or inconsistent input configurations. Thus, if the algorithm fails for an input configuration, it can be understood that this shape is unavailable for those inputs. The interface of this program is given in Figure 56.
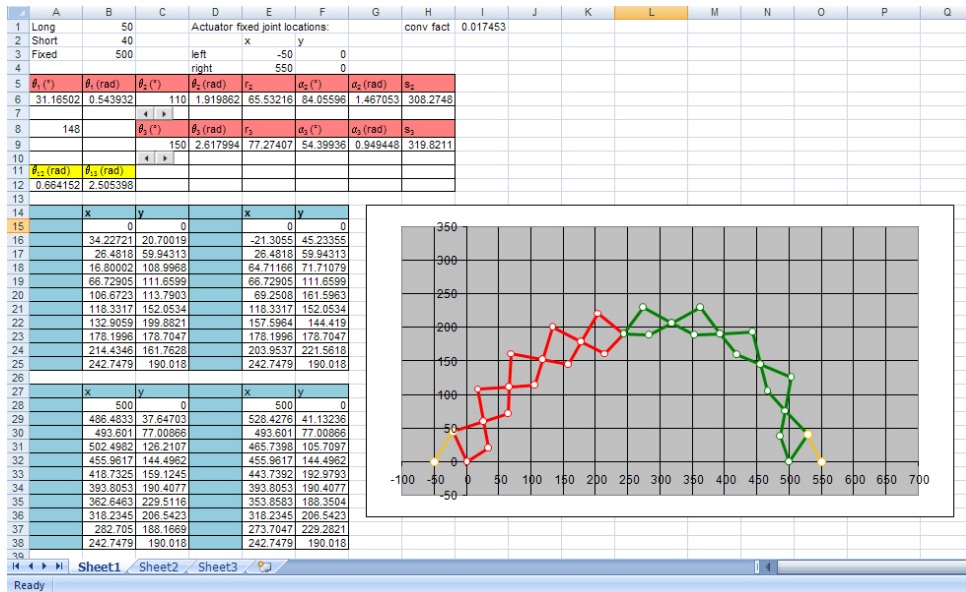
Figure 56. Interface of the computer program for M=2 condition

Some samples from the available geometric configurations of the structure with M=2, as obtained from the software described above, are illustrated in Figure 57.
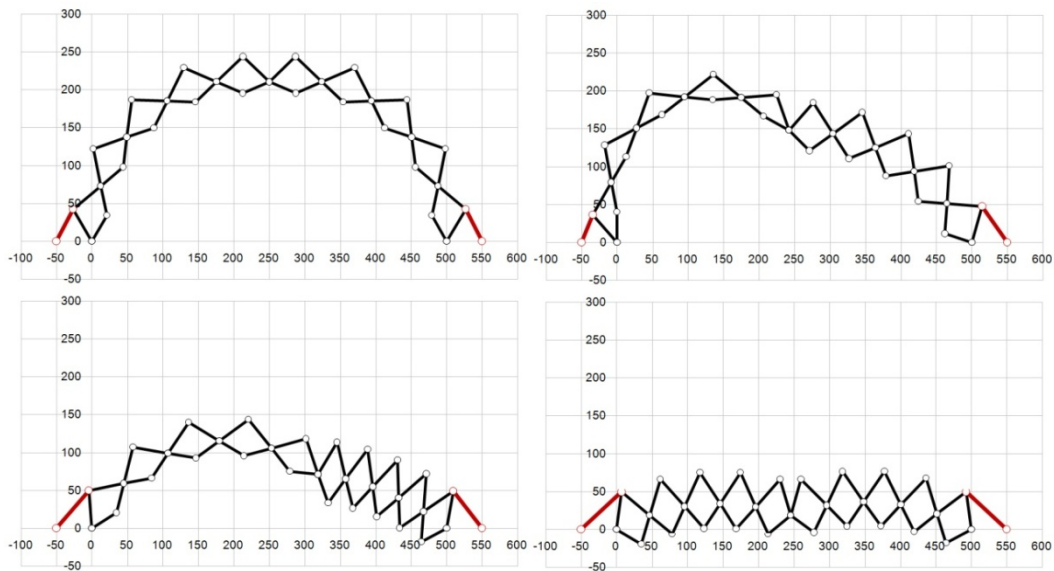
Figure 57. Successive geometries of the M=2 version of the proposed planar structure

5.4.3. Kinematic Analysis of M=4 Condition

When three scissor modules are used instead of two, a M=4 system can be obtained. In Figure 58, schematic view of this situation can be seen. When the structure in Figure 54 is investigated, it can be seen that number of bars is 27 (27th bar is the fixed ground line which connects points A_0 and A_{10}), number of revolute joints is 37 (there are two joints on points A_0 and A_{10}, three joints on A_3 and A_7) and number of loops is 11(11th loop connects points A_0 and A_{10}). According to Alizade-Freudenstein formula which was described in (3.1);

$$M = 37 - 3 \times 11 = 4$$
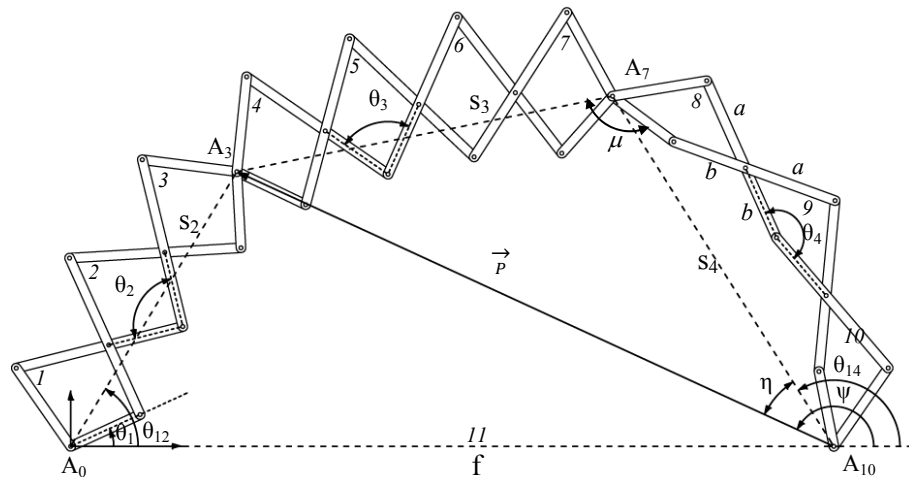
Figure 58. Proposed planar scissor-hinge structure with M=4 condition

Similar to the M=2 version, the structure in Figure 58 can also be abstracted to a mechanism with 7 bars, 4 revolute joints and 3 prismatic joints (f, s_2, s_3 and s_4 are connected with 4 revolute joints and each of s_2, s_3 and s_3 is divided into 2 by a prismatic joint). θ_1, θ_2, θ_3, θ_4 are input parameters to control the mechanism and the lengths of s_2, s_3, s_4 can be found by using θ_2, θ_3, θ_4 angles by using the methods which are described in M=2 condition. When s_2, s_3, s_4 lengths are found, with the constraint f, the system can be thought as a typical four-bar mechanism. This mechanism can be analyzed as:

$$P_x = f - s_2 \cos \theta_{12}, \quad P_y = s_2 \sin \theta_{12} \tag{5.13}$$

$$P = \sqrt{{P_x}^2 + {P_y}^2}, \psi = \angle \vec{P}, \tag{5.14}$$

$$\eta = \cos^{-1}\left(\frac{P^2 + {s_4}^2 - {s_3}^2}{2Ps_4}\right), \theta_{14} = \psi - \eta, \tag{5.15}$$

$$\mu = \cos^{-1}\left(\frac{{s_3}^2 + {s_4}^2 - P^2}{2s_3 s_4}\right), \theta_{13} = \theta_{14} - \mu, \tag{5.16}$$

This kinematic analysis method was has been tested in Microsoft Excel 2007® Medium. In Figure 59, the interface of this program is depicted.
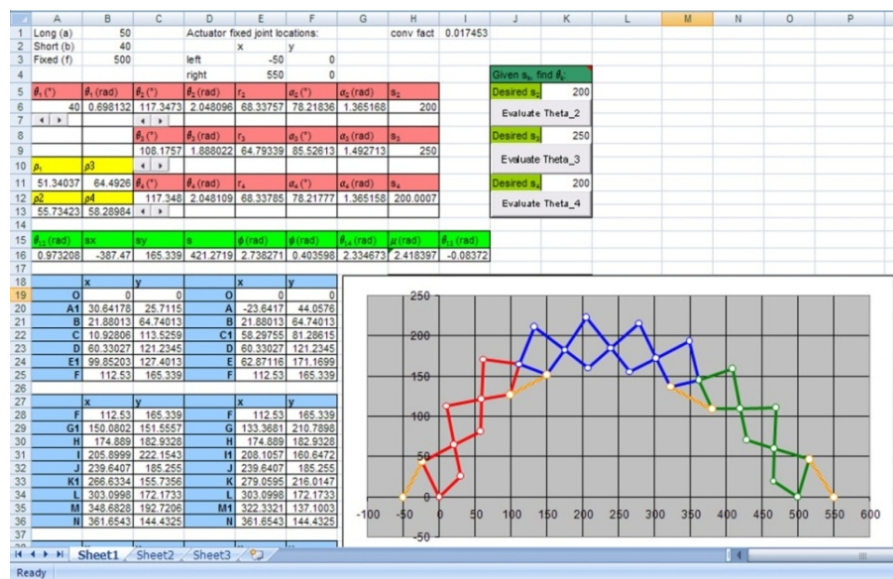
Figure 59. Interface of the computer program for M=4 condition

The inverse kinematics problem is handled with the following algorithm:

- Construct the RPRPRPR mechanism according to the desired shape; hence obtain θ_{12}, s_2, s_3 and s_4.
- Find θ_k for given s_k using a numerical algorithm, such as the Newton Raphson method (in Microsoft Excel 2007 "goal seek" tool can be used). In addition, $\theta_1 = \theta_{12} - \phi_2$.
- Perform the kinematic analysis with θ_1, θ_2, θ_3, θ_4.
- Obtain the required values for any parameter, such as the linear actuator lengths in Figure 47.

With this algorithm, any desired input parameter value can be found for a given configuration. Characteristic geometric configurations of a structure of this type, as obtained from the software described above, are illustrated in Figure 60.
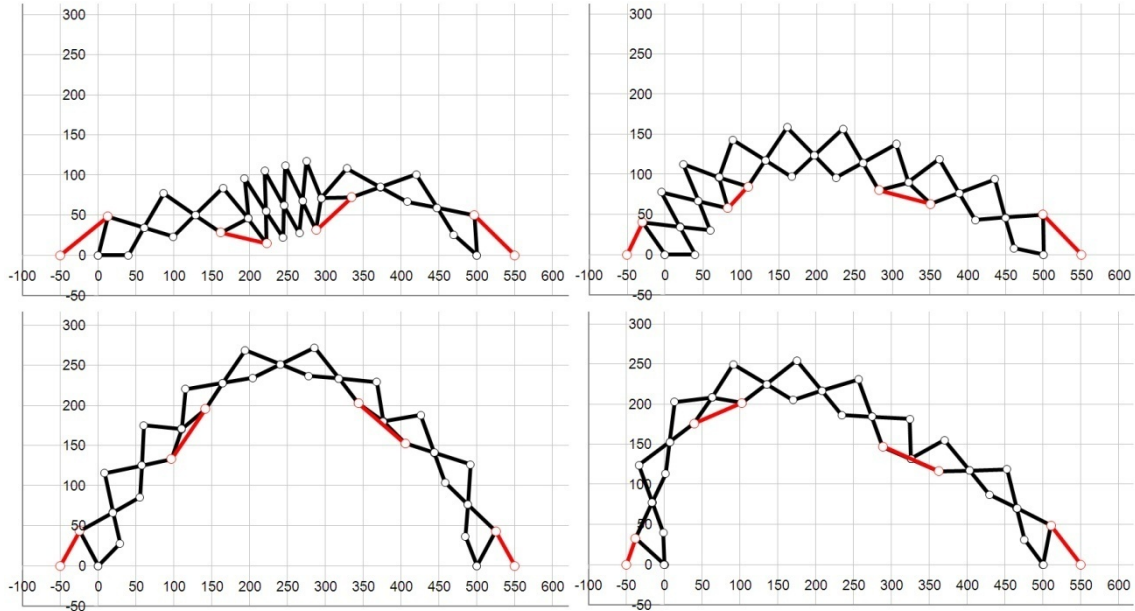
Figure 60. Successive geometries of the M=4 version of the proposed planar structure

5.5. Static Analysis of the Proposed Planar Scissor-hinge Structure

As expected, there is a price to be paid for the increased transformation capability of the proposed structure, and this is related, besides the cost associated with complicated connections between members, to the reduced stiffness and load bearing capacity in the stable, deployed configuration. In order to quantify this disadvantage, a set of structural analyses have been carried out, subjecting the structure to typical loading patterns in different geometric configurations. Additional objectives of the static analysis are to investigate how the locations of actuators influence the stiffness and strength and to find the optimum locations, as well as to obtain the minimum cross-sectional dimensions of the struts.

The structure which has been used for the static analysis (Figure 61) is formed by 14 identical SLEs and two identical M-SLEs and has a total span is 1819 cm. Each

strut is 270cm long and the pivot point of each SLE is located 120 cm from the bottom node of the strut. In this analysis, structural behaviors of a structure with two M-SLEs is investigated. This is because, such structure is geometrically more flexible but structurally weaker than the structure with one M-SLE. Findings about this structure can be valid also for the structure with one M-SLE.
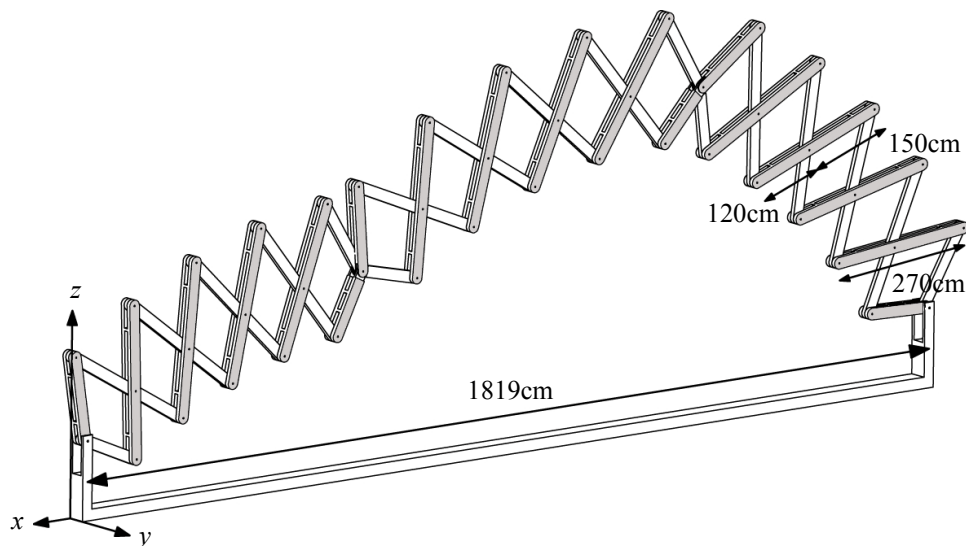
Figure 61. A snapshot of the structure which was used in the analysis

In the analysis the response of the structure against in-plane vertical and horizontal loads (through z and x direction) has been simulated. The structure was not loaded through y direction, because additional members such as crosses creates the strength of a structure against this kind of vertical loads, and these members are not in the topic of this analysis.

In this study, three different geometries (high arch, wave-shape arch, shallow arch) were analyzed, with four different actuator combinations. These three geometries are characteristic of an infinite number of different geometries that the structure can achieve. The tested geometries and alternative locations of actuators, denoted in each case as 1, 2, 3, 4, are shown in Figure 62.

Due to the relatively high flexibility, geometric nonlinearity has been taken into account in the analyses, while the material is assumed to be linear elastic, confirming this assumption later on by carrying out elastic checks for cross-sectional and member

strength. S275 steel with an elastic modulus equal to 21000kN/cm^2, Poisson's ratio equal to 0.3 and yield stress equal to 27.5kN/cm^2 is considered. The analyses are performed with the well-known finite element software ADINA. The model consisted of Hermitian beam elements with three degrees of freedom at each end and was suitably discretized in order to obtain sufficient accuracy.

High Arch   Wavelength Arch   Shallow Arch

Actuator Configuration 1

Actuator Configuration 2

Actuator Configuration 3

Actuator Configuration 4
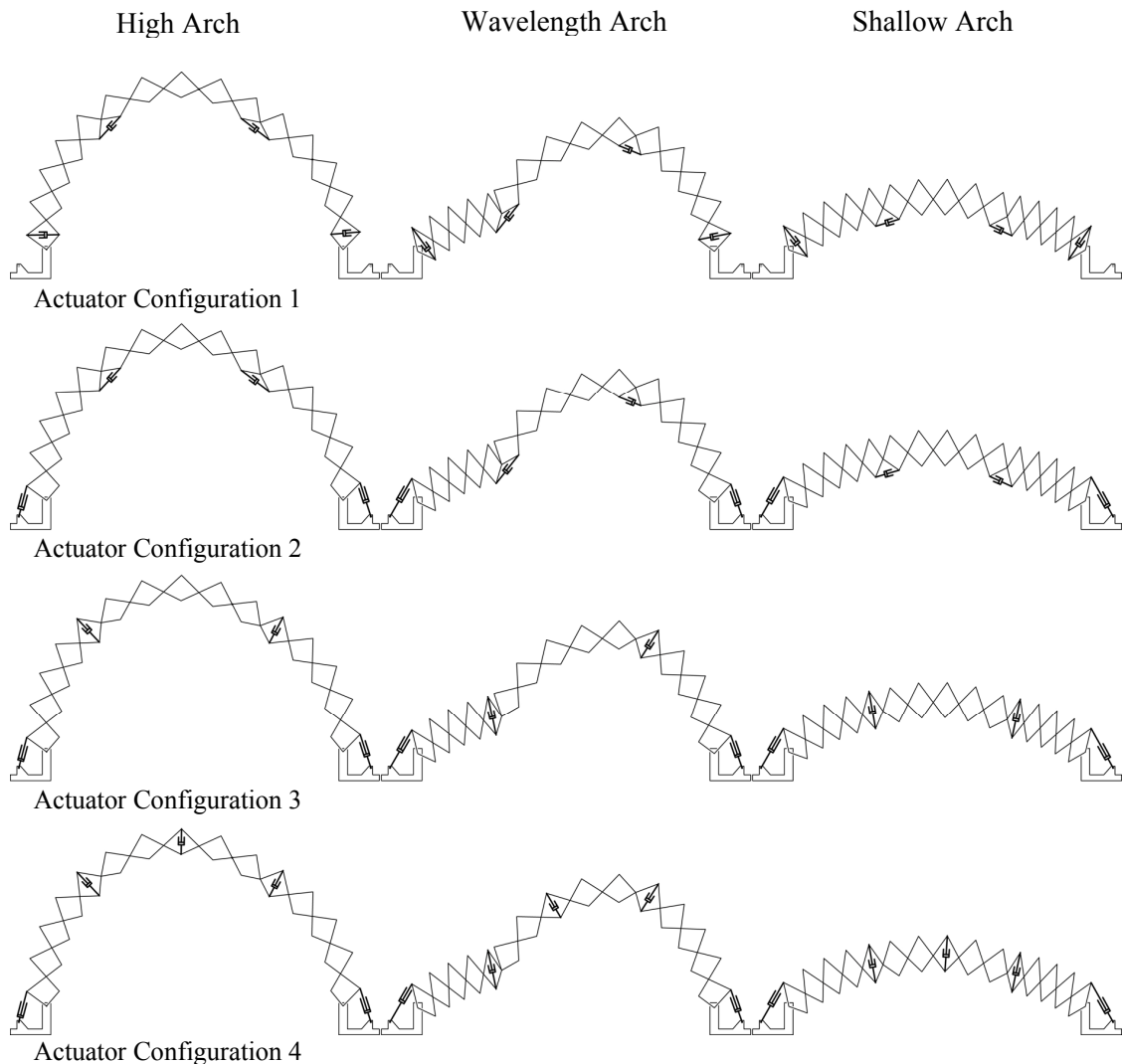
Figure 62. Tested geometries and alternative locations of actuators

Two typical load cases were considered, one consisting of a predominantly vertical load, which represents self weight (48.4kN) and snow load (0.5kN/m^2), and the second of a predominantly horizontal load, which represents wind (26m/sec). All loads

were applied as concentrated on the exterior nodes. Rectangular hollow cross-sections of 50mm x 300mm x 10mm were employed for all members. Dotted lines in Figure 62 represent pairs of bars, as seen in Figure 62, which were modeled by single members with hypothetical cross-sections of 100mm x 300mm x 10mm. Elastic strength checks of normal stresses due to axial force and bending moment were carried out, while a deflection limit of span over 200 was used for serviceability checks.

The high arch, expected to be the most efficient structural shape, was analyzed first. In the first alternative solution (Figure 62, actuator locations 1), the structure was connected to the ground via one hinge on each side, two actuators were placed on the exterior of the two bottom SLEs, while the relative rotation of the three sub-structures was partially restricted by means of two more actuators. This solution proved by the analysis to be efficient for the case of the high arch resulting to acceptable vertical deflection and amount of stress in the cross-sections. The undeformed and deformed shape, as well as the axial force and bending moment diagrams of this structure under vertical loading are shown in Figure 63.

a. Undeformed shape

b. Undeformed and deformed shape

c. Axial force diagram

d. Bending moment diagram
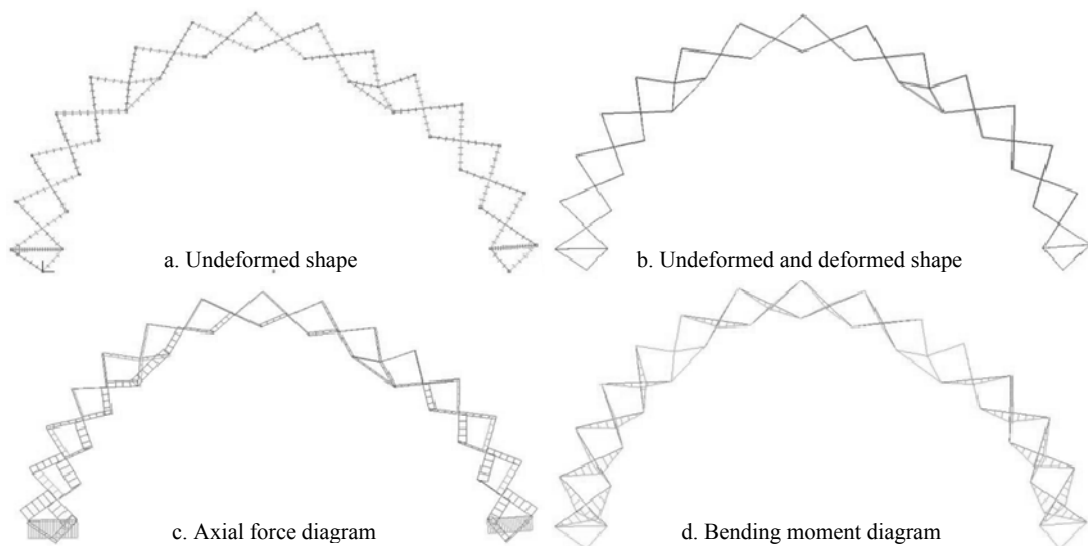
Figure 63. Response of high arch against vertical loads (actuators in location 1)

In the second alternative solution (Figure 62, actuator locations 2), the structure was connected to the ground via two actuators, while the relative rotation of the three sub-structures was partially restricted by means of two more actuators. The undeformed

and deformed shape, as well as the axial force and bending moment diagrams of the structure under vertical loading are shown in Figure 64.

| a. Undeformed shape | b. Undeformed and deformed shape |
| c. Axial force diagram | d. Bending moment diagram |
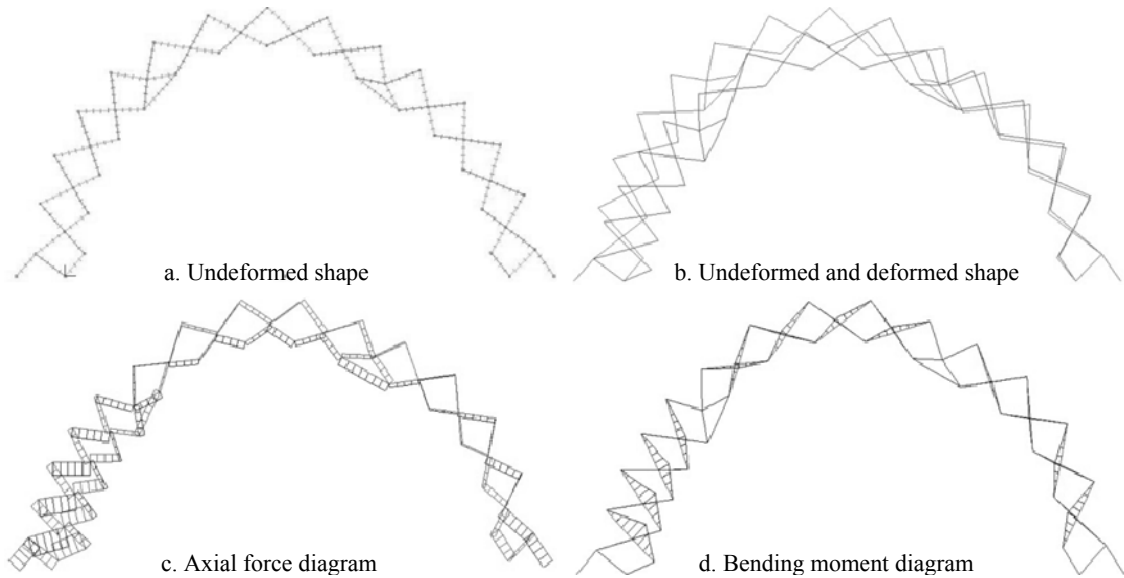
Figure 64. Response of high arch against vertical loads (actuators in location 2)

In the third alternative solution (Figure 62, actuator locations 3), the structure was connected to the ground via two actuators, while the other two actuators were placed at a suitable position, on the exterior of M-SLEs, so that overall stability is achieved. The vertical deflection was found to be equal to 52cm, which, however, is unacceptable. The stresses in some cross-sections are unacceptably high as well. The undeformed and deformed shape, as well as the axial force and bending moment diagrams of the structure under vertical loading are shown in Figure 65.

Satisfactory strength and stiffness were obtained in the fourth solution (Figure 62, actuator locations 4), which is obtained from solution 3 by adding one more actuator on the top of the arch. This actuator is not needed for deployment and it is only activated for providing increased stiffness of the deployed structure. The total deflection calculated for this case is 8cm, thus satisfying the serviceability requirement (L/200=9.1cm). Stress requirements are also satisfied. The structure is sufficiently stiff, so that geometric nonlinearity is now of limited importance. The undeformed and

deformed shape, as well as the axial force and bending moment diagrams of this structure under vertical loading are shown in Figure 66.

a. Undeformed shape

b. Undeformed and deformed shape

c. Axial force diagram

d. Bending moment diagram
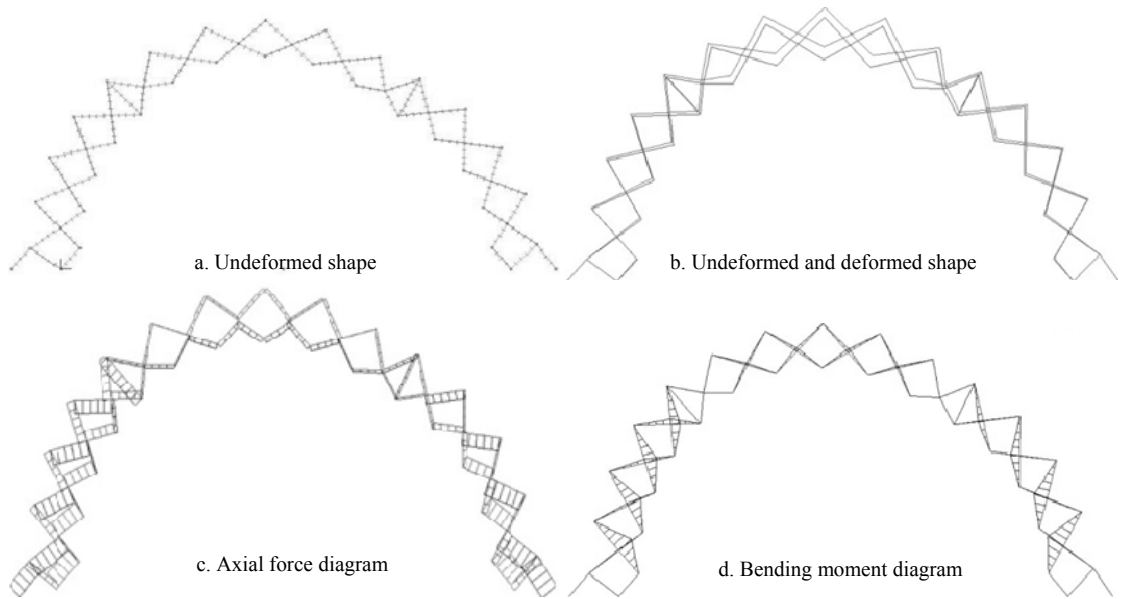
Figure 65. Response of high arch against vertical loads (actuators in location 3)

a. Undeformed shape

b. Undeformed and deformed shape

c. Axial force diagram

d. Bending moment diagram
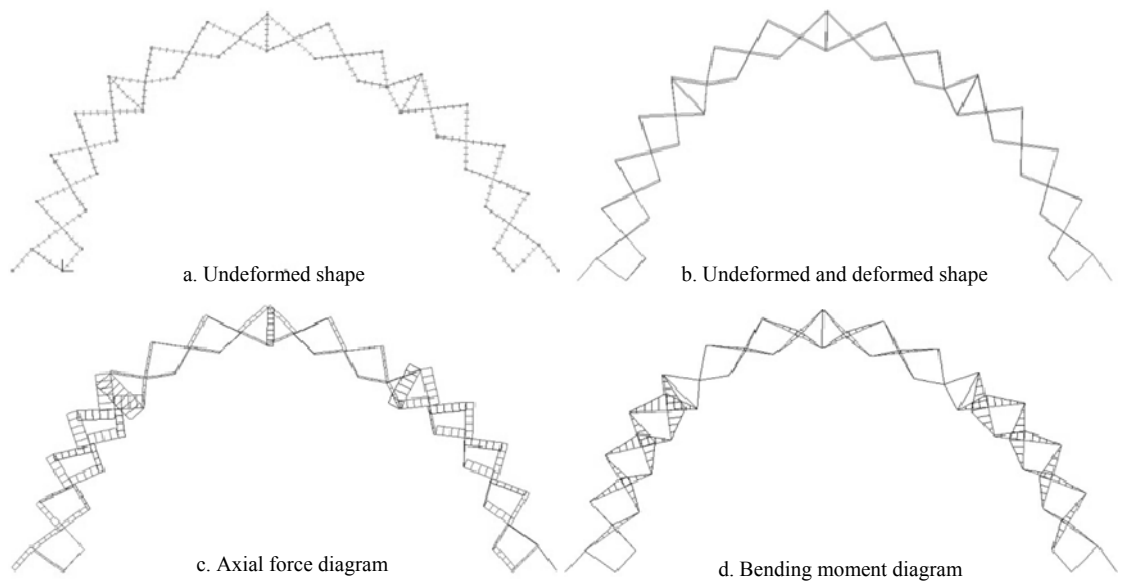
Figure 66. Response of high arch against vertical loads (actuators in location 4)

The maximum response quantities of the high arch subjected to vertical loads are summarized in Table 2, for the four alternative locations of actuators. Solution 1 is found to be the best in terms of stiffness and strength, followed by solution 4.

Table 2. Maximum response of the high arch subjected to vertical loads for the four alternative locations of actuators

Location of actuators	Vertical displacement [cm]	Normal stress [MPa]
1	5.2	200
2	200.0	1000
3	52.0	490
4	8.2	250

Lightweight roofs are particularly sensitive to wind loading, therefore, the structure was subjected to horizontal loading as well; and geometrically nonlinear analyses were performed. The load, corresponding to a wind speed of 26 m/sec, was applied as concentrated loads on the nodes, with a distribution representative of arches subjected to lateral wind, indicated in Figure 67. The maximum response quantities of the high arch subjected to horizontal loads are summarized in Table 3, for the four alternative locations of actuators. Solution 4 has been found to be by far the best.
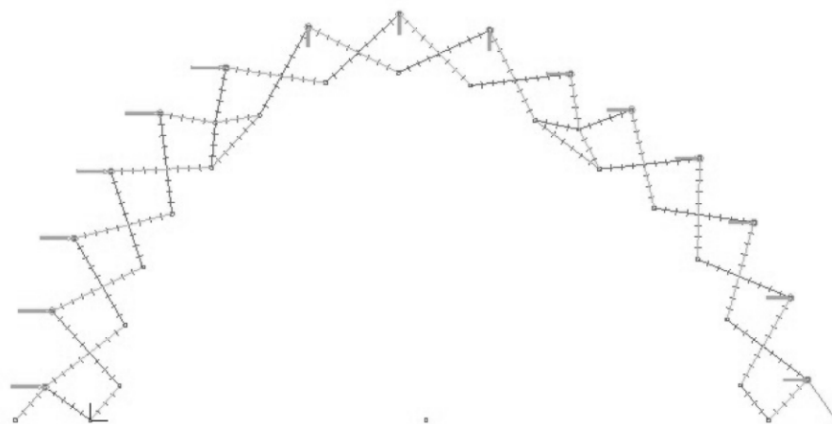
Figure 67. Distribution of loads representing wind pressure

Table 3. Maximum response of the high arch subjected to horizontal loads for the four
    alternative locations of actuators

Location of actuators	Horizontal displacement [cm]	Normal stress [MPa]
1	9.7	161
2	7.9	95
3	unstable	-
4	3.4	145

The same analyses were carried out for the wave-shape arch. The main disadvantages of this shape of structure are the fact that the "arching" action does not exist and that the accumulation of snow on it, in the case that it is used as a roof, will be larger. The results of the analyses, taking snow accumulation into account, are summarized in Table 4 and Table 5, for vertical and horizontal loads, respectively. The expected low stiffness and strength are indeed verified. The superiority of the fourth alternative for actuator locations, including a fifth actuator, is demonstrated. Even though there is a slight violation of strength and serviceability criteria, it is proven that with the use of a fifth actuator and with a modest increase of cross-sections, the structure is capable to withstand relatively light loads in this geometry as well. It is also noted that the middle substructure remains at very low levels of stress (Figure 68), as is also the case for the high arch (Figure 66), thus savings of material could be possible in that region.

Table 4. Maximum response of the wave-shape arch subjected to vertical loads for the four
    alternative locations of actuators

Location of actuators	Vertical displacement [cm]	Normal stress [MPa]
1	75.4	800
2	390.0	900
3	20.2	410
4	15.0	340

Table 5. Maximum response of the wave-shape arch subjected to horizontal loads for the four
   alternative locations of actuators

Location of actuators	Horizontal displacement [cm]	Normal stress [MPa]
1	9.3	226
2	34.2	302
3	7.2	174
4	4.6	190

a. Axial force diagram   b. Bending moment diagram
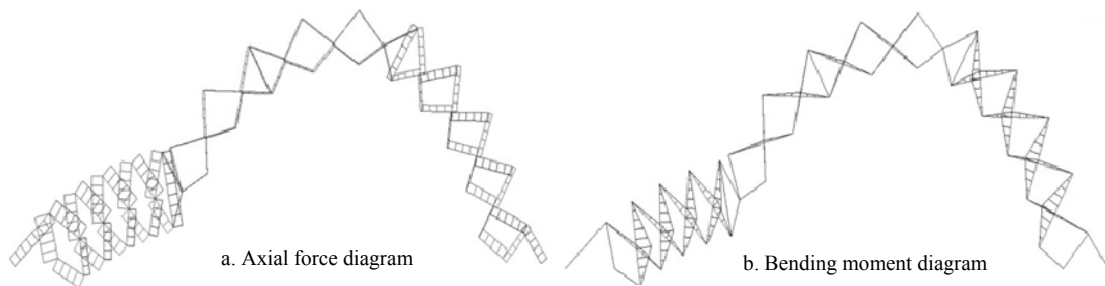
Figure 68. Response of wave-shape arch against vertical loads (actuators in location 4)

The same analyses were carried out for the shallow arch as well. The shallow arch maintains the main disadvantages mentioned in the case of the wave-shape arch. The behavior of the structure under vertical loading approaches more that of a beam and for this reason the static behavior for such long spans is not satisfactory and it is actually the worst among the three different structural geometries that have been analyzed. From this result, it is seen that the proposed planar structure as a whole cannot constitute shallow arches or planes with the existing number of actuators or materials.

This result does not mean that some parts of the structure can never form shallow geometries. As an example, wave-shape arch was investigated again. Although the left side of the wave-shape arch in Figure 68 is shallow and exceeds the serviceability requirements; it can be in the service limits by small modifications. To prove this claim, same vertical load case was applied to the structure. Nevertheless, at this loading snow loads were not taken into consideration, and the cross sections of the struts were changed from 10mm to 5mm. Response of this structure in these conditions is presented in Table 6. Fourth solution of actuators is sufficient for these cross-sections while the third one could be sufficient if a little bit larger cross-sections were used.

Table 6. Maximum response quantities of the wave-shape arch subjected to vertical dead loads
        for the four alternative locations of actuators

Location of actuators	Vertical displacement [cm]	Normal stress [MPa]
1	32.4	360
2	339	650
3	12.7	185
4	8.9	195

This small example shows that the proposed planar structure can constitute even the shallow wave-shapes as long as the estimated geometries, feasible material and cross sections are considered in structural design process.

Feasibility of the proposed planar structure is directly dependent to various variables like the expected geometry, span length, number of SLEs and M-SLEs, dimension and cross sections of the struts, type of the material and some external conditions that the snow or wind loads. According to the changes in these variables, system should be reanalyzed to find the optimum feasible solution.

Static analysis part of this dissertation has only aimed to show that this novel scissor-hinge structure can be stable in different geometries; and tried to guide to the following research on this structure.

5.6. Prospective Use of the Proposed Planar Structure

This research study provides an endeavor approach which expands the adaptability and form flexibility in the fields of deployable and transformable structures. Until now, scissor-hinge structures have been only used as the portative building components. However, the proposed structure in this study can be used as permanent adaptive building structures and skins.

As a hypothetical example, the structure analyzed in section 5.5 was implemented as an adaptive roof of an exhibition hall. However, to strengthen this structure against horizontal loads and buckling, design of the SLEs was modified. One strut of the SLE was offset 150cm and these two parallel elements were connected by steel profiles. This modified planar structure and its connection details are shown in Figure 69.

The structure in Figure 69 is multiplied five times in the same direction to cover an exhibition space which is 2400 x 3260cm. According to the activity and the necessities for the activities in that hall, these six scissor-hinge systems can be transformed individually or together; and the shape of the roof and the character of the space under the roof as well are able to be changed. Sample shape configurations of this transformable exhibition space are shown in Figure 70.
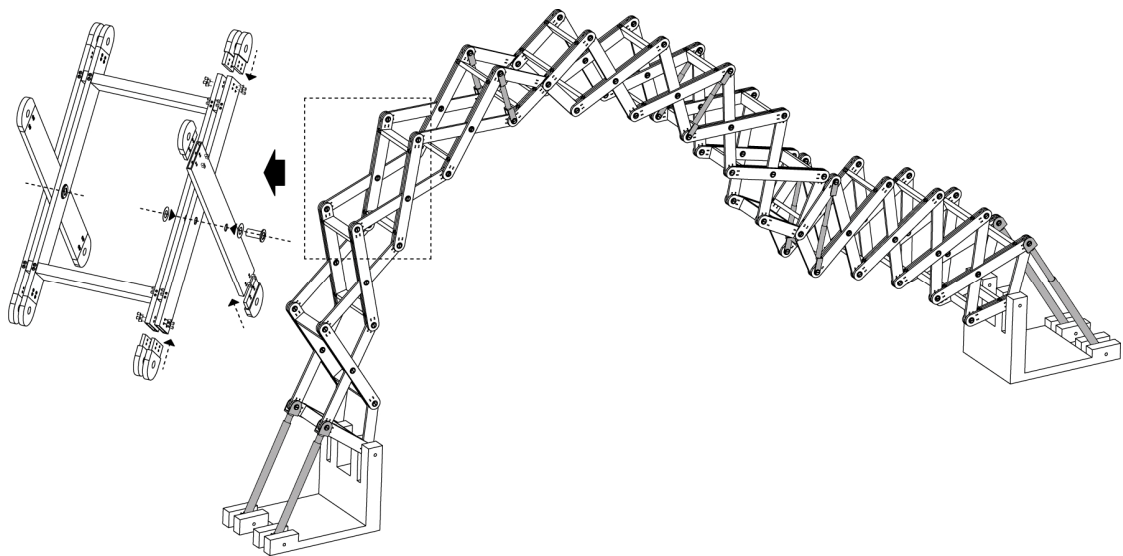
Figure 69. Parallel proposed planar scissor-hinge structure

To construct the prototype of this adaptive building, some other problems should be solved as well. For example, an additional support system against horizontal loads (such as a cable system or cross steel members) is necessary. Furthermore, a flexible cover material which can change its volume without any deformation should be developed. This cover material can be developed by using origami tessellations, pneumatic or vacuumatic skins. However, as it is mentioned in the scope of the dissertation, these problems are not in the scope of this research study.
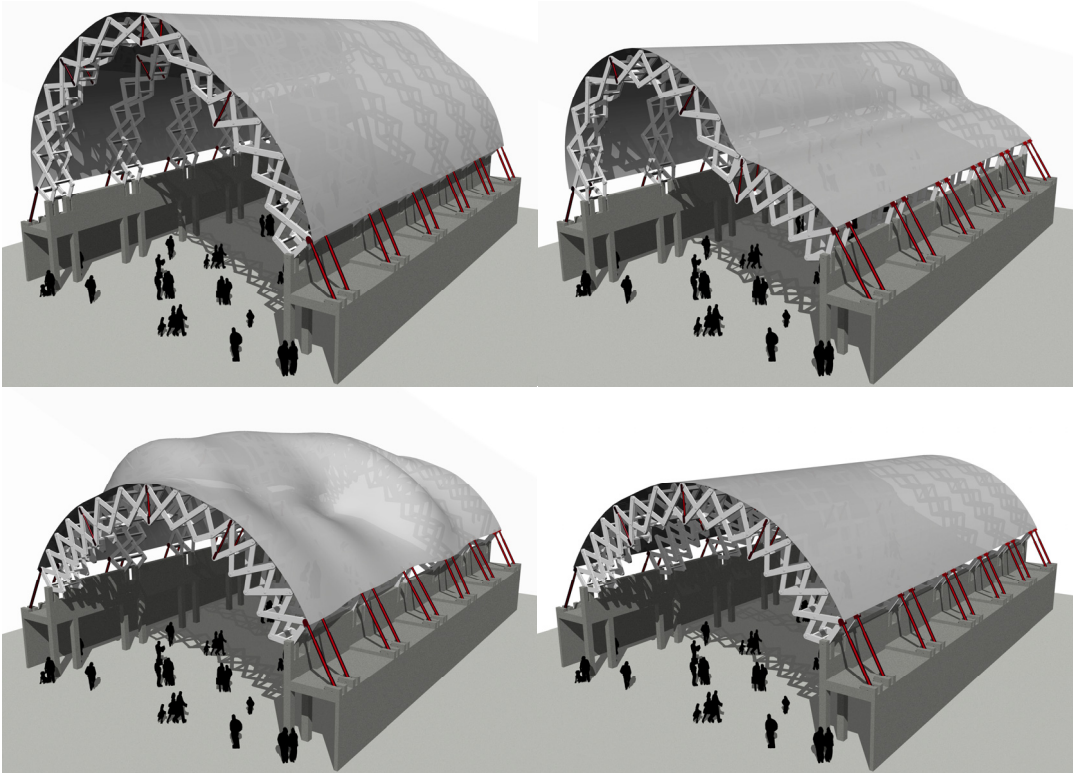
Figure 70. Proposed planar scissor-hinge structure as an adaptive roof

CHAPTER 6

PROPOSED SPATIAL SCISSOR-HINGE STRUCTURE: PRINCIPLES, ANALYSIS AND USE

This chapter mainly introduces the proposed spatial scissor-hinge structure; and highlights its originality and superiority over the common spatial scissor-hinge systems. The chapter has two main sections: In first section, M-SLE which is introduced in Chapter 5 is adapted to different type of common spatial scissor-hinge structures, and contributions of this element to the transformation capabilities of these common spatial structures are inspected.

Second section of the chapter presents the proposed spatial scissor-hinge structure: superiority of this structure over the previous examples, primary elements (S-SLEs and MS-SLEs), typologies, transformation capabilities, kinematic and static analysis, and prospective uses.

6.1. Use of M-SLEs with Common Spatial Scissor-hinge Structures

Objective of this section is to evaluate the effectiveness of the M-SLEs, when they are used as members of the common spatial scissor-hinge structures. During this evaluation, two different spatial scissor-hinge structures are experimentally tested. First structure is a combination of the proposed planar structure which is explained in Chapter 5, and common spatial scissor-hinge structures. Because of this property, this structure is called as "hybrid scissor-hinge structure". Second structure is a spatial structure which is based on current spatial scissor-hinge structures.

In order to understand the contributions of M-SLEs on these two structures, first, main properties of the common spatial scissor-hinge structures should be investigated.

When the common examples of spatial scissor-hinge structures are investigated, it can be seen that they are all M=1 structural mechanisms. This means, when a single SLE moves, all the other SLEs imitate this transformation as well. This property is graphically illustrated in Figure 71. The mechanism in this figure is fixed to the ground

from the "element A". When "element B" is slid through y axis, all the other elements adapt themselves to this movement. As a result of this movement, all distances between elements, and the size of the whole structures, change ($a_1 < a_2$, $b_2 < b_1$, $c_1 < c_2$).
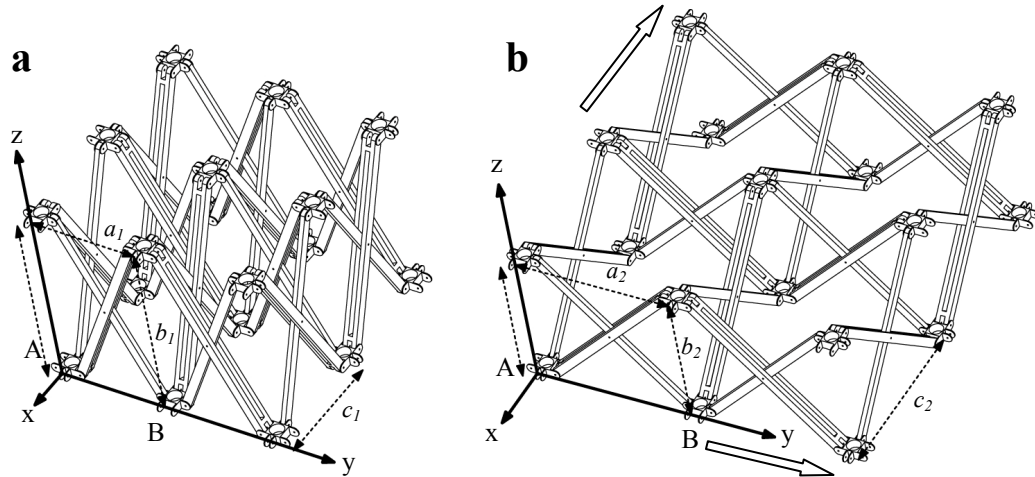
Figure 71. Transformation of a common spatial scissor structure

When Figure 71 is investigated, it can be seen that these common examples are not suitable to cover a defined area as a permanent roof. This is because, when the structure transforms, the size of the covered area under it changes. This problem constitutes one of the main topics of the research study.

Proposed planar structure which is described in Chapter 5 can overcome this problem. However, this structure is constituted by the multiplication of the parallel planar structures, so it can transform only through one direction. Thus, it is impossible to form hypersurfaces by using proposed planar structure.

6.1.1. M-SLE with Hybrid Scissor-hinge Structure

Hybrid scissor-hinge structure is a combination of the proposed planar scissor-hinge structure and common spatial scissor-hinge structures. It has M-SLEs for increasing the transformation capability and actuators to move the system, like the proposed planar structure. At the same time, its primary elements and their connection

types are the same with the common spatial examples. An example hybrid structure and its transformations are shown in Figure 73.

The hybrid structure has two different primary spatial elements which are derived from SLEs and M-SLEs. These units can be seen in Figure 72. The first unit (Figure 72a) is constituted by two different types of SLEs. For the first type of SLE, length *a* is always longer than length *b*. For the second type, pivot point is located in the middle of the strut (gray bars in the Figure 72). White SLEs are the main elements to define the shape of the whole structure. Number of the white SLEs is related to the span length; and gray SLEs are only necessary to make the structure spatial, and to increase the stability.

Second unit is the spatial version of the planar M-SLE, and it is the most important element of the hybrid structure (Figure 72b). Like its planar ancestor, this element has additional revolute joints on pivot points as well; and this increases the transformation capacity of the system.
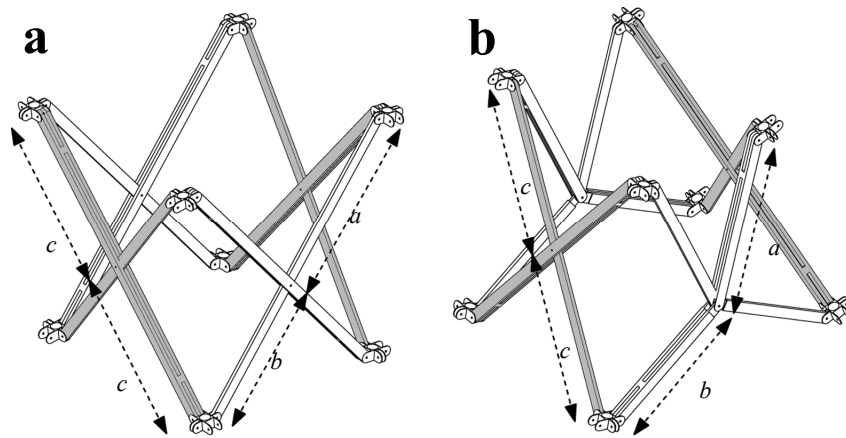
Figure 72. Primary elements of the hybrid scissor-hinge structure

To express the shortcomings of the hybrid structure, three different form configurations of the structure; high arch, shallow arch and wave-shape arch; are represented in Figure 73. The hybrid structure in this figure has four M-SLEs (two at each parallel structure), and the mobility of the structure is equal to four. Thus, four independent parameters are needed to move and control the system; and θ_1, θ_2, θ_3 and θ_4 angles are chosen as input parameters.
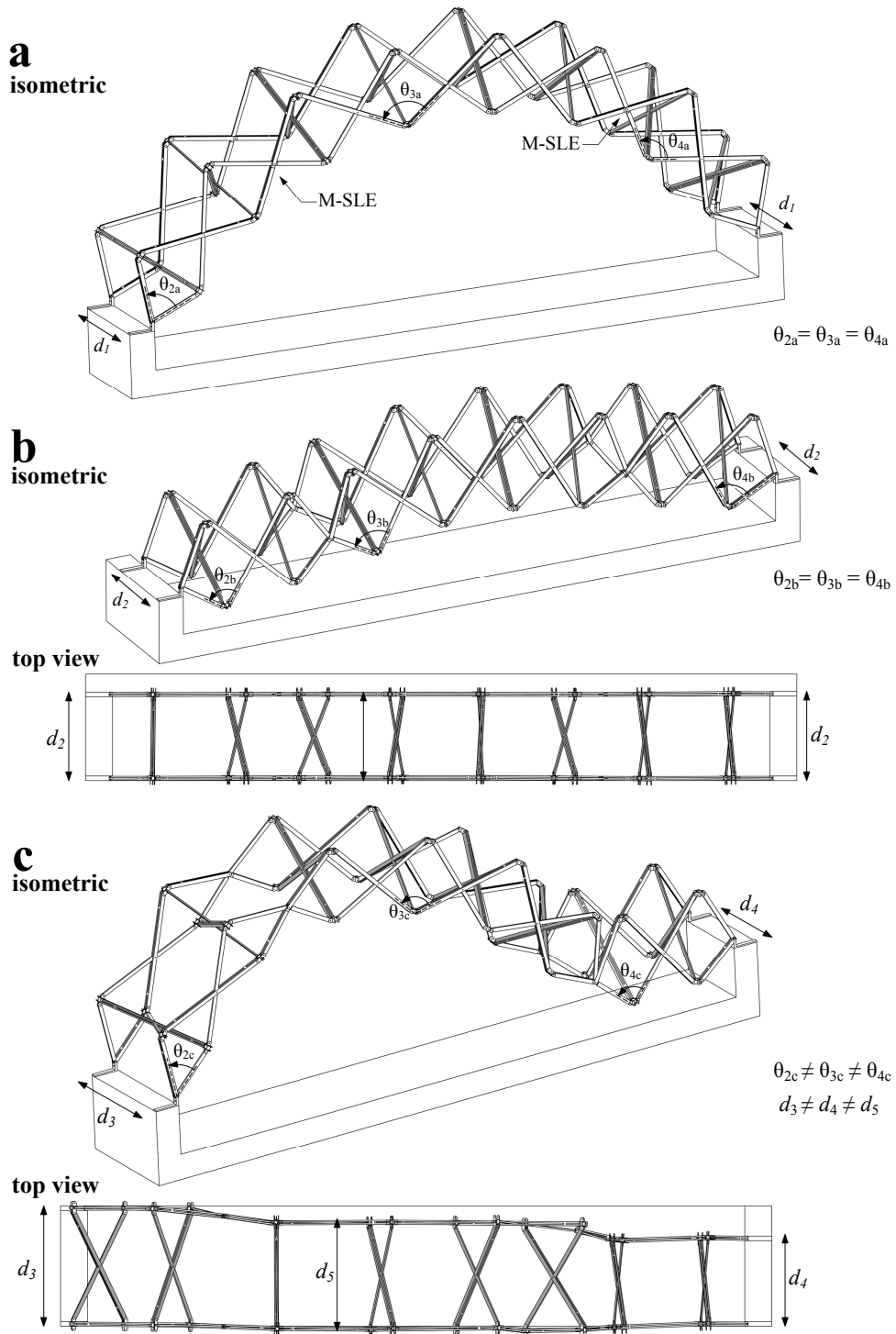
Figure 73. Sample transformations of the hybrid structure

At first sight, it can be thought that the transformation capability of the hybrid structure is very similar to the proposed planar structure. However, as it is seen in Figure 73, in the hybrid structure can only meet arcs with various radiuses. This is because, for all shape configurations, θ_2, θ_3 and θ_4 angles should always be equal. When

θ_2, θ_3 and θ_4 angles are different, depth of the structure change heterogeneously; and the structure will take a shape like as it is in Figure 73c. The hybrid structure has only revolute joints; so the form in Figure 73c is geometrically impossible. To constitute this shape with revolute joints, all joints should allow rotations perpendicular to their rotation axis; or spherical joints should be used instead of revolute joints. However, using spherical joints increase the mobility of the system and the number of actuators. This decreases the feasibility of the system. In addition, the structure in Figure 73c does not allow attaching another unit next to it; so it cannot be used as a member of a roof structure.

6.1.2. M-SLE with Common Spatial Scissor-hinge Structure

Main objective of this section is to investigate the transformation capabilities of different types of current spatial scissor-hinge structures; to expose the contribution of M-SLE to these structures, and to describe the shortcomings of these systems.

The simplest transformable spatial structure is formed by the connection of two perpendicular planar scissor-hinge structures. In this study, this structure is called as "Plus Shape System"; and an example of this structure is drawn in Figure 74. Each planar sub-structure of the Plus Shape System in the figure has two M-SLEs; but mobility of the whole system is equal to one. This is because of the joint types. At this structure, only revolute joints are used, and revolute joints can only allow planar rotations. Because of the revolute joints, each planar structure can only transform on its own plane. Intersection of two perpendicular planes constitutes an edge. For this structure, this edge is on the z axis; and the intersection element can only move through z axis.
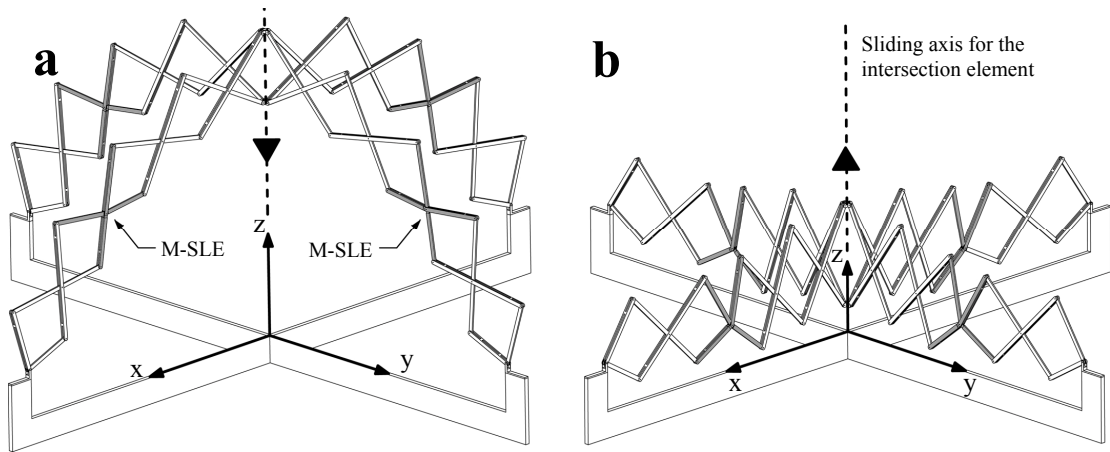
Figure 74. Plus shape system and its transformation capability

Plus shape structure cannot constitute asymmetrical shapes; and to increase the transformation capability of the structure, some of the revolute joints should be switched to spherical joints. An example switch can be seen at the structure in Figure 75. In this figure, revolute joints at the points A and B are switched to spherical joints. By this small change, the planar sub-structure on *x-z* plane can rotate around *x* axis. Theoretically, this small modification increases the transformation capability of the whole structure. However, rotation of the plane of the structure on *x-z* axis causes extra load over the perpendicular sub-structure; and this decreases the feasibility of this solution.
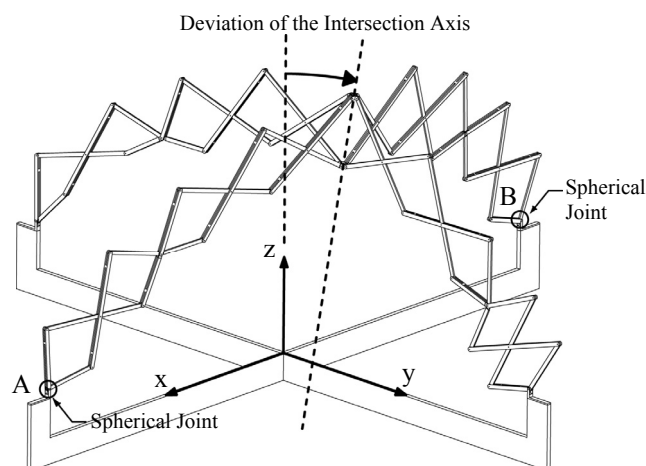
Figure 75. Transformation of the plus shape system with additional spherical joints

At the next step of the study, contributions of M-SLEs to the transformation capability of the scissor shells are investigated. In order to comprehend the geometric principles of the whole structure, first, primary elements of the scissor shell should be understood. These elements can be seen in Figure 76. Both of these elements are similar with the spatial elements of the hybrid structure; but here, only one type of SLE which meets the condition of $a>b$ is used.
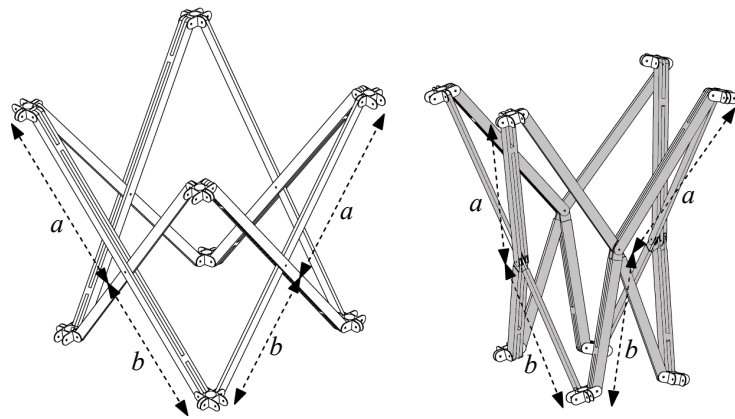
Figure 76. Primary elements of the scissor shell

The scissor shell structure which is constructed for the experimental studies can be seen in Figure 77. This structure covers an area with the dimension of 48x48 cm. Lengths of all struts are equal and 9 cm. Pivot points for each strut was at the same point, and it was 5 cm away from the upper hinge, so the structure meets $a>b$ condition. Locations of the M-SLEs on the structure are represented as grey bars at the schematic top view. All lines, such as A_1 to A_6, or A_4 to A_5, have two M-SLEs. The structure is connected to the ground from eight points (A_1, A_2 … A_8).
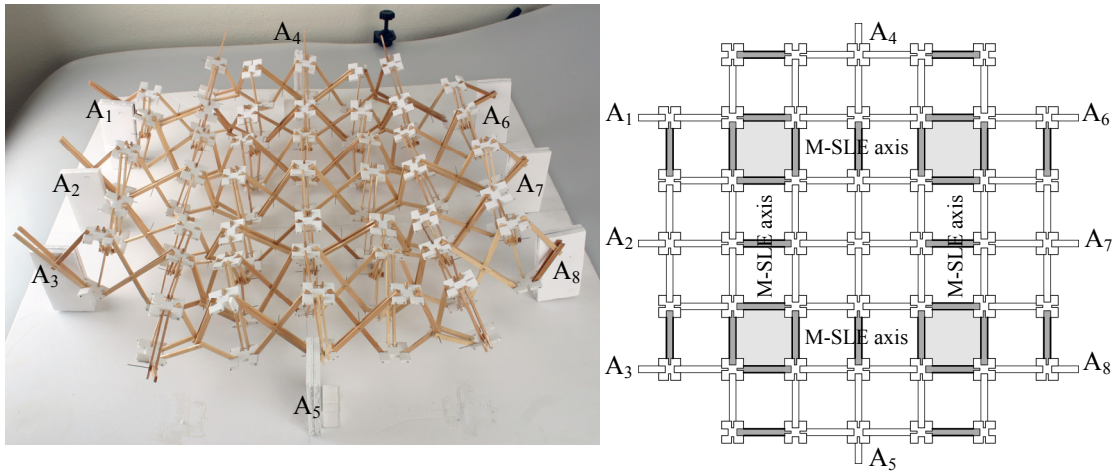
Figure 77. Model view and schematic top view of the scissor shell

During the experiments, it is understood that this structure cannot transform, unless the revolute joints at the support points (A_1 to A_8) are switched to spherical joints. Even after this switch, the mobility of this structure increases to one, and the structure can only transform between a high dome like shape and a shallow dome. Pictures of the model at these shape configurations can be seen in Figure 78.
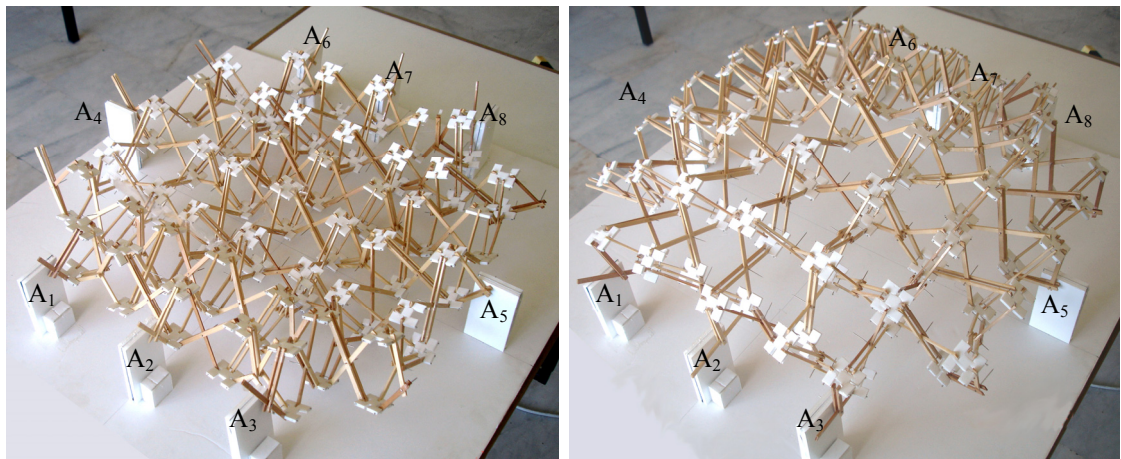
Figure 78. Model views of the scissor shell at deflated and erected positions

This research study has been thoroughly focused on the applications of the M-SLEs to the common spatial scissor-hinge structures. As a conclusion, it can be claimed

that the transformation capability of the common scissor-hinge structures are inadequate when the area they cover is fixed, even if they have several number of M-SLEs. Adaptation of the M-SLEs can only make a small contribution to the solution of this problem. Consequently, a novel spatial scissor-hinge structure is proposed to overcome the aforementioned problems.

6.2. Proposed Spatial Scissor-hinge Structure

This section of the dissertation introduces the proposed spatial scissor-hinge structure; its primary elements, transformation capabilities, structural analysis and prospective uses. As the main superiority of this structure over the aforementioned examples, this structure can achieve the transformations between various curvilinear shapes and hypersurfaces without changing the size of the covered area.

This transformation capability comes from the geometry of the primary units. Primary units and their connection details of the proposed structure are totally different from the previous examples. To understand the superiority of this structure, first, the proposed primary units should be investigated.

6.2.1. Primary Units of the Proposed Spatial Scissor-hinge Structure

Proposed spatial scissor-hinge structure has three primary elements: Spatial scissor-like element (S-SLE), Modified spatial scissor-like element (MS-SLE) and the Hybrid element which is a half MS-SLE. These elements can be seen in Figure 79.

Primary elements of the proposed spatial structure are derived from the planar SLE and M-SLE which are thoroughly described in Chapter 5. Main difference of these elements from the common spatial scissor units is the connection type of the struts. At common scissor units, struts are connected from the hinge points with an intermediate element. As it can be seen in Figure 71, when one strut of these units moves, this directly affects the other bars of the system. However, at the primary elements of the proposed structure, struts are connected from the pivot points with an intermediate element; and each strut can move individually. This individuality constitutes the main advantage of the proposed system.
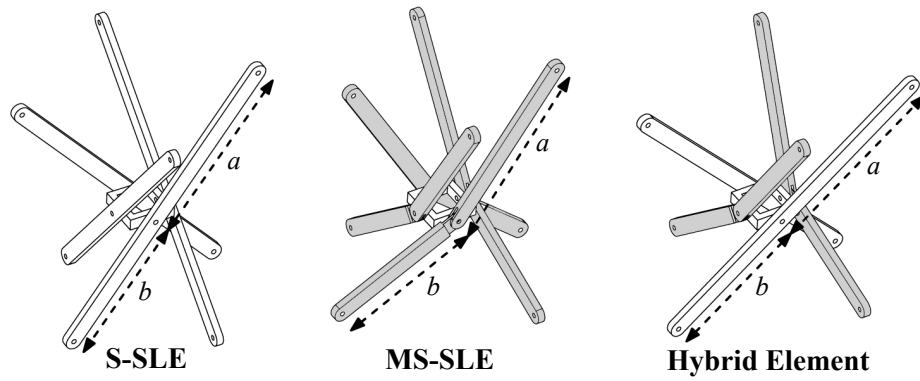
Figure 79. Primary elements of the proposed spatial scissor-hinge structure

Primary elements in Figure 79 increase the transformation capability and give a prominent superiority to the proposed spatial scissor-hinge structure over the common spatial scissor systems. One of the advantages can be expressed by an example: A scissor shell structure which is composed of the S-SLEs can be seen in Figure 80. Because of the geometry and the connection type of the S-SLEs, this structure can change its length in one direction without changing the length on the other directions. Thus, while mobility of the common spatial scissor structures is equal to one, mobility of the structure in the figure is equal to two. This makes the structure more flexible than the previous examples.
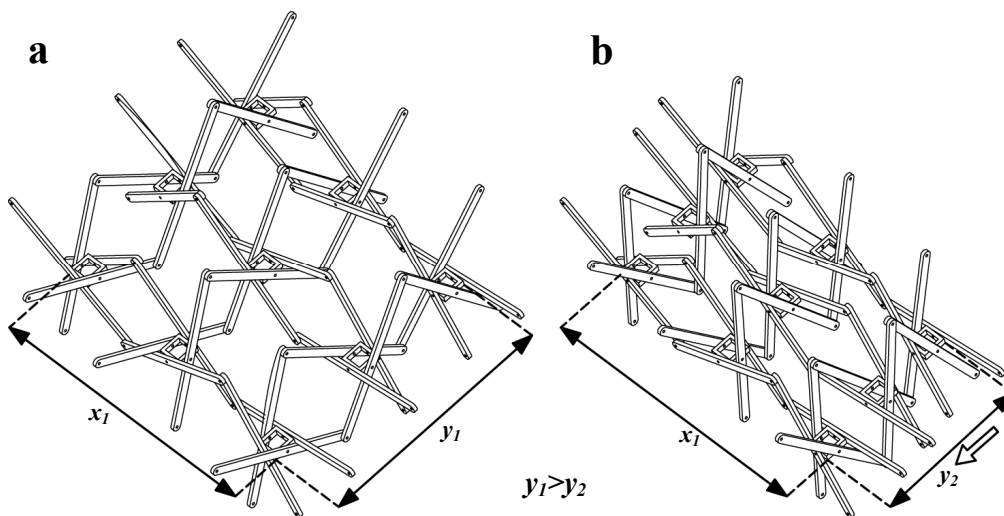
Figure 80. Transformation of a scissor shell which is composed of S-SLEs

Even the S-SLE provides partial improvement in form flexibility, the main contributions on the transformation capability are offered by the MS-SLE and the Hybrid element. To understand this contribution, Figure 81 can be investigated. Structure in this figure has four S-SLEs, four hybrid elements and one MS-SLE. The logic behind the emplacement of these elements is very similar to the proposed planar scissor-hinge structure. Every axis in both x and y direction has one M-SLE. Thus, mobility of the each axis and the whole structure as well, is equal to one. According to the emplacement of the primary elements of the proposed spatial structure, the structure can transform its shape without changing the outer dimensions of the whole structure (x_1 and y_1). Thus, this structure can achieve simple form transforms without changing the size of the covered area.
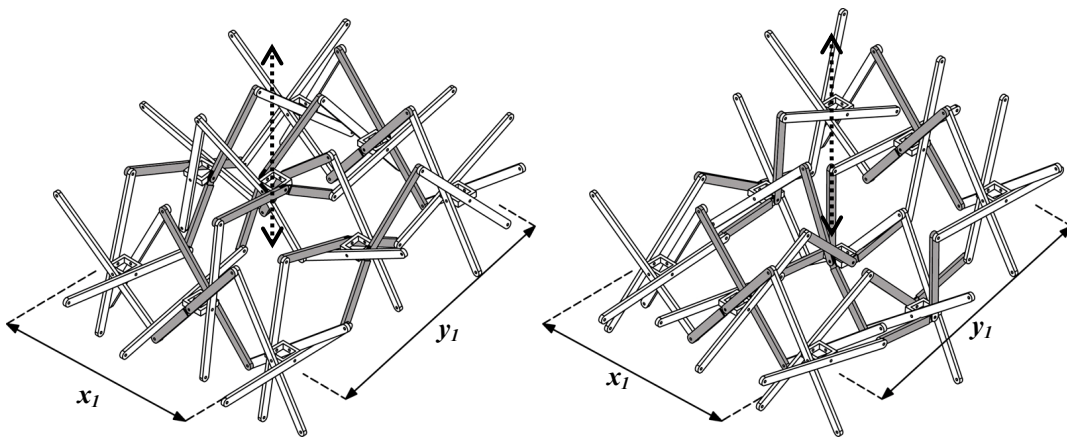
Figure 81. Transformation of a scissor shell with MS-SLEs and hybrid elements

By using the aforementioned primary elements, a transformable scissor shell structure is generated. In this dissertation, this shell structure is called as "Proposed spatial scissor-hinge structure". Perspective and top views of the structure which represents the configuration of the S-SLEs, MS-SLEs and hybrid units on the structure can be seen in Figure 82. Light grey struts in the figure express the M-SLEs. For the generation of the proposed spatial structure, various numbers of primary elements with various dimensions and various span lengths can be used. However, the structure in Figure 82 has 25 S-SLEs, 4 MS-SLEs, 20 hybrid elements and eight special SLEs for the support points. The structure is connected to the ground from eight points (A_1, A_2 …

A$_8$). Span of the structure is 14 meters in both directions; and the lengths of the struts are 270 cm. Length *a* and *b* which are described in Figure 79 are 150 cm and 120 cm. All following analyses in this chapter are done by using the structure in Figure 82.
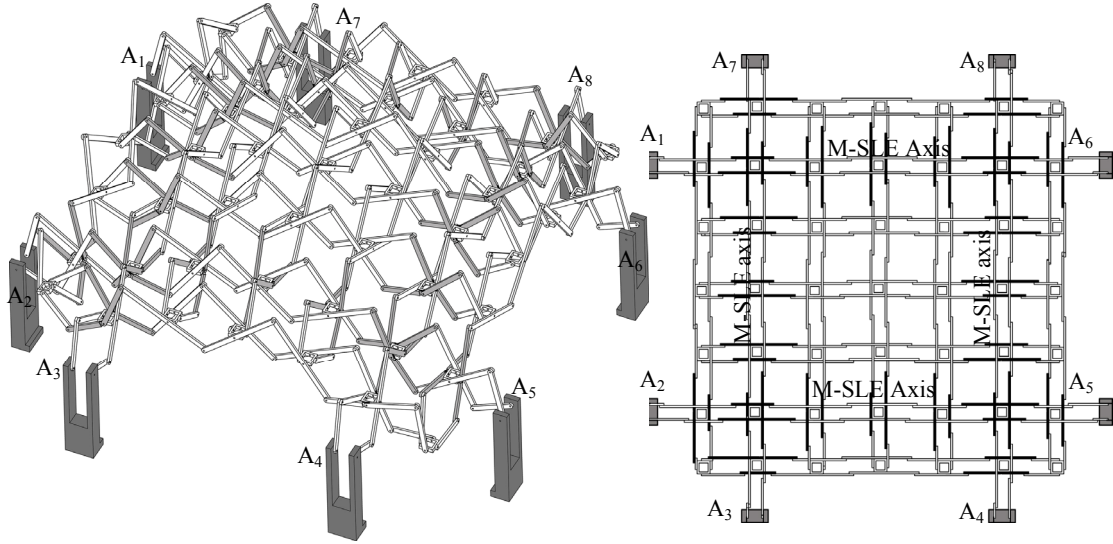
Figure 82. Perspective and top view of the proposed scissor-hinge shell structure

6.2.2. Kinematic Analysis of the Proposed Spatial Scissor-hinge Structure

Similar to its planar version, transformation capability and kinematic analysis of the proposed spatial scissor-hinge structure are investigated in two phases: Analysis of a single unit; and analysis of the whole system.

As it can be seen in Figure 79, all struts of the S-SLE can move individually and rotate 360° unless they collide with the other struts. Mobility of this unit can be found as four by Alizade-Freudenstein formula which is described in Chapter 3.2.

Transformation capability of an S-SLE is directly related to the dimensions of intermediate element and the struts. An example to express the importance of these two factors can be seen in Figure 83. In this figure, it can be seen that when the intermediate element gets bigger, α and β angles which define the rotation of struts increase as well. This means, when $l_2 > l_1$, then $\alpha_2 > \alpha_1$; $\beta_2 > \beta_1$. From this example, it can be understood that the bigger intermediate elements increase the transformation capability of the unit.

However, a bigger intermediate element increases the weight of the SLE and decreases the feasibility.

Another factor which affects the transformation capability of the S-SLE is the width (w) of the struts. When the length (w) increases, transformability range of the struts and of course α and β angles decreases.
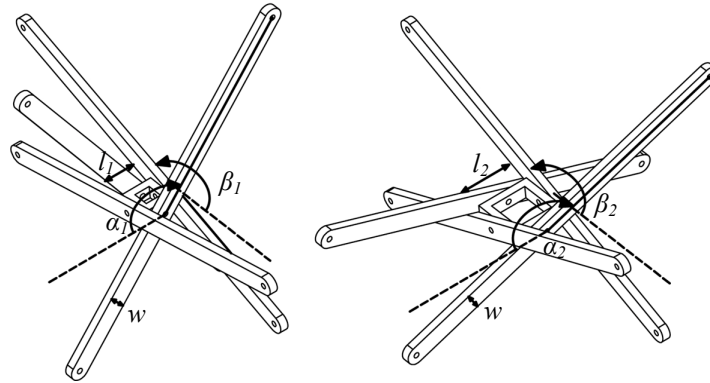
Figure 83. Transformation limits of the S-SLE

An S-SLE can be thought as the combination of two perpendicular SLEs. These SLEs constitute individual planar systems, unless they collide with the perpendicular SLE. Therefore, formulation of shape limitations for SLEs which are explained in Chapter 5.4.1, are also valid for the planar sub-systems of the S-SLE.

Similar to the common deployable structures, additional actuators are needed to fix and transform the proposed spatial scissor-hinge structure. After the experimental studies with small prototypes, it was seen that these actuators should be utilized on the scissor axes which connect the support points (A_1-A_6, A_2–A_5, A_3-A_8, A_4-A_7 axes). By this way, these four planar sub-structures become the main load bearing and transformation elements of the whole structure. The other elements which are called as the "cover scissors" are secondary members and do not have a distinguishing role at form transformations. They only adapt themselves to the actual positions of the main load bearing scissors (Figure 84). At kinematic analysis of the proposed spatial structure, transformation capability of the main load bearing sub-structures was investigated thoroughly; but the transformation of the cover scissors were not taken into consideration.
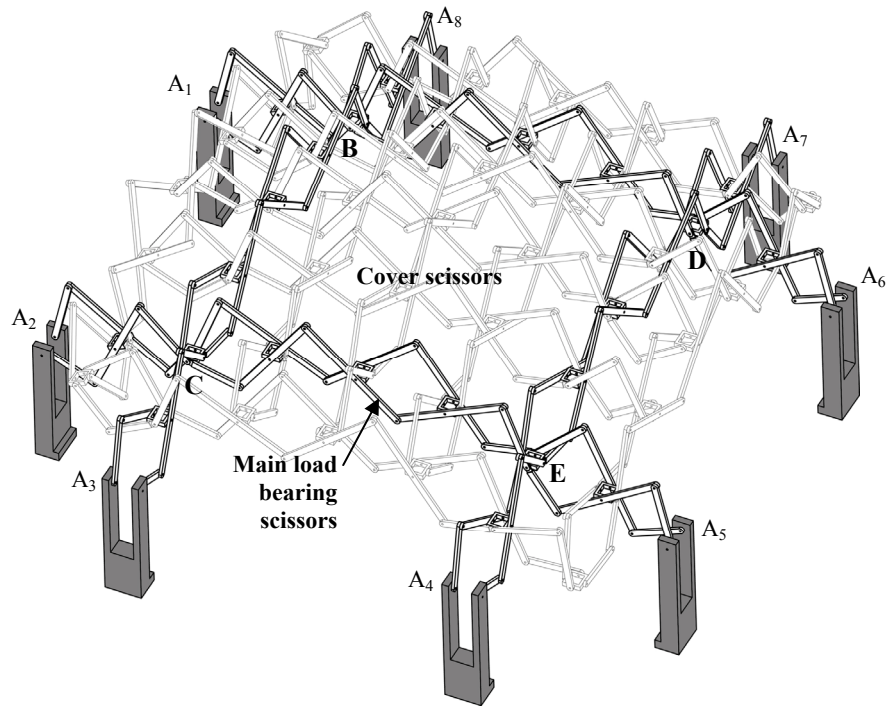
Figure 84. Load bearing and cover scissors of the spatial scissor-hinge structure

To find the number of additional actuators, mobility of the structure should be calculated. To facilitate this calculation, load bearing scissors in Figure 84 was abstracted and presented in Figure 85. At this figure, it can be seen that; due to the use of revolute joints at connections of struts, all the subsystems (A_3CBA_8, A_4EDA_7, A_2CEA_5 and A_1BDA_6) cannot deviate from their planes, and can achieve only planar transformations. Besides, subsystems intersect at some certain points (B, C, D and E) which are called as "knots". In order to keep the planes of the main axes, knots can only slide through (z) direction. This property is very important factor for the transformation capability of the proposed spatial structure.

When Freudenstein-Alizade Formula is applied to find the mobility, it is seen that the abstracted system in the figure has 40 joints and 12 loops (such as A_3CG, A_3CEA_4, A_4EI, etc.). All sub-systems are planar, so λ is equal to three. According to these variables, mobility of the system can be found as four (M=4). This means, theoretically, minimum four actuators are needed to control the geometry of the system. Feasible locations of these actuators were found in the following static analysis section.
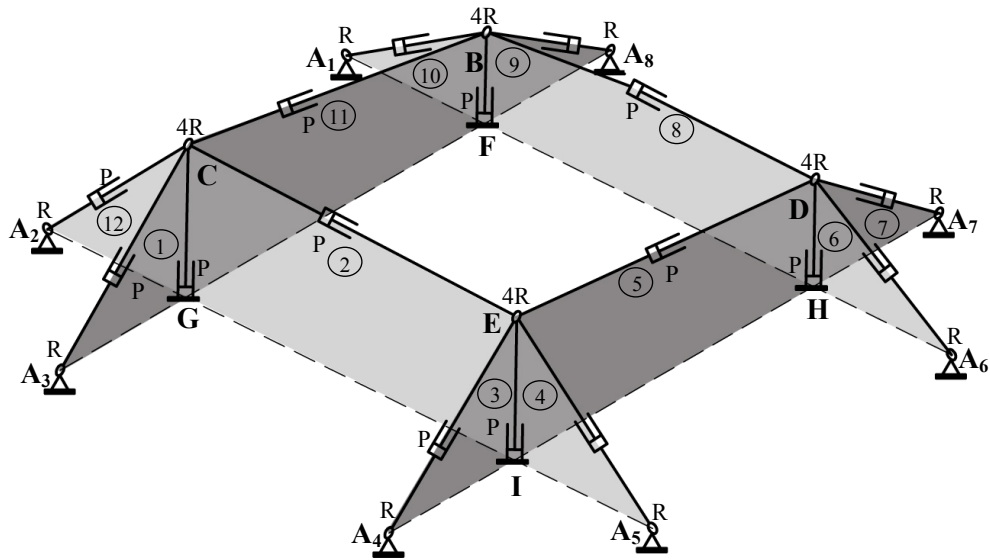
Figure 85. Abstraction of the load bearing scissors

By addition of the locations of the perpendicular axes, and the knot points as new parameters, Microsoft Excel 2007® based program, which is prepared for the planar structure and explained in Chapter 5.4.3, is updated for the spatial structure. This program is efficient to see the final shape of the main scissors according to the inputs. In this program, span of the whole structure, dimension of the elements, angles between the elements (θ_2, θ_4) and location of the perpendicular axes which define the location of knots are the input variables. By spin buttons, users can vary input angles and lengths, According to the changes on these input variables, the graphic interface can update itself simultaneously. In addition, the system gives error for unavailable shapes or inconsistent input configurations. Thus, if the algorithm fails for an input configuration, it is understood that this shape is unavailable for those inputs. The interface of this program is given below in Figure 86.
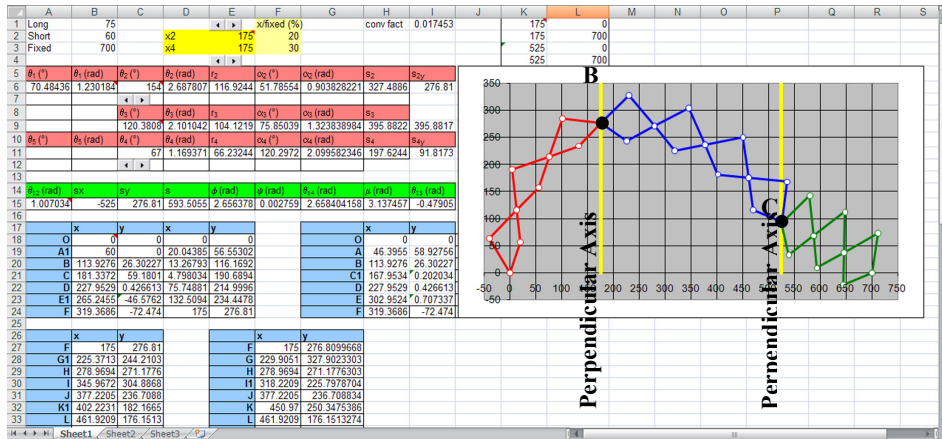
Figure 86. Interface of the computer program for the proposed spatial structure

Transformation capability of the whole structure is directly related to the transformation capability of the planar members; because the main body of the proposed spatial structure is constituted by four identical load bearing scissor structures. Some sample transformations of the whole proposed structure are represented in Figure 87. From this figure, it can be understood that the proposed structure can constitute various curvilinear shapes and hypersurfaces.
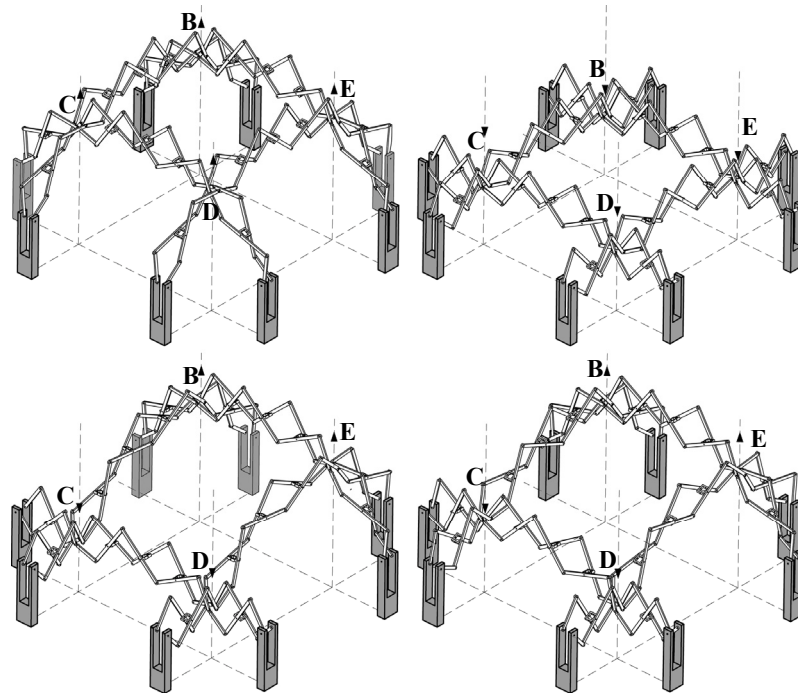
Figure 87. Successive geometric configurations of the proposed spatial structure

In order to see the transformation capability of the proposed spatial structure, a physical model was constructed. This model is 1/20 scale of the computer model in Figure 82. This structure has covered a 70cm x 70cm area. All struts were made of Plexiglas; all intermediate elements were made of polyethylene. Rivets and screws were used as revolute joints which connect the struts. Some sample shape alternatives of this physical model can be seen in Figure 88.
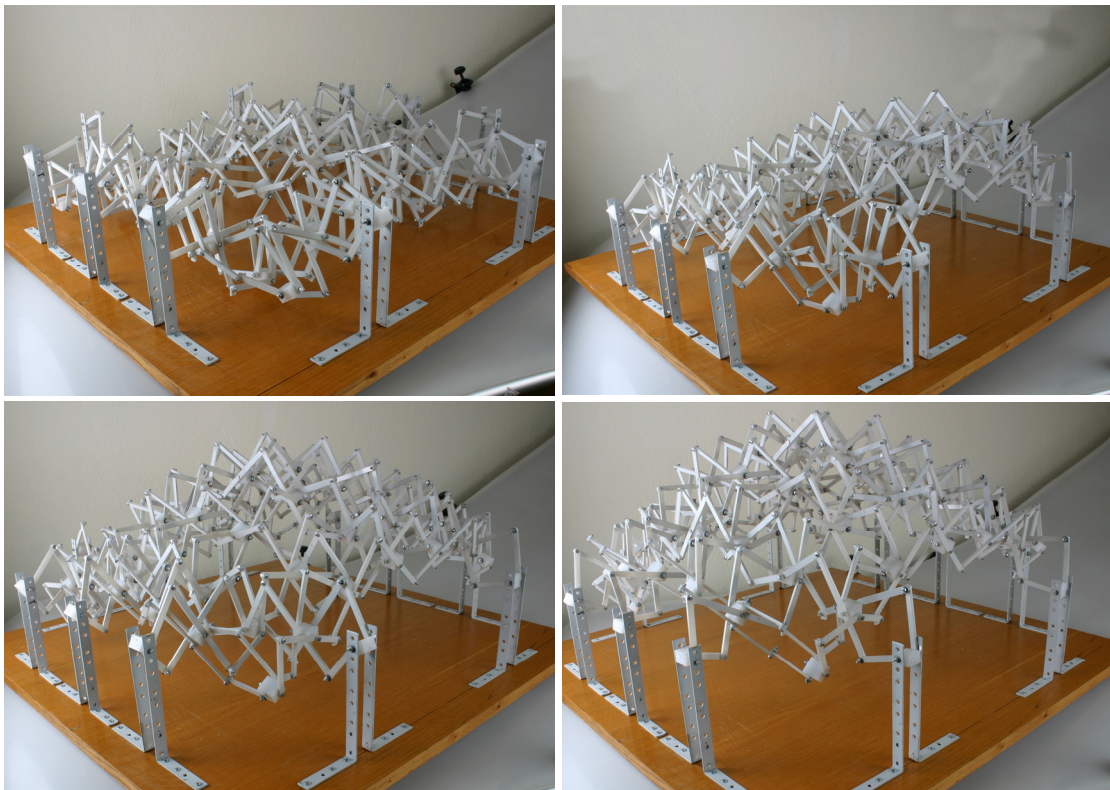
Figure 88. Physical model of the proposed spatial structure

6.2.3. Static Analysis of the Proposed Spatial Scissor-hinge Structure

In order to understand the structural behavior of the proposed spatial scissor-hinge structure, and to obtain the most feasible locations for the needed actuators, a set of structural analyses have been carried out by imposing typical loading patterns in two different geometric configurations of the structure.

The structure in Figure 82 has been used in the static analysis. However, only the main load bearing scissors in Figure 84 were taken into consideration; while the cover scissors were ignored in the analysis. This is because the cover scissors have a secondary role in transferring the loads to the support points through the main scissors, and can be studied independently. Thus, loads for the entire structure were applied directly on the main scissors.

Due to the relatively high flexibility, geometric nonlinearity has been taken into account in the analyses, while the material was assumed to be linear elastic, confirming this assumption later on by carrying out elastic checks for cross-sectional and member strength S275 steel with an elastic modulus equal to $21000kN/cm^2$, Poisson's ratio equal to 0.3 and yield stress equal to $27.5kN/cm^2$ was considered as the material of the struts. The analyses were performed with the finite element software ADINA. The model consisted of Hermitian beam elements with six degrees of freedom at each end, and was suitably discretized in order to obtain sufficient accuracy. In order to simplify the model eccentricities between struts were neglected, and all struts on each frame were assumed to be in the same plane.

Two sample geometric configurations (symmetric cross vault shape and asymmetric shape) were modeled and analyzed. The response of the structure in these two geometries against vertical load, representing self weight and snow load has been simulated. All loads were applied as concentrated on the 12 nodes where cover scissors are supported on the main scissors. Due to the arched shape of cover scissors loads exerted by them on the main scissors have not only a vertical but also a horizontal component. The total vertical component applied on each of the 12 nodes was equal to 15kN, while the horizontal component was equal to 2kN.

Rectangular hollow cross-sections of 10cm x 60cm x 1cm were employed for all members. Elastic strength checks of normal stresses due to axial force and bending moment were carried out. A deflection limit of span/200, equal to 7cm, was used for serviceability checks.

First, the structure with symmetric cross vault shape was analyzed. The structure consists of four main frames that are connected to the ground at eight points, as shown in Figure 84. In addition, there are four connections between perpendicular main frames. As these connections are at pivot locations of the main frames, it is necessary for stability that out-of-plane and torsional rotations are restricted. The capability of these connections to sustain a moment at these positions is, however, questionable from

a practical point of view. Nevertheless, in a first model it was assumed that the connections between perpendicular frames are configured so that transfer of out-of plane bending, as well as torsional moments was possible, while in-plane rotations were free. The ground supports were modeled in the same way.

From the kinematic analysis, it is known that the mobility of the structure is equal to four; so four actuators are theoretically sufficient for stabilizing the structure. Linear elastic analysis was successfully carried out for validating this fact. The four actuators were symmetrically located in the frames of one direction to prove the stability of the whole structure with minimum number of actuators. Two alternative actuator configurations are shown in Figure 89.
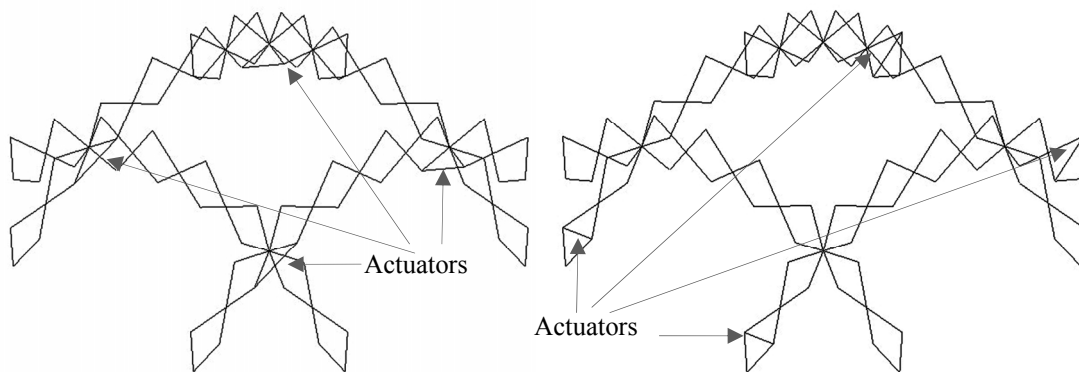
Figure 89. Two different actuator configurations for the solution with four actuators

However, the results indicated that the structure with four actuators was too flexible for this span and level of loading. Moreover, increasing the number of actuators contributed a lot more to enhanced rigidity of the structure than increasing the cross-section's dimensions. Thus, eight actuators were finally used, placed as shown in Figure 90. In this figure, applied loads can be seen as well.
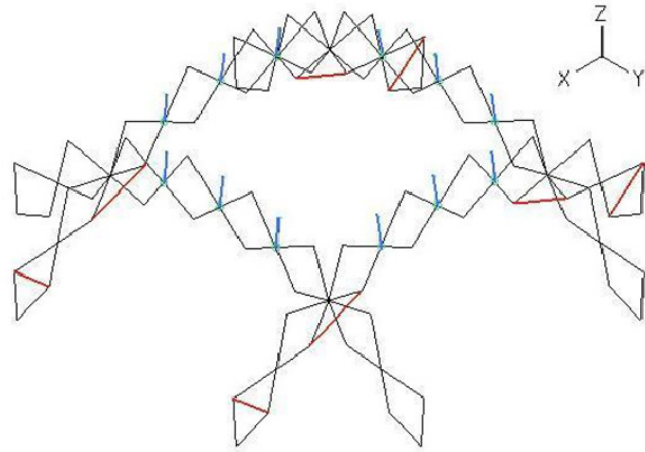
Figure 90. Applied loads on the cross vault shaped structure with eight actuators

Deformed shape, axial force and bending moment diagrams for the aforementioned load case are shown in Figure 91, Figure 92 and Figure 93, respectively. It is noted that the main frames equipped with actuators are much stiffer, thus they "attract" much larger forces.

XZ Plane   YZ Plane

Figure 91. Undeformed (black) and deformed (red) shapes of the cross vault shaped structure

XZ Plane   YZ Plane
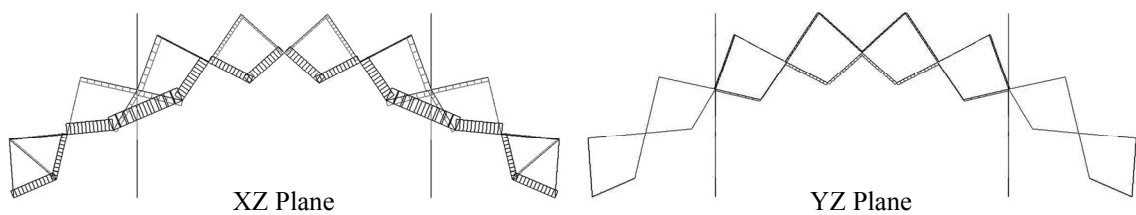
Figure 92. Axial force diagrams of the cross vault shaped structure

XZ Plane   YZ Plane
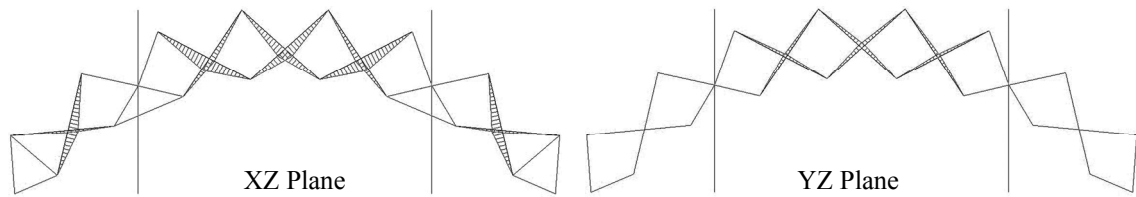
Figure 93. Bending moment diagrams of the cross vault shaped structure

The maximum displacements are given in Table 7. The maximum vertical displacement allowed for reasons of serviceability is 7cm, thus serviceability checks are satisfied. The maximum normal stress due to combined axial force and biaxial bending moment is found to be approximately equal to $9kN/cm^2$, much smaller than the yield stress $27.5kN/cm^2$. Thus, serviceability governs the design.

Table 7. Maximum displacements of the cross vault shaped structure

Maximum displacement	Value (cm)
Z (vertical)	6.70
X	3.90
Y	4.23

As mentioned above, in reality it is questionable whether the four connections between perpendicular frames can be detailed in such a way that they are capable of resisting out-of-plane and torsional rotation. For this reason it was decided to configure these connections as hinges, thus to consider that the three rotational degrees of freedom of all members converging at each of these points are free and no moments are transmitted. However, as a result, the whole structure becomes a mechanism and additional members are needed in order to stabilize it. A simple solution was adopted, providing additional members between main scissors, as shown in Figure 94. These members can be telescopic, so that their length can be adapted to the required one based on the structure's overall geometry. It should be noted that these members are not actuators and that they are pinned at their ends.
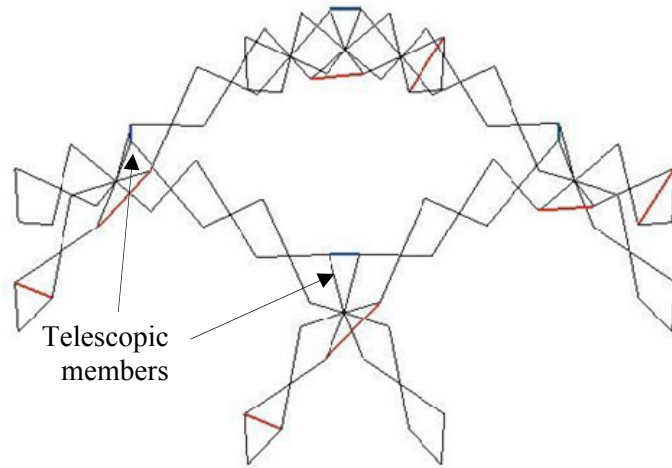
Figure 94. Cross vault shaped structure with eight actuators (red) and four telescopic members (blue)

Applying the load pattern used for the previous model, the resulting deformation and bending moment diagrams are shown in Figure 95 and Figure 96, respectively.

Detail (Out of plane of each frame)

Detail (Torsional moment)

Bending Moment (In plane of each frame)
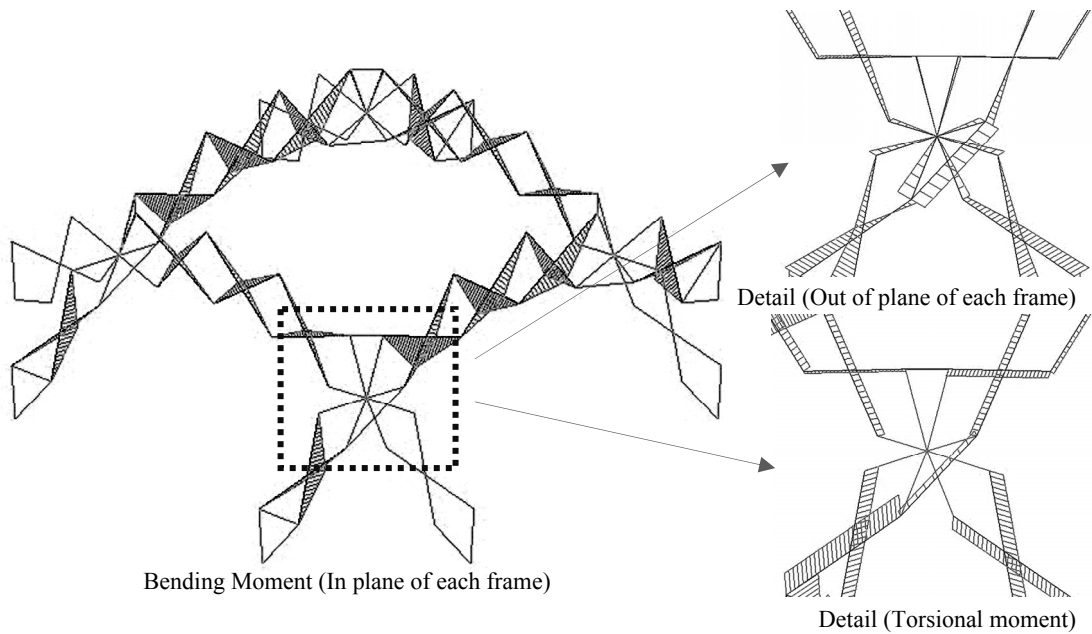
Figure 95. Bending moment diagram of the cross vault shaped structure with four telescopic members
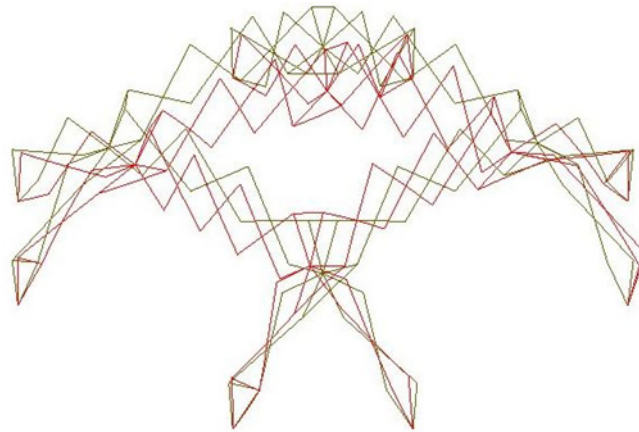
Figure 96. Deformed (red) and undeformed (black) shapes of the cross vault shaped structure with four telescopic members

The maximum displacements of the cross vault structure with eight telescopic members are given in Table 8. Deformations are now a little larger but serviceability checks are satisfied. The maximum normal stress is now approximately equal to 10kN/cm^2, thus still not critical.

Table 8. Maximum displacements of the cross vault shaped structure with four telescopic members

Maximum displacement	Value (cm)
Z (vertical)	5.90
X	1.82
Y	5.79

In the second phase of the analysis, each scissor frame has been transformed to a different geometry and the structure has now been transformed into an asymmetric shape. The number and locations of actuators and telescopic members, loading, material and cross sections of the struts are exactly the same as in the symmetric cross-vault shape structure. Views of this structure in the XZ and YZ planes are shown in Figure 97, with maximum displacements given in Table 9, while bending moment diagrams are shown in Figure 98. Vertical displacements are now smaller but significant horizontal deformations are introduced. The maximum normal stress is now found to be

approximately equal to 22kN/cm^2, still smaller than the yield stress 27.5kN/cm^2 but now nearly critical.

XZ Plane   YZ Plane
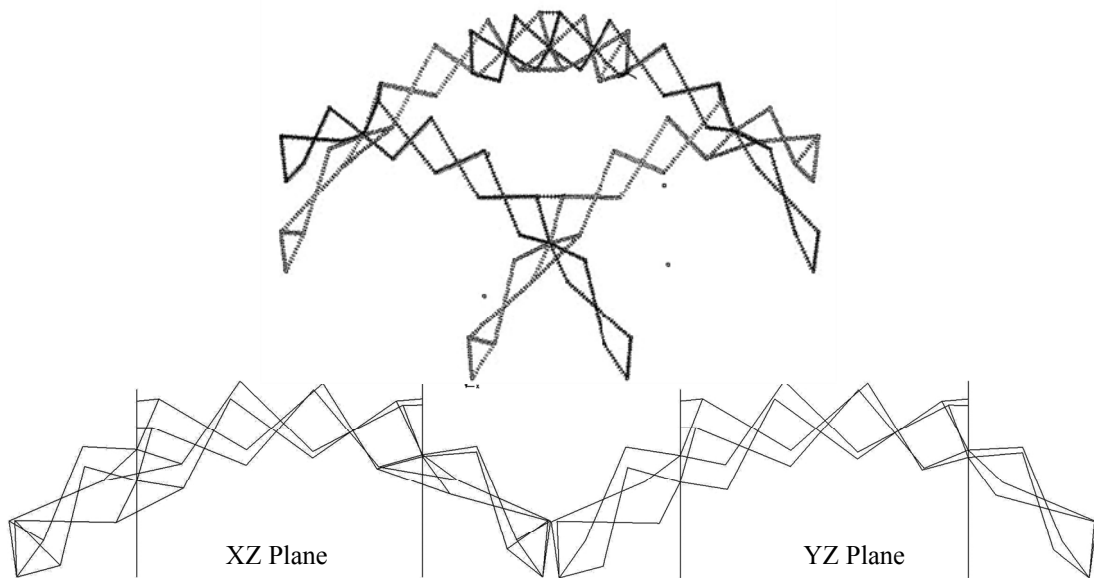
Figure 97. Views of the asymmetric structure with four telescopic members

Moments in the plane of each frame   Moments out of plane of each frame
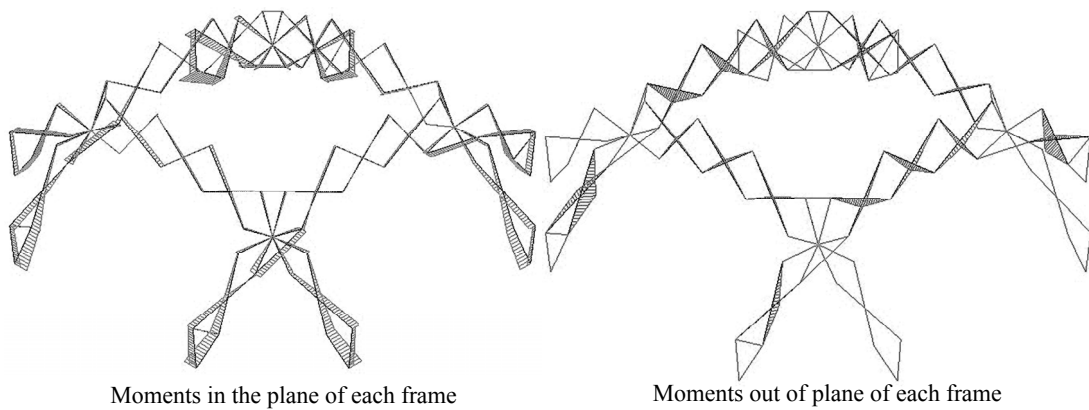
Figure 98. Bending moment diagrams of the asymmetric structure with four telescopic members

Table 9. Maximum displacements of the double-curved shape structure with four telescopic members

Maximum displacement	Value (cm)
Z (vertical)	4.74
X	2.25
Y	5.06

From the analysis results important characteristics of the proposed spatial SSM can be understood. First of all, the proposed spatial SSM is stable at both symmetric cross-vault shape and asymmetric shapes, if four actuators, which are theoretically sufficient to stabilize the structure, are used at critical locations. However, addition of four more actuators than the necessary ones has been proved to be practically needed for stiffness in the specific structure analyzed. In addition, release of the bending moments in the three spatial directions at the four critical points of intersection of perpendicular frames is a more realistic approach as far as the behavior of the connections at these points is concerned. Additional telescopic members (not actuators) should then be used for stabilizing the structure. Further optimization could be possible by distributing the actuators in main scissors of both directions, varying the cross-sections between main scissors and/or along each main scissor.

CHAPTER 7

CONCLUSIONS

In this thesis, common deployable structures and especially scissor-hinge structural mechanisms were thoroughly investigated. During this investigation, geometric and kinematic principles of these structures were examined and their shortcomings with respect to form flexibility were exposed. A novel analytical design framework and a novel scissor-hinge structure with a new primary element has been proposed to overcome these shortcomings. The proposed scissor-hinge structure has both planar and spatial versions. Planar version of the structure can constitute various curvilinear geometries. The spatial version presents remarkable form flexibility from curvilinear to double-curved shapes. These novel structures can achieve these remarkable shape transformations with minimum numbers of actuators and this increases the feasibility of these structures.

This chapter extends the aforementioned contributions of the dissertation in the development of transformable scissor-hinge structures and highlights possible future work.

7.1. Contributions of the Dissertation

Contributions of the dissertation to the literature can be thought in two groups: Contributions to the field of deployable structures and contributions to the field of architectural design.

This dissertation offers a unique and novel study approach within the field of studies in deployable structures. Until this study, deployable scissor-hinge structures have been only used as the portative building components, which can change their shapes between defined open and closed body forms. In comparison, this study proposed a novel analytical design and implementation framework which offers a wide range of form flexibility.

In the context of the aforementioned framework, a novel type of scissor unit, which is called modified scissor-like element (M-SLE), has been introduced. A novel

transformable planar scissor-hinge structure has been developed by the utilization of this unit. Furthermore, geometric, kinematic and static analyses of both this novel unit and the proposed planar scissor-hinge structure have been exposed.

Another contribution of this study to the studies in deployable structures is the proposal of a new connection detail for the spatial scissor-hinge structures. Common connection details only provide 1 DoF mechanisms, but the proposed detail allows to 2 DoF systems. A novel transformable spatial scissor-hinge structure has been proposed by the use of this connection detail and the spatial version of the M-SLE. All geometric, kinematic, and static principles and conditions of this structure have been exposed in detail. This spatial structure can achieve curvilinear shapes, ruled surfaces and hypersurfaces.

Proposed transformable scissor-hinge structure contributes to the field of architecture as well. Modern buildings are expected to be flexible and responsive. Today, various buildings are designed to allow further applications of flexibility concept. However, none of them completely responds to the functional and spatial needs. By integration of the conventional architectural design approaches with the design strategies of motion and transformation, spaces could be more flexible and respond to the requirements of any spatial need and human activity.

7.2. Recommendations for the Future Research

In the context of this dissertation, the proposed planar and spatial scissor-hinge structures have been conceived primarily as a roof structure. However, these transformable structures can be used for different functions as well. For instance, they can be used as a responsive wall surface, or as an industrial object for a specific aim, or as a transformable and retractable solar panel of a satellite. Further research on the proposed scissor-hinge structure for alternative functions will provide new research perspectives.

Because of structural stability reasons, the proposed scissor-hinge structures cannot constitute planar shapes, although it is geometrically possible. A future study could deal with this problem.

Actuators are the crucial members of such kind of transformable deployable structures. These members provide both the motion and the stability of the whole

system. In this study, linear actuators have been used and all analyses and calculations were performed according to this kind of actuators. However, location, type, and force of the actuators can be changed according to the geometric and material properties of the structure. Thus, future studies should reconsider the location and type of the actuators which are used in the study.

Although the covering materials for the proposed transformable structures are not within the scope of the thesis, the dissertation gives some clues about the prospective materials for such kind of a cover. There could be further investigations on the flexible cover materials for transformable structures. Especially, membranes with flexible materials, origami tessellations, pneumatic or vacuumatic skins have potentials to be handled.

Consequently, this study has showed that the common deployable structures can be used as transformable building members, and exposed the potentials of these structures to create responsive and adaptive structures. In this respect, this thesis is a pioneer study for the research field of transformable deployable structures. However, this study has only dealt with the scissor-hinge structures and many other deployable mechanisms such as Bennett, Brickard, and Alizade linkages can be used as transformable building components as well. Further studies can concentrate on these mechanisms and reveal novel transformable structures.

BIBLIOGRAPHY

Akgün, Y, W. Haase, and W. Sobek. "Proposal for a New Scissor-Hinge Structure to Create Transformable and Adaptive Roofs." *Proceedings of IASS 2007 (International Association of Spatial Structures) Symposium Proceedings.* Venice, 2007.

Al Khayer, M., and H. Lalvani. "Scissors-action Deployables Based on Space-filling of Polygonal Hyperboloids." Edited by S. Pellegrino and S.D. Guest. *Proceedings of IUTAM_IASS Symposium on Deployable Structures: Theory and Applications.* Cambridge, UK: IUTAM_IASS Symposium on Deployable Structures: Theory andKluwer Academic Publishers, 1998. 1-10.

Alizade, R., Ç. Bayram, and E. Gezgin. "Structural Synthesis of serial platform manipulators." *Mechanism and Machine Theory* (Elsevier Ltd.) 42 (July 2006): 580-599.

Atake, K. "New Variations of the Scissors Technique." *MARAS III: International Conference on Mobile and Rapidly Assembled Structures.* Madrid, Spain, 2000. 143-154.

Barco. *Barco: On tour this year... A 360° experience.* October 20, 2009. http://www.barco.com/en/events/reference/3807 (accessed October 20, 2009).

Bati, S.B., T.R. and M. Tupputi. "Deployable Structures: A New Kind of Self-Locking Mechanism." *Conference Proceedings of IASS-APCS.* Beijing, China, 2006.

Baverel, O., and M. Saidani. "The Multi-reciprocal Grid System." *Journal of the International Association for Shells and Spatial Structures (IASS)* 40 (1999): 33-41.

Block, P. "Scissor Hinge Deployable Membrane Structures Tensioned by Pleated Pneumatic Artificial Muscles." Faculteit Toegepaste Wetenschapen Afdeling Architectuur, Vrije Universiteit Brusel, 2003.

Bradshaw, R., D. Campbell, M. Gargari, A. Mirmiran, and P. Tripeny. "Special Structures: Past, Present and Future." *Journal of Structural Engineering*, June 2002: 691-709.

Bright-Hub. *What is kinematics.* 2009.
http://www.brighthub.com/engineering/mechanical/articles/6251.aspx (accessed January 14, 2009).

Britt, A.L., and H. Lalvani. "Symmetry as a Basis for Morphological Analysis and Generation of NASA Type Cubic Deployables." Edited by S. Pellegrino and D. Guest. *Proceedings of IUTAM IASS Symposium on Deployable Structures: Theory and Applications.* Cambridge, UK: Kluwer Academic Publishers, 1998. 45-54.

Buhl, T., F.V. Jensen, and S. Pellegrino. "Shape Optimization of Cover Plates for Retractable Roof Structures." *Computers and Structures Journal* 82 (1984): 1227-1236.

Calatrava. http://www.calatrava.com. January 13, 2009.

Calatrava. *Zur Faltbarkeit von Fachwerken.* PhD Thesis, Zurich, Switzerland: ETH, 1981.

Calladine, C.R. "Deployable Structures: What can We Learn from Biological Structures?" Edited by S. Pellegrino and S.D. Guest. *Proceedings of IUTAM_IASS Symposium on Deployable Structures: Theory and Applications.* Cambridge, UK: Kluwer Academic Publishers, 1998. 463-476.

Chelyshev, V.A., V.N. Zimin, and V.E. Meshkovsky. "Self-deployable Truss Structures." *MARAS III: International Conference on Mobile and Rapidly Assembled Structures.* Madrid, Spain, 2000. 165-173.

Chen, W., F. Guan, X. Chen, and H. Qiu. "Design and Analysis of a Deployable/Retractable Mast." *Journal of the International Association for Shells and Spatial Structures (IASS)* 39 (1998): 111-116.

Chen, W., G. Fu, J. Gong, Y. He, and S. Dong. "A New Design Conception for Large Span Deployable Flat Grid Structures." *International Journal of Space Structures* 17, no. 4 (2002): 293-299.

Chen, W., Y. Luo, G. Fu, J. Gong, and D. Shilin. "Design Conception and Deployment Simulation for a Extendable/Retractable Mast." *International Journal of Space Structures* Vol. 16, no. 4 (2001): 261-269
.
Chen, Y. *Design of Structural Mechanisms.* PhD Thesis, Department of Engineering Science, Oxford: University of Oxford, 2003.

Chen, Y. "Threefold-symmetric Bricard linkages for deployable structures." *International Journal of Solids and Structures 42*, 2005: 2287–2301.

Chen, Y. and Z. You. "Square Deployable Frames for Space Applications Part 1 Theory." *Proceedings of the I MECH E Part G Journal of Aerospace Engineering.* 2006. 347-354.

Chilton, J.C. "Research and Teaching of Space Structures." *International Journal of Space Structures* 17, no. 2-3 (2002): 93-105.

Clarke, R.C. "The Kinematics of a Novel Deployable Space Structure System." Edited by H. Nooshin. *Proceedings of the 3rd International Conference on Space Structures.* Guildford, UK: Elsevier Applied Science Publishers, 1984. 820-822.

Cozar, J.C.G. and R.G. Dieguez. "System for the Construction of Double Layer Deployable Structures: Processes of Formal Definition." *Proceedings of MARAS III: International Conference on Mobile and Rapidly Assembled Structures.* Madrid, Spain, 2000. 103-112.

Denavit, J. and R.S. Hartenberg. "A Kinematic Notation for Lowe-pair Mechanisms based on Matrices." *Journal of Applied Mechanics*, 1955: 215-221.

Deployable Structures. http://www-civ.eng.cam.ac.uk/dsl/ (accessed January 06, 2009).

Dieguez, R.G. and J.C.G. Cozar. "Florin System Double Layer Spatial Deployable Structures, with Frames of Rhombuses and Scissors." Edited by S. Pellegrino and S.D. Guest. *Proceedings of IUTAM IASS Symposium on Deployable Structures: Theory and Applications.* Cambridge, UK: Kluwer Academic Publishers, 1998. 117-126.

Ebara, M. and K. Kawaguchi. "Foldable Grid Connections,." Edited by S. Pellegrino and S.D. Guest. *Proceedings of IUTAM-IASS Symposium on Deployable Structures: Theory and Applications.* Cambridge, UK: Kluwer Academic Publishers, 1998. 97-105.

Ekmekçi, Ç. *Mimari Yapılarda Hareket Çeşitlerinin İncelenmesi ve Haareketin Mimari Tasarımda Kullanılması.* MSc Thesis, İstanbul: Yıldız Technical University, 2005.

Escrig, F. "Expandable Space Frame Structures." Edited by H. Nooshin. *Proceedings of the 3rd International Conference on Space Structures.* Guildford, UK: Elsevier Applied Science Publishers, 1984. 845-850.

Escrig, F.. "Expendable Space Structures." *Space Structures Journal* 1, no. 2 (1985): 79-91.

Escrig, F. "General Survey of Deployability in Architecture." Edited by F. Escrig and C.A. Brebbia. *Proceedings of MARAS'96:2nd International Conference on Mobile and Rapidly Assembled Structures.* Seville, Spain: Computational Mechanics Publications, 1996. 3-22.

Escrig, F. and J.P. Valcarcel. "Analysis of Expendable Space Bar Structures." Edited by K. Heki. *Proceedings of IASS Symposium on Shells, Membranes, and Space Frames.* Osaka, Japan: Elsevier Science Publishers, 1986. 269-276.

Escrig, F. "Great Size Umbrellas with Expendable Bar Structures." *Proceedings of the 1st International Conference on Lightweight Structures in Architecture.* Sydney, Australia, 1986. 676-681.

Fox, M.A. «Novel Affordances of Computation to the Design Process of Kinetic Structures.» MSc Thesis, Depatment of Architecture, MIT, Boston, USA, 1996.

Freudenstein, F. and R. Alizade. "On the Degree of Freedom of Mechanisms with Variable General Constraint." *IV. World IFToMM Congress.* England, 1975. 51-56.

Galinsky. *Milwaukee Art Museum by Santiago Calatrava.* October 27, 2009. http://www.galinsky.com/buildings/milwaukeeart/ (accessed October 27, 2009).

Gan, W.W., and S. Pellegrino. "Closed-Loop Deployable Structures." *Proceedings of 44th AIAA/ASME/ASCE/AHS/ASC Structures, Structural Dynamics and Materials Conference.* Norfolk, VA, 2003.

Gan, W. and S. Pellegrino. "Numerical Approach to the Kinematic Analysis of Deployable Structures Forming a Closed Loop." *Proceedings of the I MECH E Part C Journal of Mechanical Engineering Science.* Professional Engineering Publishing, 2006. 1045-1056.

Gantes, C.J. «A Design Methodology for Deployable Structures.» PhD Thesis, Department of Civil Engineering, MIT, Boston, USA, 1991.

Gantes, C.J. and E. Konitopoulou. "Geometric Design of Arbitrarily Curved Bi-Stable Deployable Arches with Discrete Joint Size." *International Journal of Solids and Structures* 41, no. 20 (2004): 5517-5540.

Gantes, C.J. *Deployable Structures: Analysis and Design.* Boston, USA: WIT Press, 2001.

Gantes, C.J., A. Giakoumakis and P. Vousvounis. "Symbolic Manipulation as a Tool for design of Deployable Domes." *Computers & Structures Journal* 64, no. 1-4 (1997): 865-878.

Gantes, C.J., D.N. Tsouknaki and S.C. Kyritsas. "Combining Active and Passive Sub-structures in Snap-through Type Deployable Structures." Edited by S. Pellegrino and S.D. Guest. *Proceedings of IUTAM IASS Symposium on Deployable Structures: Theory and Applications.* Cambridge, UK: Kluwer Academic Publishers, 1998. 107-116.

Gantes, C.J., J.J. Connor and R.D. Logcher. "A Systematic Design Methodology for Deployable Structures." *International Journal of Space Structures* 9, no. 2 (1994): 67-86.

Gantes, C.J., J.J. Connor and R.D. Logcher. "Simple Friction Model for Scissor Type Mobile Structures." *Journal of Engineering Mechanics* 119, no. 3 (1993): 456-475.

Gantes, C.J., J.J. Connor, R.D Logcher and Y. Rosenfeld. "Structural Analysis and Design of Deployable Structures." *Computers & Structures* 32, no. 3/4 (1989): 661-669.

Gantes, C.J., R.D. Logcher, J.J. Connor and Y. Rosenfeld. "Deployability Conditions for Curved and Flat, Polygonal and Trapezoidal Deployable Structures." *International Journal of Space Structures* 8 (1993): 97-106.

Gantes, C.J., R.D. Logcher, J.J. Connor and Y. Rosenfeld. "Geometric Design of Deployable Structures with Discrete Joint Size." *International Journal of Space Structures* 8 (1993): 107-117.

Gutierrez, E.M., and J.B.P. Valcarcel. "Generation of Foldable Domes formed by Bundle Modules with Quadrangular Base." *Journal of the International Association for Shells and Spatial Structures (IASS)* 2 (2002): 133-140.

Hachem, C., E. Karni and A. Hanaor. "Evaluation of Biological Deployable Systems." *International Journal of Space Structures* 20, no. 4 (2005): 189-200.

Hanaor, A. "Double-Layer Tensegrity Grids as Deployable Structures." *International Journal of Space Structures* 8 (1993): 135-143.

Hanaor, A., and R. Levy. "Evaluation of Deployable Structures for Space Enclosures." *International Journal of Space Structures* 16, no. 4 (2001): 211-229.

Heatherwick-Studio. *Heatherwick Studio - Rolling Bridge.* January 12, 2009. http://www.heatherwick.com/index.php?option=com_content&task=view&id=19&Itemid=48.

Hoberman. *Hoberman Transformable Design.* Hoberman Associates - Transformable Design. October 20, 2009. http://www.hoberman.com.

Hoberman, C. "Unfolding Architecture: An Object that is Identically a Structure and a Mechanism." *Architectural Design* 63 (1993): 56-59.

Hollaway, L. "Numerical Analysis of an Energy Loaded Joint for a Deployable Satellite Structure." *International Journal of Space Structures* 10, no. 1 (1995): 47-55.

Inoue, F. "Development of Adaptive Construction Structure by Variable Geometry Truss." In *Robotics and Automation in Construction*, edited by C Balaguer and M Abderrahim, 253-272. InTech Education and Publishing, 2008.

Inoue, F., K. Kurita, R. Moroto, and N. Furuya. "Development of Adaptive Structure by Variable Geometry Truss." *Proceeding of 23th International Symposium on Automation and Robotics in Construction.* Tokyo, 2006. 704-709.

Jensen, F., and S. Pellegrino. "Expandable Structures Formed by Hinged Plates." Edited by G.A.R. Parke and P. Disney. *Proceedings of 5th International Conference on Space Structures.* London: Thomas Telford Publishing, 2002. 263-272.

Karni, E. "Deployable Swimming Pool Enclosures." Edited by S. Pellegrino and S.D. Guest. *Proceedings of IUTAM IASS Symposium on Deployable Structures: Theory and Applications.* Cambridge, UK: Kluwer Academic Publishers, 1998. 183-191.

Kaveh, A., A. Jafarvand and M.A. Barkhordari. "Optimal Design of Pantograph Foldable Structures." *International Journal of Space Structures* 14, no. 4 (1999): 295-302.

Kaveh, A. and A. Davaran. "Analysis of Pantograph Foldable Structures." *Computers & Structures* 59, no. 1 (1996): 131-140.

Kawaguchi, M. and S. Mitsumune. "A Domical Space Frame Foldable during Erection." Edited by H. Nooshin. *Proceedings of the 3rd International Conference on Space Structures.* London: Elsevier Applied Science Publishers, 1984. 982-987.

Kinematics - Britannica Online Encyclopedia. 2009. http://search.eb.com/eb/article-9045488 (accessed January 13, 2009).

Kinetic Art Association. June 20, 2008. http://www.kinetic-art.org.

Kokawa, T. "Structural Idea of Retractable Loop Dome." *Journal of the International Association for Shells and Spatial Structures (IASS)* 41 (2000): 111-115.

Kokawa, T. and T. Hokkaido. "Cable Scissors Arch-Marionettic Structure: Structural Morphology, Towards the New Millennium." *Proceedings of International Conference of IASS.* Nottingham, 1997. 107–116.

Korkmaz, K. "An Analytical Study of the Design Potentials in Kinetic Architecture." PhD Thesis, Department of Architecture, İzmir Institute of Technology, Izmir,Turkey, 2004.

Kovacs, F. "Foldable Bar Structures on a Sphere." Edited by Pellegrino S. and S.D. Guest. *Proceedings of IUTAM IASS Symposium on Deployable Structures: Theory and Applications.* Cambridge, UK: Kluwer Academic Publishers, 1998. 221-228.

Kresling, B. "Coupled Mechanisms in Biological Deployable Structures." Edited by S. Pellegrino and Guest S.D. *Proceedings of IUTAM IASS Symposium on Deployable Structures: Theory and Applications.* Cambridge, UK: Kluwer Academic Publishers, 1998. 229-238.

Kronenburg, R. *Portable Architecture.* Boston, USA: Architectural Press, 1996.

Kronenburg, R. *Houses in Motion: The Genesis, History and Development of the Portable Building.* London: Academy Editions, 1995.

Kronenburg, R. *Transformable Environments, papers from the International Conference on Portable Architecture.* London: E&FN Spon Press, 1997.

Kronenburg, R. *Flexible: Architecture that Responds to Change.* Laurence King Publishers, 2007.

Kukreti, A.R. and N.D. Uchil. "Dynamic Response Analysis of Large Latticed Space Structures." *International Journal of Space structures* 4, no. 1 (1989): 25-42.

Kwan, A.S.K. "A Parabolic Pantographic Deployable Antenna." *International Journal of Space Structures* 4 (1995): 195-203.

Kwan, A.S.K., Z. You and S. Pellegrino. "Active and Passive Cable Elements in Deployable Retractable Masts." *International Journal of Space Structures* 8 (1993): 29-40.

Langbecker, T. "Kinematic Analysis of Deployable Scissor Structures." *International Journal of Space Structures* 14, no. 1 (1999): 1-15.

Liapi, K. "Geometry in Architectural Engineering: Education Revisited." *Journal of Architectural Engineering* 8, no. 3 (2002): 80-88.

Liapi, K. "Transformable Structures Design Features and Preliminary Investigation." *Journal of Architectural Engineering* 1 (2001): 13-17.

Lin, G. and Y.R. Lin. "The Design and Research of Revolving Openable Roof System for Shangai Qi-Zhong Stadium." *Proceedings of IASS-APCS.* Beijing, China, 2006.

McNulty, O. "Foldable Space Structures." Edited by K. Heki. *Proceedings of IASS Symposium on Shells, Membranes, and Space Frames.* Osaka, Japan: Elsevier Science Publishers, 1986. 277-284.

Natori, M., K. Miura and H. Furuya. "Deployable Truss Concepts in Space Technology." Edited by K. K. Heki. *Proceedings of IASS Symposium on Shells, Membranes, and Space Frames.* Osaka, Japan: Elsevier Science Publishers, 1986. 261-268.

Neogi, D. and C.D. Douglas. "Design and Development of a Self-deployable Structural Element." *International Journal of Space Structures* 13, no. 3 (1998): 77-87.

Norton, R.L. *Design of Machinery: An Introduction to the Synthesis and Analysis of Mechanisms and Machines.* 3rd Edition (International Edition). Singapore: McGraw Hill Education, 2004.

Otto, F. and B. Rasch. *Finding Form : Towards an Architecture of the Minimal.* Stuttgart: Axel Menges, 1995.

Piekarski, M. "Constructional Solutions for Two-way-fold Deployable Space Trusses." Edited by S Pellegrino and S.D. S.D. Guest. *Proceedings of IUTAM IASS Symposium on Deployable Structures: Theory and Applications.* Cambridge, UK: Kluwer Academic Publishers, 1998. 301-310.

Pinero, E.P. "Project for a Mobile Theatre." *Architectural Design* 12 (1961): 570.

Raskin, I. "Stiffness and Stability of Deployable Pantographic Columns." PhD Thesis, Faculty of Architecture, University of Waterloo, Ontario, Canada, 1998.

Raven, F H. "Velocity and Acceleration Analysis of Plane and Space Mechansims by Means of Independent-Position Equations." *Trans ASME* 25 (1958): 1-6.

Rippmann, M. *Curtain Wall: Building Design Semesterarbeit.* Stuttgart: Universität Stuttgart-ILEK, 2007.

Rizzuto, J.P., M. Saidani and J.C. Chilton. "The Self Supporting Multi-reciprocal Grid (MRG) System Using Notched Element." *Journal of the International Association for Shells and Spatial Structures (IASS)* 41 (2000): 125-131.

Robbin, T. *Engineering a New Architecture.* New Haven and London: Yale University Press, 1996.

Rodriguez, C. and J. Chilton. "Swivel Diaphragm A New Alternative for Retractable Ring Structures." *Journal of the International Association for Shells and Spatial Structures (IASS)* 1 (2002): 181-188.

Rosenfeld, Y., Y. Ben-Ami and R.D. Logcher. "A Prototype "Clicking" Scissor-Link Deployable Structures." *International Journal of Space Structures* 8 (1993): 85-95.

Saar, O. "Self-Erecting Two-Layer Steel Prefabricated Arch." Edited by H. Nooshin. *Proceedings of the 3rd International Conference on Space Structures.* Guildford, UK: Elsevier Applied Science Publishers, 1984. 823-827.

Saar, O.S. "A New Type of Hardening Structure." *Proceedings of MARAS III, International Conference on Mobile and Rapidly Assembled Structures.* Madrid, Spain, 2000. 113-124.

Saidani, M. and O. Baverel. "Retractable Multi-Reciprocal Grid Structure." *Journal of the International Association for Shells and Spatial Structures (IASS)* 39 (1998): 141-146.

Schmidt, L.C. and H. Li. "Geometric Models of Deployable Metal Domes." *Journal of Architectural Engineering, ASCE* 1, no. 3 (1995): 115-120.

Schmidt, L.C. and H. Li. "Shape Formation of Deployable Metal Domes." *International Journal of Space Structures* 4 (1995): 189-194.

Söylemez, E. *Mechanisms.* Ankara: Middle East Technical University Press, 1999.

Stach, E. and D. Smith. "Kinetic Structures and Sculptures." *Proceedings of IASS-APCS.* Beijing China, 2006.

Tanami, T. "Tools of Analysis on Mobility and Structural Morphology." Edited by S. Pellegrino and S.D. Guest. *Proceedings of IUTAM IASS Symposium on Deployable Structures: Theory and Applications.* Cambridge, UK: Kluwer Academic Publishers, 1998. 425-434.

Tarczewski, R. "Variable Rigidity as a Tool of Shaping of Self Erecting Structures." *Proceedings of MARAS III, International Conference on Mobile and Rapidly Assembled Structures.* Madrid, Spain, 2000. 125-129.

Tibert, G. "Deployable Tensegrity Structures for Space Applications." PhD Thesis, Department of Mechanics, Royal Institute of Technology, Sweden, 2002.

Tischhauser, A. and S. von Moos. *Calatrava: Public Buildings.* Basel, Switzerland: Birkhauser Press, 1998.

Tsai, L. *Robot Analysis: The Mechanics of Serial and Parallel Manipulators.* New York: John Wiley and Sons Press, 1999.

TurboSquid 3D Marketplace. October 23, 2009. http://www.turbosquid.com/FullPreview/Index.cfm/ID/215432 (accessed October 23, 2009).

Tzonis, A. *Santiago Calatrava: The Poetics of Movement.* New York: Universe Publishing, 1999.

Tzonis, A. and L. Lefaivre. *Movement, Structure and the Work of Santiago Calatrava.* Basel, Switzerland: Birkhauser Press, 1995.

Usiukin, V.I. "Dynamics of Large Deployable Structures." Edited by Pellegrino S. and S.D. Guest. *Proceedings of IUTAM IASS Symposium on Deployable Structures: Theory and Applications.* Cambridge, UK: Kluwer Academic Publishers, 1998. 447-456.

Vincent, J.F.V. "Deployable Structures in Nature: Potential for Biomimicking." *Proceedings of the Institution of Mechanical Engineers.* 2000.

Vu, K.K., J.Y. Richard Liew and K. Anandasivam. "Deployable Tension-Strut Structures: Structural Morphology Study and Alternative Form Creations." *International Journal of Space Structures* 21, no. 3 (2006): 149-164.

Wagner, R. and A. te Bögle. "Double-Curved Space Structures – Function and Construction." *International Journal of Space Structures* 17, no. 2-3 (2002): 117-127.

West-8. *Schouwburgplein.* January 12, 2009. http://www.west8.nl/projects/public_space/schouwburgplein/.

Wikipedia, The Free Encyclopedia. http://en.wikipedia.org/wiki/Analytical_dynamics (accessed April 1, 2009).

Wu, A.H.K. and H. Lalvani. "A Class of Periodic Deployable Space Frames Using Regular Prismatic Nodes." *Journal of the International Association for Shells and Spatial Structures (IASS)* 39 (1998): 37-41.

Yeh, B. "Kinetic Wall." MSc Thesis, Department of Architecture, Massachusetts Institute of Technology, Cambridge, USA, 1998.

You, Z. "A New Approach to Design of Retractable Roofs." Edited by S. Pellegrino and S.D. Guest. *Proceedings of IUTAM IASS Symposium on Deployable Structures: Theory and Applications.* Cambridge, UK: Kluwer Academic Publishers, 1998. 477-483.

You, Z. and S. Pellegrino. "Foldable Bar Structures." *International Journal of Solids and Structures* 34, no. 15 (1997): 1825-1847.

Zanardo, A. "Two Dimensional Articulated Systems Deployable on a Single or Double Curvature Structure." *Meccanica* Vol. 21 (1986): 106-111.

Zhao, J.S. and Z.J. Feng. "The mechanism theory and application of deployable structures." *Mechanism and Machine Theory* (Elsevier) 44 (2009): 324-335.

Zuk, W. "The Next 100 Years of Architecture." *The Futurist*, 1994: 16-19.

Zuk, W., and R. Clark. *Kinetic Architecture.* New York: Van Nostrand Reinhold Press, 1970.

VITA

Yenal AKGÜN

EDUCATION

2004-2010   **PhD in Architecture,** Izmir Institute of Technology, Department of Architecture, Turkey
Thesis: "A Novel Transformation Model for Deployable Scissor-hinge Structures"

2000-2004   **Master of Architecture,** Izmir Institute of Technology, Department of Architecture, Turkey
Thesis: "Perception of Space through Representation Media: A Comparison between 2D Representation Techniques and 3D Virtual Environments"

1996-2000   **Bachelor of Architecture**
Istanbul Technical University, Department of Architecture, Turkey

TEACHING EXPERIENCE

2002-2010   **Research Assistant,** Izmir Institute of Technology, Department of Architecture, Turkey

1999-2000   **Student Assistant,** Istanbul Technical University, Department of Architecture

PROFESSIONAL EXPERIENCE

2001-2002   **Office Architect,** Tekser Engineering and Construction Company, Turkey

2000-2001   **Office Architect,** Azan Kozbe Construction Company, Turkey